To mimic microbes with models: Development and application of the microbially explicit soil model MIMICS+ in cold climates

Elin Ristorp Aas

Supervisors:
Terje Koren Berntsen
Alexander Eiler
Helge Hellevang

Department of Geosciences

Series of dissertations submitted to the
Faculty of Mathematics and Natural Sciences, University of Oslo
No. 2784

ISSN 1501-7710

Cover: UiO.
Print production: Graphic center, University of Oslo.

Abstract

Whether soils will act as a net sink or a net source of atmospheric carbon in the future is a major uncertainty in current climate projections. Soil processes have traditionally been underrepresented in Earth System Models, and to increase our understanding of soil responses to climate change, we need soil models that explicitly represent microbial groups like bacteria and fungi, which can respond non-linearly to changes in their environment. This work presents a soil biogeochemistry model, MIMICS+, which is developed with a particular focus on boreal areas. The model is built on the existing model MIMICS, which represents the decomposition of plant litter and soil organic matter by two functionally different microbial pools. With MIMICS+, we extend this framework by introducing two additional microbial pools, representing ectomycorrhizal and arbuscular mycorrhizal fungi. In addition, a nitrogen (N) cycle, and vertical layers are introduced in MIMICS+. We show that the model performs better, or on par with a traditional soil model when we compare to forested sites in Norway, both in terms of carbon (C) content and soil C:N ratio. We also show that the model broadly captures climatic and litter quality controls on decomposition rates. Through a sensitivity study of ectomycorrhizal turnover times, we show how the presence of mycorrhiza affects soil dynamics through nutrient competition with microbial decomposers. In the future, MIMICS+ will represent an improved soil sub-model in the Norwegian Earth System Model, thus contributing to a deeper understanding of how soil and its microorganisms can affect climate projections.

Sammendrag

Hvorvidt jordsmonn vil være et netto tap eller en netto kilde til atmosfærisk karbon i fremtiden er en stor usikkerhet i klimaprognoser. Jordprosesser har tradisjonelt vært underrepresentert i jordsystemmodeller. For å øke vår forståelse av hvordan jordsmonn responderer på klimaendringer, trenger vi jordmodeller som eksplisitt representerer mikrobielle grupper som bakterier og sopp, som kan reagere ikke-lineært på endringer i omgivelsene. Denne avhandlingen presenterer en jordbiogeokjemimodell, MIMICS+, som er utviklet med et spesielt fokus på boreale områder. Modellen er bygget på den eksisterende modellen MIMICS, som representerer dekomponering av dødt plantemateriale og organisk materiale gjennom to funksjonelt forskjellige mikrobielle grupper. Med MIMICS+ har vi utvidet dette rammeverket ved å introdusere ytterligere to mikrobielle grupper, som representerer ektomykorrhiza og arbuskulær mykorrhiza sopp. Vi har også lagt til en nitrogensyklus og gjort modellen vertikaloppløst. Vi viser at modellen presterer bedre, eller på nivå med en tradisjonell jordkarbonmodell når vi sammenligner med observasjoner fra norske skoger, både når det gjelder karboninnhold og jordens C:N-forhold. Vi viser også at modellen i store trekk fanger opp hvordan klima og kvaliteten av plantemateriale påvirker dekomponeringshastigheter. Gjennom en sensitivitetsstudie av levetider for ektomykorrhiza viser vi hvordan mykorrhiza kan påvirke karbon- og nitrogenkretsløpet gjennom konkurranse med mikrobielle nedbrytere. I fremtiden vil MIMICS+ representere en forbedret jordmodell i den norske klimamodellen "the Norwegian Earth System Model", og dermed bidra til en dypere forståelse av hvordan jorden og dens mikroorganismer kan påvirke klimaprojeksjoner.

Contents

Preface

This synthesis and collection of papers are submitted for the degree of philosophiae doctor (PhD) in terrestrial modeling at the Section for Meteorology and Oceanography (MetOs), Department of Geosciences, University of Oslo. The work has been conducted in the period from November 2018 until April 2024. The research has been supervised by Terje Koren Berntsen (MetOs), Alexander Eiler (Biosciences), and Helge Hellevang (Geosciences). The funding for this research is from the interdisciplinary Centre for Biogeochemistry in the Anthropocene (CBA), as well as the Norwegian Research Council funded projects EMERALD (294948) and FUNDER (315249). The thesis includes one introductory part (Part I) and one part consisting of three research papers (Part II). Chapter 4 presents summaries of all papers, including author contributions.

Paper I

Elin R. Aas, Heleen A. de Wit, and Terje K. Berntsen (2024), "Modeling boreal forest soil dynamics with the microbially explicit soil model MIMICS+ (v1.0)". Published in Geoscientific Model Development. DOI: https://doi.org/10.5194/gmd-17-2929-2024

Paper II

Elin R. Aas, Inge Althuizen, Hui Tang, Sonya Geange, Eva Lieungh, Vigdis Vandvik, and Terje K. Berntsen (2024), "Implications of climate and litter quality for simulations of litterbag decomposition at high latitudes". In review for Biogeosciences. The version presented in this thesis is revised based on reviewer comments, and takes into account the CLM bug described in Section 3.2.2. DOI for pre-print version: https://egusphere.copernicus.org/preprints/2024/egusphere-2024-340/

Paper III

Elin R. Aas, Elisabeth Wörner, and Terje K. Berntsen, "Ectomycorrhizal turnover times affect soil dynamics in boreal ecosystems; A model study". in prep. for Soil Biology and Biochemistry.

Acknowledgements

This thesis would not have been possible without the support from many people and institutions. I want to thank my supervisor Terje K. Berntsen, who gave me the opportunity to work on this project. Your open-door policy have been invaluable for navigating between the modeling-world and the real-world.

Also a big thanks to other colleagues at the CBA, from which I have learned so much through conversations and seminars.

Thanks to Hui Tang, Rosie Fisher, and Kjetil Aas for helping with everything related to CLM, from technical issues to process understanding.

I also want to thank Will Wieder, Dave Lawrence and other colleagues at NCAR, Colorado, for allowing me to visit and gain a deeper understanding of the MIMICS model. Thanks also to the Kristine Bonnevie scholarship for funding the research stay there.

Thanks to my colleagues at MetOs, for interesting scientific and not-so-scientific discussions, table tennis matches, and after-work activities. Thanks to Betty for much needed help with illustrations, and for being a great office mate. A special thanks also to Tim, Rob, and Franziska for their support, and for constructive feedback on the thesis text.

A big thanks also to Einar for being supportive and patient, and making sure I had dinner and clean clothes, even during the busiest of times.

Part I

Part 1: Thesis

Chapter 1

Introduction

1.1 Motivation

In addition to being a component of the greenhouse gas CO_2, carbon atoms are essential building blocks for all living things, from the largest trees to the smallest bacteria. Carbon is stored in, and cycled between different reservoirs on Earth; soils, living biomass, ocean, sediments, fossil reservoirs, rocks, and the atmosphere. We assume that the carbon cycle was more or less at steady-state in pre-industrial times, but anthropogenic emissions of greenhouse gases have shifted this stable state. The responses of soil organic carbon to increasing atmospheric CO_2 concentrations and climate change are not well constrained by observations and represent a key uncertainty in climate projections (Jia et al., 2019). Given that soils store more than twice as much carbon than what is present in the atmosphere, whether they will act as a net source or a net sink of atmospheric carbon in the future is an important but unanswered question (Shi et al., 2024).

So-called feedback mechanisms can either amplify (positive feedback) or dampen (negative feedback) the effect of a forced change on the climate system. How the carbon cycle responds to increased atmospheric CO_2 and climate change can be characterized in two different feedbacks. The *carbon-concentration feedback* quantifies responses to changes in atmospheric CO_2 concentrations, while the *carbon-climate feedback* quantifies responses to changes in the physical climate (Arora et al., 2020). Model intercomparison studies have shown that the carbon-concentration feedback is generally negative (from the atmosphere perspective), as increased atmospheric concentration leads to greater uptake of carbon by the ocean and over land through photosynthesis and thereby a reduced accumulation of carbon in the atmosphere (Arora et al., 2013; Friedlingstein et al., 2006). The carbon-climate feedback effect was found to be positive from the atmosphere perspective in the model intercomparisons, as increased temperature reduces the carbon holding capacity of the land and the ocean. The results from Arora et al. (2020), where they look at CMIP5 (Taylor et al., 2012) and CMIP6 (Eyring et al., 2016) models[1], showed a striking difference in the uncertainty of the feedback

[1]The Coupled Model Intercomparison Project (CMIP) is a collaborative framework for comparing state-of-the-art Earth System Model simulations of the past, current, and future climate.

strength between land models and ocean models, with estimates over land being one order of magnitude more uncertain than estimates over the ocean. The terrestrial responses to increased CO_2 and climate change are largely governed by biological processes that are much less understood, which in turn limits the models ability to capture these responses. The differences in uncertainty between land and ocean components of Earth System Models (ESMs) were also addressed by Bonan and Doney (2018), who showed that the majority of uncertainty in land models comes from model structure and parameters, reflecting a lack of representation of essential biogeochemical processes.

The historical development of ESMs originating from purely physical general circulation models (Fisher and Koven, 2020), together with the limited amount of observed data about soil processes and biodiversity (Guerra et al., 2020), has led to an under-representation of soil processes in general, and the role of microbial activity specifically. With new technologies for observing soil processes, it has become evident that microbial activity, nutrient availability, and plant- and mineral interactions cannot be ignored when modeling future climate projections, as these processes are sensitive to changes in climate and CO_2 concentrations. Proper representation of interactions between biogeochemical cycles, like how the carbon cycle is affected by the cycling of nutrients like nitrogen or phosphorus, is also lacking from most ESMs (Jia et al., 2019). To better understand the role of soils as a source and/or a sink of atmospheric carbon, we need to reduce the uncertainties related to the carbon feedbacks of terrestrial systems.

Although the spread among ESM projections of warming-induced soil carbon loss is large, most of the models represent soil decomposition in a structurally similar manner, using the microbially implicit CENTURY approach (Parton et al., 1988). As argued by Bradford et al. (2016), the large spread among model projections is, therefore, largely a consequence of parameter uncertainty. If we want to increase confidence in the direction and magnitude of the carbon feedbacks, we need a better understanding also of the structural uncertainty. This can be achieved by using soil sub-models that represent structurally different hypotheses about carbon exchange and stabilization in the ESMs.

The new generation of soil models represent microbial activity explicitly, and challenges the traditional view of Soil Organic Matter (SOM) as inherently stable humic substances, with the emergent view of SOM as a continuum of progressively decomposing organic compounds (Lehmann and Kleber, 2015; Chandel et al., 2023). These models can give more realistic and diverse representations of the terrestrial carbon cycle in ESMs, as the explicit representation of microorganisms allows for modeling nonlinear responses to changes in climate and/or CO_2 concentration. By incorporating such models into ESMs, it is possible to assess the structural uncertainties associated with the carbon feedbacks and increase confidence in the projected responses to climate change.

Previous CMIP phases have mainly used concentration-driven emission scenarios to project future climate. This approach does not capture the carbon cycle uncertainty in the scenario outcomes, thus missing an important piece of information. A proposed method to overcome this issue is to use emission-driven scenarios in the model simulations (Sanderson et al., 2023). This approach requires

ESMs to represent complete cycles of green house gases, which further motivates the incorporation of more realistic cycling of carbon and nitrogen in ESMs.

A major challenge in soil models is to translate complex biogeochemical processes and mechanisms into equations and parameters (Chandel et al., 2023). Historically, ecological observations have often been performed without considering the usefulness for process model development, and empirical observations have been used carelessly to inform models (Kyker-Snowman et al., 2022). With more careful consideration of how models and field experiments can complement each other, the development of these microbially explicit models can be a valuable tool in bridging the gap between empirical observations and model development (Kyker-Snowman et al., 2022; Halbritter et al., 2020).

A complicating factor when modeling terrestrial ecosystems is the vast difference in the behavior of different biomes across Earth. Rapid turnover of carbon and nutrients in the tropics leads to relatively small amounts of carbon stored in the soils compared to vegetation. In contrast, boreal ecosystems, with slower turnover and less nutrients store a disproportionately large amount of the total terrestrial carbon in the soils (Crowther et al., 2019). Many soil models and ESMs are developed from a global perspective and do not necessarily consider mechanisms that are particularly important in colder climates, like nutrient competition and mycorrhizal associations[2]. Therefore, there is an urgent need for more knowledge about how high-latitude ecosystems respond to climate change, and a need to ensure that these processes are also represented in global simulations with ESMs. The focus of this thesis is to further our understanding of high-latitude soil process responses to a changing climate through the development of a soil biogeochemistry model with a particular focus on these ecosystems. To make full use of the soil model to quantify the carbon-climate and carbon-concentration feedbacks, the model is intended to be incorporated first into the Community Land Model (CLM; (Lawrence et al., 2019)) and then further into the fully coupled Norwegian Earth System Model (NorESM; Seland et al., 2020).

[2]Mycorrhiza: symbiotic associations between plants and fungi

1.2 Objectives

To address the challenges mentioned above, **the main objective of this work has been to establish a microbially explicit soil biogeochemical model, which is capable of representing processes relevant to boreal ecosystems but also simple and general enough to be incorporated into an ESM**. A large part of the project has been devoted to formulating a model fit for this purpose, by combining existing work with new ideas and observations. The result is the decomposition model MIMICS+ which has been used to address the following sub-objectives:

1. Gain a better understanding of the processes that are important for boreal soils, and investigate the soil dynamics related to them within the modeling framework. In particular;
   (a) How the availability of nutrients (nitrogen) affects microbial activity and microbe-microbe interactions[3] in nutrient poor environments.
   (b) How temperature and moisture affect soil carbon storage and decomposition.
   (c) How the quality (chemical composition) of plant litter can impact microbial decomposition.
2. Gain a better understanding of how microclimatic forcing can impact model results.
3. Contribute to bridging the gap between model requirements and measurements, by identifying key parameters and processes.

Paper I presents MIMICS+ as a useful tool to investigate soil processes and their responses to anthropogenic climate change. The paper describes how MIMICS+ is built on the existing microbially explicit model MIcrobial-MIneral Carbon Stabilization (MIMICS; Wieder et al., 2015) and extended with a nitrogen cycle, additional microbial groups, and vertical layers. In addition to microbial decomposers, we added mycorrhizal fungi, which form important but less understood symbiotic relationships with plants. In this paper, we also perform a nitrogen enrichment experiment to investigate below-ground responses to increased nutrient availability in Norwegian forest soils. In addition to the main objective, paper I addresses sub-objectives 1a, 1b, 2, and 3.

A key control of the carbon exchange between soils and the atmosphere is the microbial decomposition of plant litter. In paper II, MIMICS+ was used to simulate two litterbag decomposition experiments, both performed at high latitudes (Canada; Trofymow and CIDET Working Group (1998) and the Vestland Climate Grid (VCG) in Southern Norway; Vandvik et al., 2022) but with different durations and spatial scales, to examine how well the model reproduced the impact of climatic factors and litter quality on decomposition rates. We

[3]In this work "microbe-microbe interactions" mainly refer to interactions between saprotrophs and mycorrhizal fungi.

performed experiments using measurements of soil temperature and moisture for the Norwegian sites, as well as improved model surface parameters in the MIMICS+ simulations. In contrast to expectations, simulations using observed microclimate and/or improved surface parameters did not improve the modeled results, but rather highlighted several challenges connected to snow and freezing conditions when modeling microbial decomposition at high latitudes. Paper II addresses the main objective, and sub-objectives 1b, 1c, 2 and 3.

While paper II mainly investigated the role of saprotrophic decomposers, paper III focuses on the ectomycorrhizal fungi, and interactions between the saprotrophic and ectomycorrhizal pools. Observational evidence from boreal forests indicated that the proportion of ectomycorrhizal fungi compared to saprotrophic fungi is larger in reality than what is modeled with the MIMICS+ version presented in paper I. In paper III, we performed sensitivity tests of mycorrhizal turnover time to examine how model parameters can be modified to better represent observations at high latitudes. We also tested sensitivity to ectomycorrhizal necromass composition. We investigated the consequences for the rest of the modeled soil system, in particular how microbe-microbe interactions affected soil carbon storage. Paper III addresses sub-objective 1a and 3.

1.3 Thesis outline

Part I of this thesis is structured as follows: An overview of the scientific background relevant to the work in this thesis is given in Chapter 2. Chapter 3 describes the model development process of MIMICS+, as well as a description of how it uses CLM-produced forcing data. A summary of the scientific findings of the papers is found in Chapter 4, while conclusions and outlook are presented in Chapter 5. Part II contains the scientific papers.

Chapter 2

Background

This chapter first presents an introduction to the terrestrial cycling of carbon and nitrogen, and soil microbial processes (Section 2.1). Then, Land Surface Models (LSMs) and relevant sub-models within them, as well as microbially explicit soil models are presented (Section 2.2).

2.1 Terrestrial cycling of carbon and nitrogen

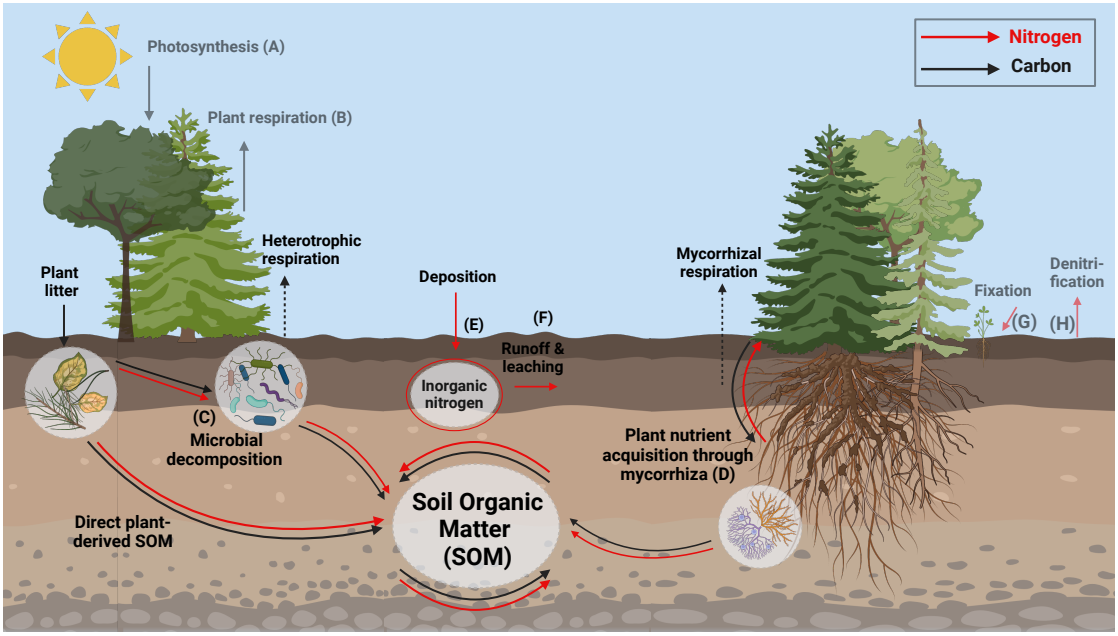

Figure 2.1: Simplified illustration of the terrestrial cycling of carbon (black) and nitrogen (red). Carbon is exchanged with the atmosphere through photosynthesis (A) and respiration by microbial decomposers, mycorrhizal fungi, and vegetation. Nitrogen is exchanged through atmospheric deposition (E), leaching (F), fixation (G), and denitrification (H). Within the soil, carbon and nitrogen is cycled between litter, microbial, SOM, and inorganic nitrogen pools. Processes in full colors are represented in MIMICS+, while processes in faded colors are not. Created with BioRender.com.

The main processes of the terrestrial carbon and nitrogen cycles are illustrated in Fig. 2.1. In the following text, letters in parenthesis correspond to letters in the figure. Through photosynthesis, plants transform atmospheric CO_2 into energy i.e. carbohydrates (A). The fate of the carbon assimilated through photosynthesis depends on how the plant allocates it to different processes. This is influenced by plant species and resource availability. At the ecosystem scale, photosynthesis can be approximated by Gross Primary Production (GPP) (Chapin et al., 2011). About half of GPP is used for plant respiration and will return relatively quickly to the atmosphere (Schlesinger and Bernhardt, 2013) (B). The remaining carbon (GPP minus respiration) makes up the Net Primary Production (NPP). Most NPP is allocated to plant biomass, which eventually will enter the soil as dead plant material (plant litter). Decomposers break down this material (C), and in the process release a fraction of the carbon back into the atmosphere as heterotrophic respiration. Plants also allocate a fraction of NPP to nutrient acquisition, either directly through roots or through symbiotic associations with mycorrhizal fungi (D).

Nitrogen and phosphorus are the two most important macronutrients in terrestrial ecosystems. Plants and soil organisms depend on these components to function properly, and competition for nutrients can limit productivity even if carbon is abundant (Chapin et al., 2011). Du et al. (2020) showed a strong latitudinal shift in the nutrient limitation of primary production, with a transition from phosphorus-limited in the tropics, to nitrogen-limited at higher latitudes. Since nitrogen is the most limiting nutrient at high latitudes, this work focuses on the role of nitrogen as a nutrient.

2.1.1 Plant litter

On top of the soils we find plant litter, which is dead plant material in various forms: leaves, twigs, branches, and dead roots. Litter from different species and parts of the plant vary widely in terms of nutrient content and chemical recalcitrance. Litter that can provide easily accessible resources to the microbes, either by consisting of easily degradable (metabolic) compounds or having a high nitrogen content is of "high quality". Recalcitrant litter, on the other hand, has a high amount of complex, organic compounds and/or low nitrogen content, and is considered to be of "poor quality". We can use the lignin content of litter to determine the chemical recalcitrance, while the carbon:nitrogen (C:N) ratio (stoichiometry) is often used to determine the litter nutrient content (Bardgett, 2005).

2.1.2 Soil Organic Matter

Soils consist of mineral material (sand, clay, silt, and inorganic compounds), plant roots, water, gases, and organic matter, and are thus complex, multiphased systems. Soils are also home to a vast variety of organisms, from microbes like bacteria and fungi, to macrofauna like earthworms and beetles (Bardgett, 2005).

The part of soils that holds the most carbon is SOM. Chapin et al. (2011) defines SOM as "Dead organic matter in the soil that has decomposed to the point that its original identity is uncertain". Advances in observational technologies have led to findings that challenge the traditional view of SOM as consisting mostly of stable, humic substances (Schmidt et al., 2011). The emergent understanding of SOM is that it consists of a continuum of organic compounds at different decomposition stages that can interact with other molecules in their environment (Lehmann and Kleber, 2015). These interactions can stabilize the SOM through mineral association and the formation of aggregates. Mineral-associated organic matter forms chemical bonds with mineral soil particles, which physicochemically protect the SOM from being decomposed by microbes. Aggregation formation between organic and mineral compounds makes the SOM less accessible to microbes, leading to a physical protection of the SOM molecules from microbial decomposition (Angst et al., 2021). The more "traditional" form of chemical protection based on recalcitrance of lignin-rich substances, also contributes to the protection of SOM from microbial decomposition.

2.1.3 Soil microbes

The global biomass of soil fungi and bacteria is estimated to be 12 GtC and 7 GtC, respectively, while soil animals only account for approximately 2 GtC, globally (Bar-On et al., 2018). These organisms greatly affect soil formation, composition, and dynamics. Since the vast majority of soil organisms are microscopic, MIMICS+ and many other soil models (Chandel et al., 2023) focus on microbial activity, but acknowledge that larger organisms also contribute to soil dynamics (Grandy et al., 2016).

Soil microbial biomass has a narrower and lower stoichiometrical constraint than the resources it consumes. Global averages suggest that microbial biomass has a carbon:nitrogen ratio of around 7:1, while plant litter and SOM have ratios of 71:1 and 17:1, respectively (Mooshammer et al., 2014). To keep a relatively constant C:N ratio, microbes can only invest a fraction of the carbon they take up in biomass production. The ratio of carbon invested in growth versus total carbon uptake is called Carbon Use Efficiency (CUE). Generally, different microbial groups have different stoichiometrical constraints and optimal CUEs, as described below.

Saprotrophic bacteria and fungi

The word *saprotroph* comes from Greek, and translates to "feeding on decaying matter". Saprotrophic bacteria and fungi acquire energy from dead organic material, and together they account for about 95 % of total decomposer biomass and respiration (Chapin et al., 2011). Although a myriad of different species exist within each of the groups, there are some general differences in the functioning of fungal versus bacterial decomposition, which is useful for simplifying microbial decomposition dynamics in a model.

Fungi produce networks of hyphae that can span vast areas, allowing the fungi to acquire carbon and nutrients at different locations. Fungal decomposers are often specialized in decomposing more recalcitrant substrates than bacterial

decomposers. This means that they often have slower decomposition rates, but higher CUE than bacterial decomposers (Chapin et al., 2011).

Bacteria can not spread out through hyphae in the same way, making them more dependent on carbon and nutrients in their immediate surroundings. Therefore, they are often more dominant in nutrient-rich environments, and nutrient hot-spots like the rhizosphere (close to plant roots). In general, they have a more opportunistic behavior than fungi, with higher decomposition rates but lower CUE (Chapin et al., 2011).

To break down complex organic matter into simpler molecules that the decomposers can assimilate and use, they produce extracellular enzymes that depolymerize the complex substrates. This process results in soluble products that can be used in the microbial metabolism (Chapin et al., 2011). The speed at which decomposers break down the substrates depends on climatic factors, like temperature and moisture. Generally, microbial decomposition rates increase with temperature. However, decomposition responses to changes in temperature are unclear, as there is evidence that microbial communities adapt to their environment, and therefore might respond differently than expected to changes in local temperature (German et al., 2012). When it comes to moisture, both too much and too little limits decomposition. The microbes are dependent on the diffusion of substrates towards them (or their enzymes). This diffusion is dependent on the presence of moisture films on the soil surfaces, which is reduced or removed under dry or freezing conditions. In the case of water-logged soils, microbes lose access to the oxygen needed for the metabolic process, and decomposition is inhibited.

Mycorrhizal fungi

The word *mycorrhiza* is also of Greek origin, and translates to "fungus-root". Mycorrhizal fungi forms symbiotic relationships with plants. The fungi receive carbon from the plant, and provide nutrients, like nitrogen and phosphorus, in return. In contrast to saprotrophs, the energy source for mycorrhizal fungi is fresh carbon from the plant, not dead plant material. Globally, it is estimated that 3.58 GtC is allocated from terrestrial plants to mycorrhizal fungi every year (Hawkins et al., 2023), and that plants allocate 4–20 % of NPP to mycorrhizal associations (Chapin et al., 2011).

The two main types of mycorrhiza are Arbuscular Mycorrhiza (AM) and ectomycorrhiza (EcM). 70 % of land plant species associate with AM, covering 57 % of global vegetation, while about 2 % associate with EcM, covering 25 % of global vegetation (Hawkins et al., 2023). Many boreal tree species, like spruces and pines associate with EcM, explaining the high land coverage compared to species association. While AM mostly scavenge for nutrients in inorganic forms, EcM have been found to depolymerize organic matter to access nutrients. Thus, EcM can indirectly contribute to decomposition by "mining" SOM for nitrogen (Lindahl and Tunlid, 2015).

Microbial interactions

Although the saprotrophic microbes and mycorrhizal fungi get their carbon from different sources, they compete for the same nitrogen. Competition between EcM fungi and saprotrophic fungi can introduce the so called Gadgil effect (Gadgil and Gadgil, 1971; Gadgil and Gadgil, 1975), where saprotrophic decomposition is suppressed because nitrogen are removed from SOM by EcM. The reduced decomposition leads to more carbon stored in the soils.

The presence of mycorrhiza can also promote saprotrophic decomposition through so-called priming effects, where provision of high quality substrates increase the saprotrophic decomposition rates. These substrates can be mycorrhizal necromass which have a relatively low C:N ratio (Phillips et al., 2012), or the release of easily decomposable enzymes (Kaiser et al., 2015). Both the Gadgil effect and priming effects are assumed to be context dependent, affcted by resource availability and climatic factors (Fernandez and Kennedy, 2016).

2.1.4 Climate change in high latitude ecosystems

It is well known that Arctic amplification causes Northern high latitudes to warm faster than the rest of the globe (Rantanen et al., 2022). According to Crowther et al. (2019) the highest abundances of both soil carbon and soil microbial biomass are found at these latitudes. Thus, the accelerated warming has the potential to cause large responses in biogeochemical cycles and the carbon-climate feedback. Thawing permafrost and related processes are also a considerable consequence of the increased warming, and much research has focused on this topic (e.g. Schädel et al., 2018; Miner et al., 2022; Smith et al., 2022). However, the general representation of soils in LSMs and ESMs should reflect an "average" soil, and not the special case of permafrost. Therefore, the focus in this thesis is on "regular soil" processes, that is, soils that experience seasonal or intermittent freezing. The presented model structure could also be well suited for modeling permafrost conditions, but that will need careful examination and likely changes to parameter values. In this section I will briefly introduce some mechanisms that are particularly relevant for these high-latitude soils.

Snow effects on soil temperature

In addition to being a source of soil water when melting, snow cover has an insulating effect on soil temperature, making snow a regulator of temperature and moisture dependent decomposition rates. When the soils freeze, the soil water will become unavailable to the microbes, which leads to reduced or halted decomposition.

Vegetation composition

Increased temperatures lead to longer growing seasons which again can cause vegetation shifts like shrubbification and tree line migration (Vowles and Björk, 2019; Hansson et al., 2021). These shifts also affect below-ground processes

by modifying the input rates of organic matter from plants. Since mycorrhizal associations are species-dependent, vegetation shifts might also cause shifts in dominant mycorrhizal association, however, the rates and consequences of this are still highly uncertain.

Nutrient availability

In boreal forests, the internal turnover of nitrogen, i.e., litterfall, plant uptake, and microbial mineralization and immobilization, is much larger than the external input and output (nitrogen fixation[1], deposition[2], leaching, and denitrification[3], (E), (F), (G), and (H) in Fig. 2.1). This means that the nitrogen cycle is relatively closed, and that the interactions between the living components of the ecosystems largely control the nitrogen dynamics (Högberg et al., 2017). Microbes and plants compete for the nitrogen resources in the soil, which is available in organic (SOM) and inorganic (NH_4 and NO_3) forms (Daly et al., 2021). Due to the limited amount of available nitrogen, these systems will likely respond with increased plant growth if nitrogen is added, either through increased atmospheric deposition, or for fertilization purposes (Högberg et al., 2017).

2.2 Land Surface Models (LSMs)

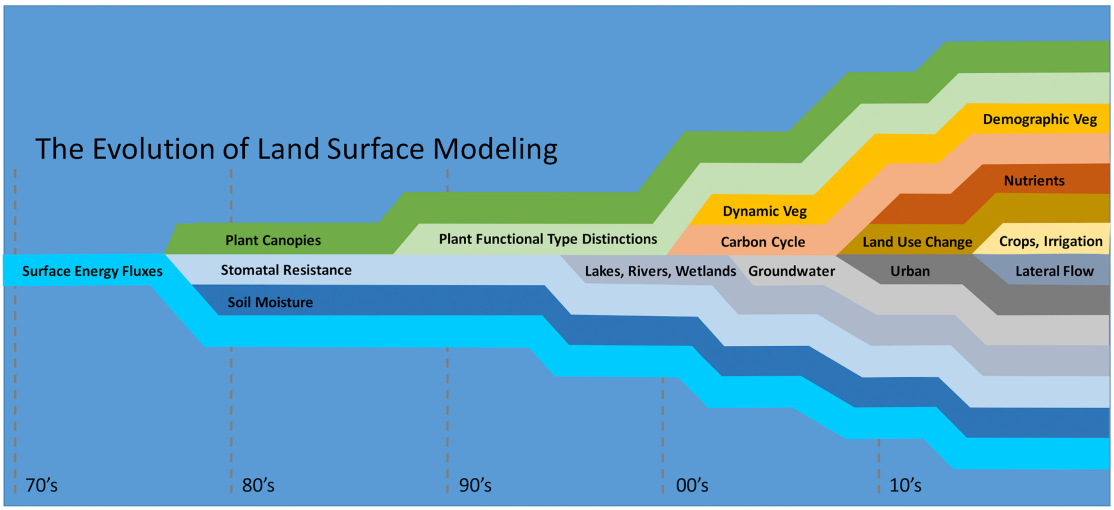

Figure 2.2: A schematic depiction of the evolution of land surface model process representation through time, representing the approximate timing of emergence of different model components as commonly employed features of Earth system models. Note that all modeling groups follow a different pathway and that this diagram is primarily intended to act as an illustration of increasing complexity through time. Adopted from Fisher and Koven (2020).

[1] conversion of N_2 gas to ammonium
[2] atmospheric input of nitrogen to the ecosystem
[3] conversion of NO_3 to gaseous forms

In an ESM, the Earth is divided into gridcells, in which mathematical equations are used to represent physical processes, timestep by timestep. The ESM combines sub-models that represent different parts of the Earth system, typically a land model, an ocean model, an atmosphere model, and ice models (at sea and on land). In a fully coupled ESM, LSM actively exchanges momentum, water, energy, carbon, and other compounds with the atmospheric ESM component. LSMs can also be used in "offline" mode, in which the atmospheric input comes from prescribed datasets containing surface temperature, precipitation, wind, solar radiation, and humidity. LSMs (and ESMs) can be run globally, regionally or as single-cell simulations.

Due to the complexity and heterogeneity of the processes presented in Section 2.1, representing them in a mechanistic modeling framework is a major challenge. Carbon cycle processes have only been a part of LSMs since the early 2000s, while nutrients (mainly in the form of nitrogen) are an even more recent addition (Fig 2.2, Fisher and Koven (2020)).

When LSMs are expanded with new features or processes, it is often done by developing and testing smaller, stand-alone process models which then can be incorporated into the larger modeling framework. This is the approach we, and several other research groups, are using to incorporate microbial activity into LSMs, and later into to fully coupled ESMs.

2.2.1 The Community Land Surface Model (CLM)

CLM constitutes the LSM of the Earth system models NorESM (Seland et al., 2020) and CESM (Danabasoglu et al., 2020). The primary processes and functionality of the current version of CLM (version 5, CLM5) are illustrated in Fig. 2.3. In CLM, the soil is represented as a column of discrete layers. The thickness of the layers increase exponentially with depth. The default model setup has 20 hydrologically and biogeochemically active layers, reaching a soil depth of 8.6 m (custom configurations allow shallower soils, see Section 3.1.6). This means that soil water, heat, carbon, and nitrogen can be transported up and down the soil column. Note that the discrete soil layers in CLM are not based on real-world soil horizons that are a consequence of soil formation processes. The soil column is connected to a vegetated land unit, where the vegetation is represented by one or more of 14 natural Plant Functional Types (PFTs, Fig. 2.4). The PFTs are broad representations of plant species that share functional features, e.g. "broadleaf deciduous boral tree" and "C3 nonarctic grass".

The processes illustrated in Fig. 2.3 are represented by many sub-models within CLM. Sections 2.2.2 and 2.2.3 give an overview of two of the sub-models used in CLM5: the microbially implicit CENTURY model and the FUN model. The CENTURY model traditionally has been used to represent soil decomposition in CLM and many other LSMs (Parton et al., 1988). The FUN model includes the current representation of mycorrhizal association in CLM5.

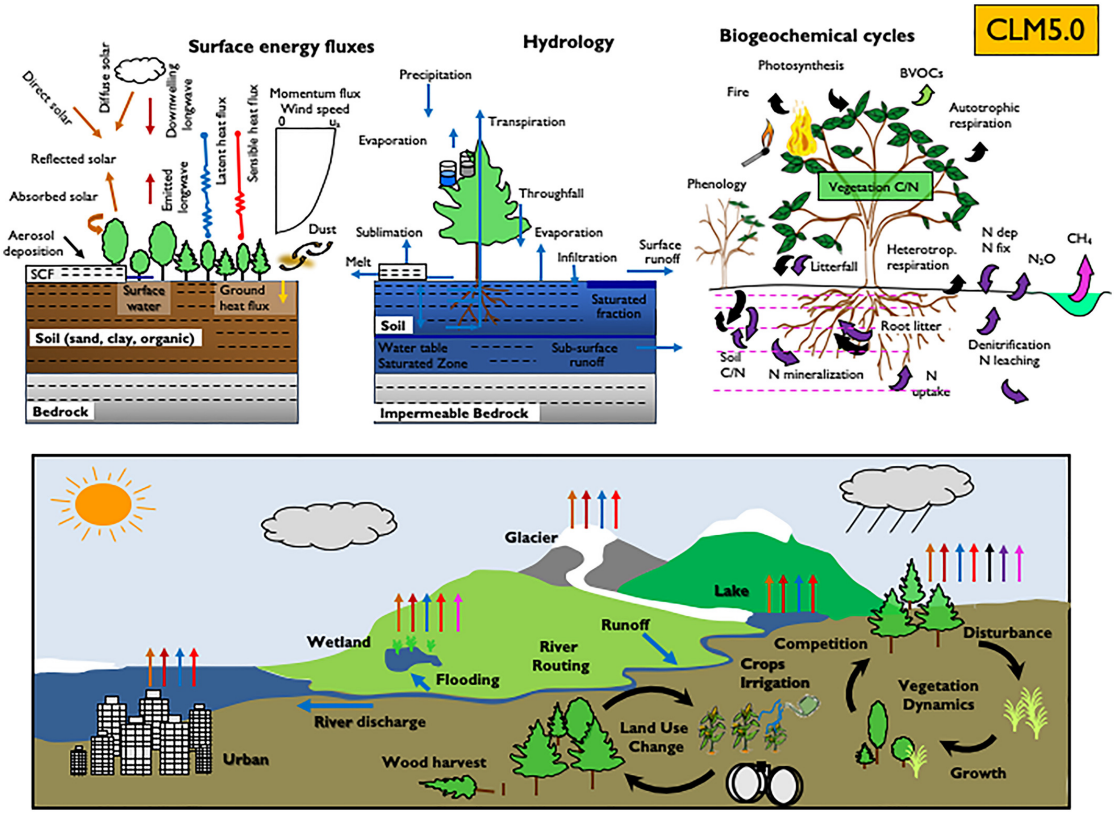

Figure 2.3: Schematic representation of primary processes and functionality in CLM5. SCF = snow cover fraction; BVOC = biogenic volatile organic compounds; C/N = carbon and nitrogen. For biogeochemical cycles, black arrow denotes carbon flux, and purple arrow denotes nitrogen flux. Note that not all soil levels are shown. Not all processes are depicted. Adopted from Lawrence et al. (2019).

.

2.2.2 The CENTURY decomposition model

The CENTURY model was developed by Parton et al. (1988), and has been used for representing decomposition in CLM4.5 and CLM5 (Lawrence et al., 2019). Here, fresh litter decomposes to more and more recalcitrant forms through a cascade of transformations from litter and coarse wood, to SOM pools (Fig. 2.5). During a transformation step, carbon is moved from a donor pool to a receiver pool determined by constant decomposition rates, and where constant fractions are lost to respiration. The decomposition rates can be modified by simple environmental modifiers, as well as nutrient limitations. These modifications are simple and general, and cannot capture shifts or changes in microbial communities as a response to climate change. Since there are no explicit microbial pools, the model assumes that microbial abundance will never limit decomposition rates. It also assumes that there is no competition or other interactions between different microbial groups that can affect the decomposition rates (Chandel et al., 2023).

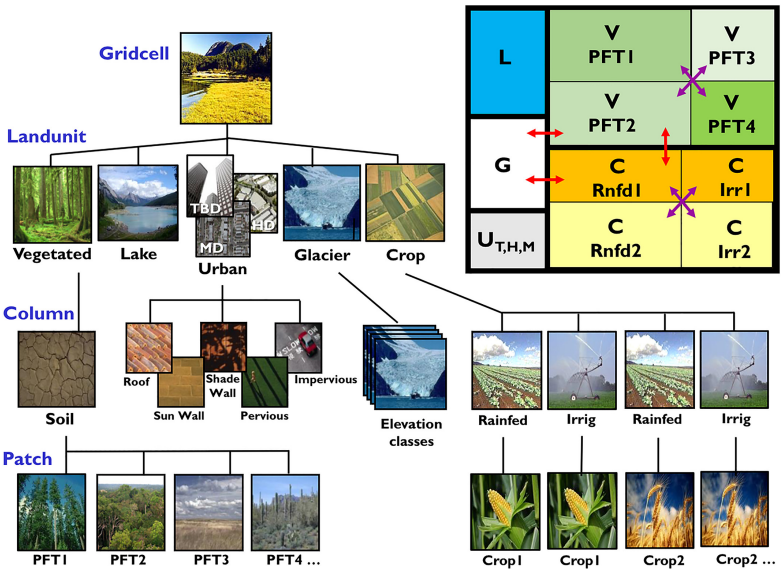

Figure 2.4: Configuration of the CLM subgrid hierarchy. Box in upper right shows hypothetical subgrid distribution for a single grid cell. Note that the Crop land unit is only used when the model is run with the crop model active. Abbreviations: TBD = Tall Building District; HD = High Density; MD = Medium Density, G = Glacier, L = Lake, U = Urban, C = Crop, V = Vegetated, PFT = Plant Functional Type, Irr = Irrigated, UIrr = Unirrigated. Red arrows indicate allowed land unit transitions. Purple arrows indicate allowed patch-level transitions. Adopted from Lawrence et al. (2019).

2.2.3 The FUN model

FUN stands for Fixation and Uptake of Nitrogen and calculates the carbon cost for plants to acquire nitrogen through different pathways. These pathways include passive uptake through fixating bacteria or retranslocation, and active uptake through EcM, AM, or directly through roots (Fisher et al., 2010; Brzostek et al., 2014; Shi et al., 2016). FUN moves nitrogen from the inorganic pools in the soil (i.e. not including EcM mining for organic nitrogen) into the plant pools. The carbon cost for this transfer is calculated as a function of plant root biomass and inorganic nitrogen availability. Since there are no explicit mycorrhizal pools represented in CLM, the carbon cost is assumed to immediately respire from the plant into the atmosphere, omitting an important mechanism for transferring organic carbon from plants into the soil. In Section 3.1.5 I explain how MIMICS+ brings this carbon into the soil through its mycorrhizal pools, thereby opening up for exploring processes related to mycorrhizal mining and turnover.

2.2.4 Microbially explicit soil models

To replace traditional, CENTURY-based soil models in ESMs, new microbially explicit models need to be formulated and tested before incorporation into a fully coupled system. A recent review by Chandel et al. (2023) showed that of 71 microbial models published since 1975, 58 of them were published between 2007 and 2022. This recent surge of interest in microbial models illustrates the increased

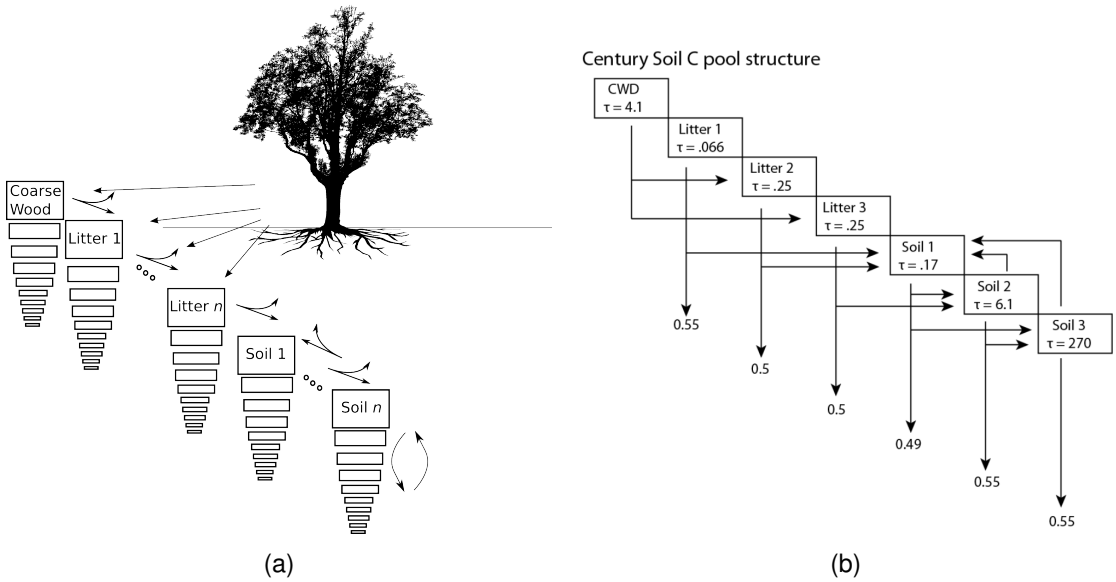

Figure 2.5: Illustrations of the CENTURY-based decomposition model used in CLM5. (a) Decomposition of coarse wood and litter leads to heterotrophic respiration and formation of SOM. Each decomposing carbon and nitrogen pool is defined at each soil vertical level, with vertical mixing within each pool. (b) Pool structure, transitions, respired fractions (numbers at end of arrows), and turnover times (numbers in boxes, in years) for the CENTURY soil carbon pool structure. Adopted from Koven et al. (2013).

awareness of the critical role of soil dynamics in terrestrial responses to climate change. There is a consensus among the models that microbes degrade complex substrates by producing extracellular enzymes that break down the substrate into compounds that can be used for microbial growth or respiration (Chandel et al., 2023). However, which processes are rate-determining, which pools are represented, and which parameters depend on biotic/abiotic factors, vary among the models. Some key differences in process representation are illustrated by Sulman et al. (2018) in Fig. 2.6. Choices about the kinetics that determine decomposition rates (yellow circles), abiotic controls of microbial turnover (blue squares), and explicit representation of enzymatic pools (brown triangles) can all fundamentally affect responses to climate change. The microbial models represent different hypotheses about the governing (nonlinear) processes which can lead to divergent model projections of for example total soil carbon (Wieder et al., 2017). When these soil sub-models are incorporated into ESMs, they will likely increase the spread among model projections even more. However, this is a necessary first step towards a better understanding of the structural uncertainty linked to the carbon-climate feedback (Bradford et al., 2016).

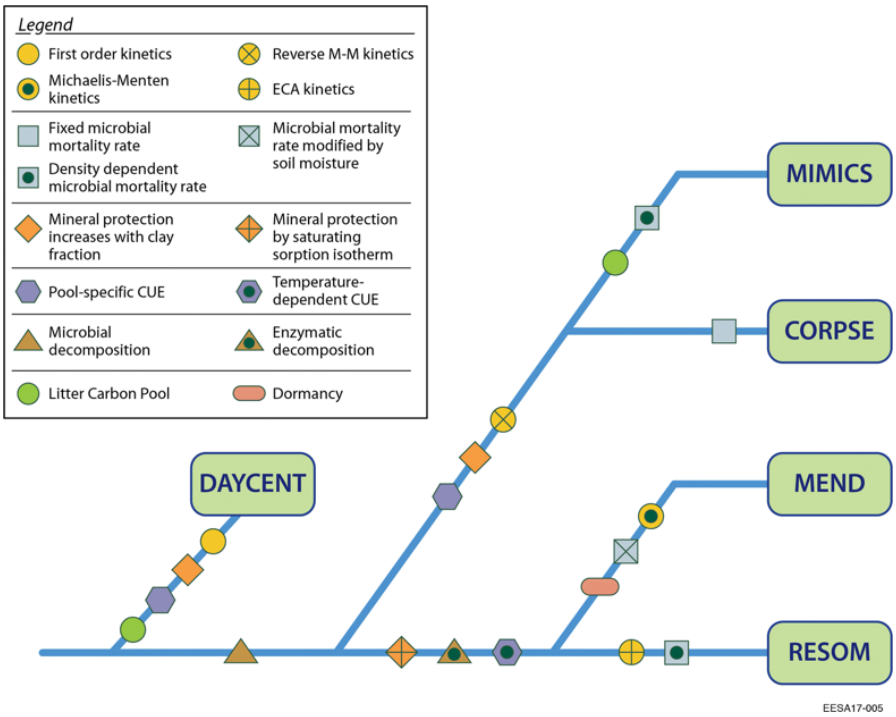

Figure 2.6: Microbially explicit models with different process representations. The models are arranged in a tree based on major differences in explicit process representation. Specific processes are indicated with symbols. Adopted from Sulman et al. (2018)

Chapter 3

Methods

The main tool in this thesis is the soil biogeochemistry model MIMICS+[1], which is described and applied in paper I, and applied in papers II and III. The model is an extension of the MIMICS model (Wieder et al., 2015), designed to be incorporated into CLM, but is used in an offline version in this thesis. This section will first describe the development process of MIMICS+, before giving an overview of the CLM simulations performed for this thesis. The CLM simulations have been used to produce input data for MIMICS+, as well as to provide soil carbon and nitrogen stocks for comparison in paper I.

3.1 Model development

As MIMICS+ is thoroughly described in paper I, the focus here is the development process and reasoning for choices made along the way. Tables with detailed information about equations and parameters are found in Appendix A of paper I.

3.1.1 From MIMICS to MIMICS+

Our point of departure for development of MIMICS+ was the carbon-only, single-layer version of the MIMICS model, developed by Wieder et al. (2015) (Fig. 3.7). To avoid confusion, this version will be referred to as MIMICS-Wieder hereafter. The model is microbially explicit, and puts particular emphasis on mineral-stabilization of SOM which incorporates the emergent view of SOM as a continuum of progressively decomposing organic compounds (Lehmann and Kleber, 2015). As discussed in Section 2.2.4, a range of microbially explicit models with different features and process representations exist. The structure of MIMICS-Wieder allowed for modifications suitable for our purposes, and was particularly attractive since the goal was incorporation of the framework into CLM, which is the land model used in NorESM. I will first describe the pools and processes that are shared between the two model formulations, before giving an overview of the expansions and modifications that were done to the modeling framework to get to MIMICS+.

[1]Github repository for the model code, written in Fortran90: https://github.com/ecaas/MIMICSplus

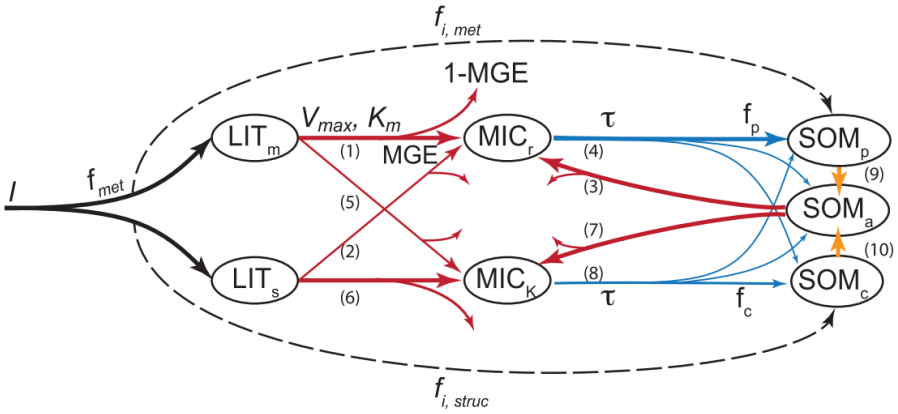

Figure 3.7: Soil C pools and fluxes represented in MIMICS. Litter inputs (I) are partitioned into metabolic and structural litter pools (LIT_m and LIT_s) based on litter quality (f_{met}). Decomposition of litter and available SOM pools (SOM_a) are governed by temperature sensitive Michaelis–Menten kinetics (V_{max} and K_m), red lines. Microbial growth efficiency (MGE) determines the partitioning of C fluxes entering microbial biomass pools vs. heterotrophic respiration. Turnover of the microbial biomass (τ, blue) depends on microbial functional type (MIC_r and MIC_K), and is partitioned into available, physically protected, and chemically recalcitrant SOM pools (SOM_a, SOM_p, SOM_c, respectively). Bracket numbers correspond to the equations for fluxes described in Appendix A1 in (Wieder et al., 2015). The definition and values of parameters are included in Table B1 in (Wieder et al., 2015). Adopted from Wieder et al. (2015).

Both models include two litter pools, two decomposing microbial pools and three SOM pools, of which only one is available for microbial decomposition (Fig. 3.7, Fig. 3.8). Incoming litter is partitioned between a structural and a metabolic pool based on the calculated metabolic fraction, f_{met}, which is a function of the lignin:N ratio of the litter (see Table A5 in paper I). Lignin-rich litter is recalcitrant (structural) and takes longer to decompose, which is reflected in the lower base decomposition rates of the structural litter pool (LITs) than the metabolic litter pool (LITm). A fraction of the incoming litter is transferred directly to the protected SOM pools to represent mechanisms that convert litter to SOM without going through the microbial pathway (direct plant-derived SOM).

In MIMICS-Wieder the two microbial pools are named MIC_r and MIC_k, and represent two functional trait groups; opportunistic, fast-growing r-strategists, and slower-growing k-strategists (Wieder et al., 2014). This divides the microbes into ecologically meaningful groups, however, these groups are difficult to measure, and direct comparisons between modeled and observed quantities are therefore difficult. An alternative way of dividing the microbial groups into two observable categories is to use the two major decomposer groups; bacteria and fungi (Strickland and Rousk, 2010). In MIMICS+ we therefore chose to separate the decomposing microbes into saprotrophic bacteria (SAPb) and saprotrophic fungi (SAPf). As mentioned in Section 2.1.3, bacteria are generally more opportunistic than fungi, hence our SAPb and SAPf pools are in many ways comparable to MIC_r and MIC_k in MIMICS-Wieder, respectively.

The MIMICS framework uses either forward (Wieder et al., 2015) or

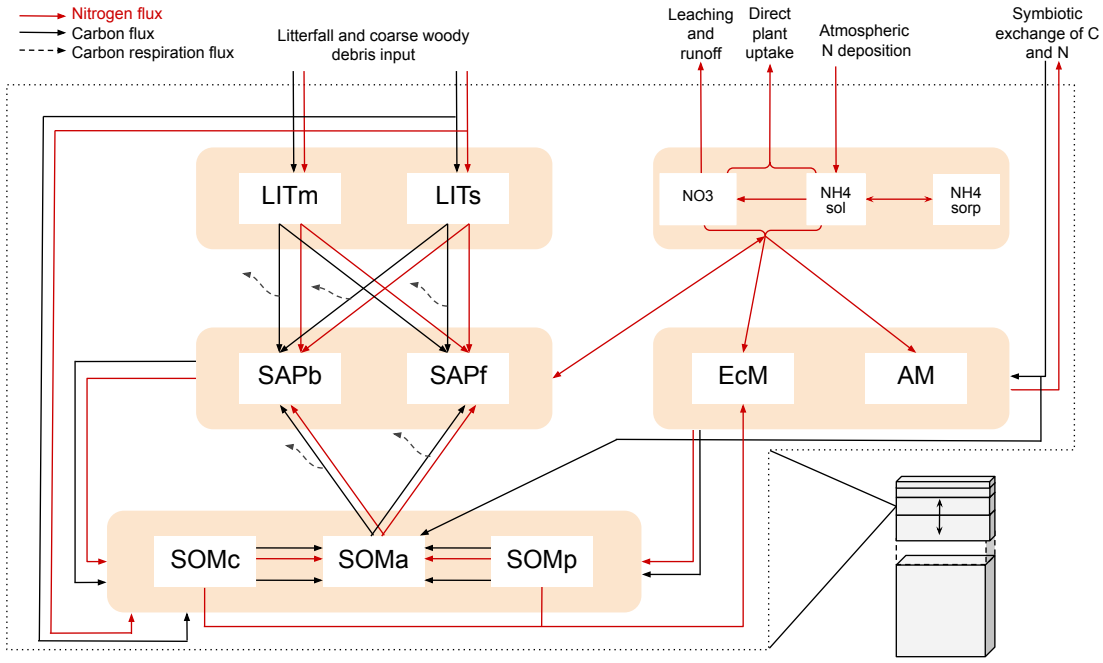

Figure 3.8: Schematic of the MIMICS+ structure, showing C and N flows within each layer of the model. Black arrows indicate carbon fluxes ($gCm^{-3}h^{-1}$) while red arrows indicate nitrogen fluxes ($gNm^{-3}h^{-1}$). The dashed black arrows symbolize C leaving the system as heterotrophic respiration. LITm, LITs: metabolic and structural litter. SAPb, SAPf: saprotrophic bacteria and fungi. EcM, AM: ecto- and arbuscular mycorrhizal fungi. SOMc, SOMa, SOMp: chemically protected, available and physically protected soil organic matter. NO_3, $NH4_{sol}$, $NH4_{sorp}$: Inorganic N in the form of NO_3, NH_4 in solution and NH_4 sorbed to particles, respectively. Adopted from Aas et al. (2024).

reverse (Wieder et al., 2017) Michaelis Menten Kinetics (MMK) to determine decomposition rates. Both approaches are nonlinear, as they are dependent on the amount of both substrates and microbial exoenzymes. While forward MMK depends linearly on the concentration of enzymes and nonlinearly on the substrate, reverse MMK assumes that soil carbon decomposition depends nonlinearly on enzyme concentration and linearly on substrate concentration (Wang et al., 2016). The reverse and forward MMK kinetics are derived based on exoenzyme concentration, not microbial biomass concentration. In the MIMICS-based models, there are no explicit enzyme pools and they therefore rely on the assumption that exoenzyme production linearly depends on microbial biomass (Chandel et al., 2023). It has been shown that forward MMK may be more prone to oscillatory model behavior (Wang et al., 2016). The MIMICS-Wieder version that is currently being implemented into CLM uses reverse MMK, and we therefore decided to use the same in MIMICS+. The general form of the decomposition rates, F ($gC \cdot m^{-2} \cdot h^{-1}$), using reverse MMK, and described in terms of MIMICS+ pools can be written as

$$F_{SUB,SAP} = CUE \cdot \frac{V_{max}(T,\Theta) \cdot SAP \cdot SUB}{K_m(T) + SAP} \tag{3.1}$$

where SUB is substrate (LITm, LITs or SOMa in Fig. 3.8), SAP is saprotrophic group (SAPb or SAPf in Fig. 3.8), CUE is the carbon use efficiency, V_{max} is the temperature (T) and moisture (Θ) dependent MMK maximum reaction velocity, and K_m is a temperature dependent MMK half-saturation constant. The MMK parameters are exponential functions of temperature based on German et al. (2012), while the moisture dependence of V_{max} is represented by a unimodal function of soil water, also used by Wieder et al. (2017) and Sulman et al. (2014) (see Table A5 in paper I for parameters and functions).

During the decomposition process a fraction of carbon, determined by the CUE, goes into the microbial pools (biomass growth), while the rest is respired out of the system (heterotrophic respiration). In MIMICS+ the CUE varies with nutrient availability, further described in Section 3.1.4 here, and in Section 2.1.2 of paper I.

In both model versions, dead microbial biomass is distributed among all three SOM pools. SOM moves from the physically and chemically protected pools to the available pool through desorption and depolymerization, respectively.

Based on insights gained during the model development process and from other studies, some key parameter values were changed to better represent the boreal ecosystems that are the focus in this thesis. These are described in Sections 3.1.2 and 3.1.3.

3.1.2 The direct plant-derived fraction

In Wieder et al. (2015), 5 % of the structural and metabolic litter input was directly transferred to SOMc and SOMp, respectively. In a version of the model including a nitrogen cycle (MIMICS-CN), Kyker-Snowman et al. (2020) increased the fraction of structural litter going to SOMc to 30 % to produce reasonable values

of total SOM C:N ratio. When plant litter is converted to SOM by going through the microbial decomposition process, the C:N ratio of the resulting SOM is much lower than the C:N ratio of the original plant litter due to the strict stoichiometrical constraint on the saprotrophs. However, if plant litter is converted to SOM directly (direct-sorption pathway; Sokol et al. (2019)) the C:N ratio of the resulting SOM will still be high. How much of SOM is going through the direct plant-derived pathway versus the microbial pathway is uncertain, but recent evidence indicate that forest soils and podzols have a high fraction of direct plant-derived SOM (Angst et al., 2021; Whalen et al., 2022). These soils are common in boreal areas, and total SOM C:N ratio can be high compared to global values, as illustrated by the soil profile data from Strand et al. (2016) which was used in Paper I. We therefore decided to increase the direct plant-derived fraction to 50 % for both structural and metabolic litter, which allows for higher values, and a broader range of total soil C:N in the model (Paper I).

3.1.3 Desorption parameter

In the MIMICS framework, SOM moves from the protected pools to the available pool but not the other way around. The rates at which SOM is made available for microbial decomposition (and thereby removal of carbon by respiration) therefore largely controls the soil carbon storage capacity. In MIMICS, the desorption rate, which moves carbon and nitrogen from SOMp to SOMa, is a function of clay content. Compared to MIMICS-CN (Kyker-Snowman et al., 2020) we doubled the desorption coefficient, but this is still one order of magnitude lower than the value that was used in the carbon-only version of MIMICS (Wieder et al., 2015). In the above-mentioned studies and in this work, this parameter has been adjusted to match observed data.

3.1.4 Addition of a nitrogen cycle

As described in Section 2.1.4, boreal soils are often nutrient-poor, and competition for nutrients among microbes, and between plants and microbes is expected to impact soil dynamics. To capture interactions among the different microbial groups, we decided to expand the model with a nitrogen cycle. This was done by adding parallel nitrogen pools to the existing carbon pools, as well as adding three inorganic nitrogen pools; NO_3 (dissolved), NH_4 (dissolved) and NH_4 (sorbed). The C:N ratio of the litter and SOM pools are determined by their input and are therefore variable, while the microbial pools have constant stoichiometrical demands causing them to reduce their CUE if there is a shortage of nitrogen in the system. Adding nitrogen pools parallel to carbon pools is common also in other models, like CLM and the MIMICS-CN model established by Kyker-Snowman et al. (2020).

A novelty in MIMICS+ is the representation of the inorganic N pools. NH_4^+ ions can be adsorbed or absorbed by soil particles (often clay particles), which can make them less available for uptake (by microbes or plant roots) than NH_4 or NO_3 available in the soil solution (Nieder et al., 2011). While in this "sorbed"

state, the nitrogen is also protected from leaching and runoff processes, and can thus work as a long term supply that slowly releases nutrients into a soluble, more accessible form.

For the conversion of ammonium between sorbed and dissolved pools we developed an algorithm based on work by Sieczka and Koda (2016) which uses a Langmuir isotherm to determine the equilibrium fraction between the $NH4_{sol}$ and $NH4_{sorp}$. The equilibrium fraction is calculated at every timestep, and NH4 is moved to or from the "sorbed" pool depending on the equilibrium status. Detailed equations for this mechanism is found in Section 2.1.3 of paper I. Sieczka and Koda (2016) studied agricultural soils, and the parameter values derived from there might not be the best fit for natural soils. However, the current implementation of the process in MIMICS+ serves as a starting point that can be further refined in the future.

Nitrification of $NH4_{sol}$ to NO3 is modeled based on the same algorithm that is used in CLM which again is based on work by Parton et al. (1996), Parton et al. (2001), and Del Grosso et al. (2000).

The input of nitrogen to the model comes from plant litter (added to the litter pools) and nitrogen deposition (added to $NH4_{sol}$), while it is lost through leaching of NO_3 and through the mycorrhizal exchange.

3.1.5 Addition of mycorrhizal fungi

As the objective was to incorporate processes that are important in boreal ecosystems, including mycorrhizal fungi was a natural choice. As described in Section 2.1.3, the main types are AM and EcM, which are also most commonly represented in models. Another type, that associates with many shrub-, and dwarf shrub species is ericoid mycorrhiza. In early model formulations of MIMICS+ we also included an ericoid mycorrhizal pool, as it is relevant for vegetation changes in boreal regions (Vowles and Björk, 2019). However, as there are limited observations to inform model parameterizations, and the complexity of the model already was quite high, we decided to leave it out for the MIMICS+ version presented in this thesis. As more observations become available, the code allows for extending the model with an ericoid pool in the future.

Each PFT from CLM associates with EcM, AM or a combination. The plant cost function for uptake of nitrogen through the mycorrhizal pathway in FUN (Section 2.2.3) is specific to each association. Within the CORPSE model framework, Sulman et al. (2019) have developed a method for calculating plant allocation of carbon to symbiotic associations dynamically via a Return Of Investment function (ROI). To be able to capture shifts in plant carbon allocation if above- and/or belowground species shift, MIMICS+ uses the ROI method from Sulman et al. (2019) to determine how much of the allocated carbon from CLM (see Section 3.2) is transferred to EcM versus AM, independent of the type of PFT (see Eq. (8) and (9) in paper I). When MIMICS+ is coupled to vegetation this structure allows for experiments on vegetation shifts promoted by belowground conditions and vice versa.

Although Sulman et al. (2019) represent EcM mining within their modeling framework, it is not particularly designed for boreal systems. Therefore, we turned to Baskaran et al. (2017) for determination of mining rates. Based on the "mycorrhizal decomposition theory" that EcM contributes to the decomposition process when mining for organic nitrogen (Lindahl and Tunlid, 2015), they presented a model where EcM "decomposition" was modeled as a multiplicative function of EcM biomass and SOM. For MIMICS+ we adapted this theory by using the multiplicative function to represent carbon fluxes from the protected SOM pools to SOMa. Based on the C:N ratio in the protected pools, the associated nitrogen from this calculation is transferred to the EcM pool. To represent the enzymatic cost of the mining process, a fraction of the carbon allocated to EcM from plants is directly transferred to the SOMa pool. In addition to the mining, EcM can also get nitrogen from the available inorganic nitrogen pools, NO3 and $NH4_{sol}$. The AM pool is only acquiring nitrogen from the inorganic nitrogen pools, giving EcM a competitive advantage over AM in the model when the soils are nutrient poor. Both mycorrhizal pools are assumed to have a constant C:N ratio of 20, and the surplus of acquired nitrogen is transferred to the plant (out of the system in this uncoupled model setup). Mortality is modeled as a first order loss from the mycorrhizal pools, and the dead mycorrhizal biomass is divided between the three SOM pools.

3.1.6 Addition of vertical layers

To facilitate future incorporation into CLM, MIMICS+ soil layers follow the same structure, with increasing layer thickness with depth. In a default CLM setup there are 20 biochemically active layers. However, it is possible to specify depth-to-bedrock, either with the default dataset (Pelletier et al., 2016), or user-specified custom values. In this thesis, we specified the depth-to-bedrock to the Pelletier et al. (2016) dataset (except for the VCG simulations in paper II, in which we set depth-to-bedrock as shallow as possible, which is 40 cm). Therefore, the number of MIMICS+ layers are determined by the number of active layers in the CLM simulations. In MIMICS+, the fluxes between the pools in the same layer are calculated first, then the vertical transport is determined using a diffusion equation from Soetaert and Herman (2009). The diffusion transports carbon and nitrogen towards layers with lower concentrations within a pool. This means that the model structure does not capture fungal growth towards nutrient-rich areas, or horizontal growth.

3.1.7 Parameter choices and calibration

MIMICS+ is an expanded version of MIMICS-Wieder, but a formal re-calibration has not been done. With a few exceptions, most parameter values were kept the same as they were in their original versions (Wieder et al., 2015; Kyker-Snowman et al., 2020; Baskaran et al., 2017; Sulman et al., 2019; Sieczka and Koda, 2016). The exceptions include the direct plant-derived fraction (Section 3.1.2), the desorption parameter value (Section 3.1.3), an increase of the mycorrhizal mining rate value

(K_{MO} in Table A5, paper I) compared to Baskaran et al., 2017, and an increase in V_{max} for saprotrophic fungi decomposing structural litter (compared to the value for k-strategist decomposition of structural litter in MIMICS, Wieder et al., 2015). The model setup and parameter choices produced carbon stocks and C:N ratio values comparable to measured values from soil profiles from Norwegian forests (Strand et al., 2016), as well as reasonable values for microbial percentage (1–3 % Frey, 2019), see paper I. Based on this, we deemed the model suitable to represent boreal conditions. However, we cannot rule out that some model prediction error is caused by poorly fitted parameter values within the new model framework.

3.1.8 Limitations

Like all models, MIMICS+ has limitations and shortcomings. By extending the MIMICS-Wieder framework with additional processes, we also introduced many new parameters, some of which are poorly constrained by observations. The increased complexity can make it challenging to interpret model results, and whether we get the right answer for the right reason. The lack of a plant pool has limited our opportunity to investigate plant-microbe interactions. However, additional pools would further increase the model complexity. As the intention of MIMICS+ is to be coupled to CLM (which includes vegetation), we decided to focus on the soil dynamics and microbe-microbe interactions in this work. Further limitations of the model are discussed in Chapter 5.

3.2 Input data from CLM

As the MIMICS+ version is offline, i.e. not coupled to an LSM, it needs input of litter, carbon allocated to mycorrhiza, and nitrogen deposition. Since some of the fluxes are dependent on temperature, moisture, and clay content, the model also needs this environmental information as input data. During the work with this thesis I have used CLM5 in single-site mode to produce the required input data for MIMICS+. A full list of all the CLM variables used as input is found in Table A6 in the Appendix of paper I. I have also used the soil carbon content from CLM simulations (which are calculated using the CENTURY approach) for comparisons in paper I. I will here briefly explain the setup and the atmospheric forcing used in the CLM simulations.

For the single-site simulations in this work, we have set the land unit to be 100 % vegetated. Except for the simulations of the VCG sites in paper II, the composition of PFTs is determined by the default present-day dataset used in CLM. For the VCG sites, we also ran simulations where the vegetation cover was set to 100 % C3 grass (see Table D3 in paper II).

The above-ground composition of PFTs share the same soil column (see Fig. 2.4). Each of the 14 natural PFTs in CLM has a prescribed association to either EcM or AM[2] (Shi et al., 2016). The plant root profile is determined by the

[2]except for the PFT "broadleaf deciduous temperate tree", which associates 50/50 with the two mycorrhizal types

PFTs, so the PFT distribution therefore determines the carbon cost of nitrogen acquisition through FUN (which is a function of root biomass). A bug related to the calculation of this cost was discovered during the work with paper III, this is described in Section 3.2.2. The total cost of active uptake of nitrogen by plants calculated by FUN (which in CLM is lost to respiration) is transferred to the mycorrhizal pools in MIMICS+. The partitioning between EcM and AM is determined by the ROI function in MIMICS+, so the division between the two pools in MIMICS+ is independent of the prescribed associations in CLM (although the CLM associations affect the amount of carbon that is directed to mycorrhizal uptake).

3.2.1 CLM atmospheric forcing

When CLM is run as a stand-alone model, it needs prescribed atmospheric forcing (air temperature, precipitation, wind, humidity, surface pressure, and downwelling short- and longwave radiation). For papers I and III we used the default atmospheric forcing dataset for CLM, the Global Soil Wetness Project 3 version 1 (GSWP3v1, https://hydro.iis.u-tokyo.ac.jp/GSWP3), which has a spatial resolution of 0.5° x 0.5° and a temporal resolution of three hours. The coarse resolution of this dataset inevitably contributes to discrepancies between observations and model results. The GSWP3v1 dataset only runs through the year 2014. As the VCG experiments in paper II were performed in 2016/2017 we used the alternative forcing data from COSMO-REA6 which has a spatial resolution of 6 km (Bollmeyer et al., 2015). The higher spatial resolution should make this dataset more suitable for modeling site simulations. However, it has been shown that CLM forced with either GSWP3v1 or COSMO-REA6 forcing can give inaccurate representations of snow depth at high latitudes (Lambert, 2022).

3.2.2 Mycorrhizal carbon allocation issue

During the work with paper III, I discovered an issue related to the cost functions that determine the amount of carbon the plant uses for uptake of nitrogen through mycorrhiza in CLM (determined by the FUN model). Due to a mix-up of names in the parameter file of CLM, too much carbon was allocated to the pathway "direct root uptake" compared to mycorrhizal uptake. I addressed this issue on the CLM Github page[3], which is used to maintain the model. The collaborative efforts that followed proved to be a great example of how the community approach can benefit model development. The issue turned out to have a relatively small impact on CLM results, as all of this carbon is directly respired to the atmosphere in CLM. However, for MIMICS+ this had large consequences as the modeled mycorrhizal biomass became very low due to the low input rates of carbon. CLM test simulations with the corrected setup indicated a slight increase in total cost of active nitrogen uptake, and that the majority of the cost was allocated to mycorrhizal uptake. For all three papers it was decided to run the MIMICS+ simulations again using the total amount of carbon allocated to active uptake (i.e.

[3]https://github.com/ESCOMP/CTSM/issues/2120

mycorrhizal uptake and direct root-uptake) from the original CLM simulations as input to the mycorrhizal pool. This assumes that the allocation to direct root-uptake is a small fraction of the total carbon allocated to active uptake in CLM.

Chapter 4

Presentation of findings

4.1 Paper I: Modeling boreal forest soil dynamics with the microbially explicit soil model MIMICS+ (v1.0)

Objectives

- Present and evaluate MIMICS+, a microbially explicit soil biogeochemical model which is capable of representing processes relevant to boreal ecosystems but is also general enough to be incorporated into an ESM.

- Evaluate model performance and model structure by comparing simulated vertical soil carbon content along a climatic gradient with observations and simulated soil carbon from the microbially implicit model CLM5.

- Investigate below-ground responses to nutrient changes by performing a nitrogen enrichment experiment using MIMICS+.

Summary

This model description paper introduces MIMICS+ and describes how the MIMICS-Wieder framework (Wieder et al., 2015) have been expanded with mycorrhizal pools, a nitrogen cycle, and vertical layers. It provides detailed descriptions of the structure and parameter choices of the model. To evaluate MIMICS+, soil carbon and nitrogen content are compared to observed soil profiles from Norwegian forests (Strand et al., 2016) and carbon and nitrogen content from CLM simulations. The paper also presents a deeper analysis of the results from MIMICS+, including how carbon is distributed between the different pools, and correlations between various variables. An idealized nitrogen enrichment experiment is also presented.

Main findings

- MIMICS+ performed better or on par with the state-of-the art land surface model CLM5 when compared to 50 podzolic forested sites in Norway.
- Site-to-site correlation with the observations gave poor results for both models, which illustrates the challenge of modeling processes that happen on a subgrid scale, and are thus not captured by the model. Inaccuracies in the coarse-resolution atmospheric forcing are likely also a contributing factor.
- SOM C:N ratios modeled with MIMICS+ matched observations significantly better than CLM5. This is largely explained by a high fraction of direct plant-derived input to SOM.
- The percentage of microbes in the soil modeled by MIMICS+ agreed with literature values. Saprotrophic fungi (SAPf) was the largest microbial pool in the model, giving a high fungal:bacterial ratio.
- Both models gave higher values of total soil carbon for the warmer half of the sites compared to the colder half of the sites, in line with the observations. Both models predicted more carbon at sites with lower mean annual precipitation than sites with higher mean annual precipitation, while the observations indicate the opposite.
- The results indicated that plant productivity drives total soil carbon in these Norwegian forest soils, as there was a strong positive correlation between litter input and total soil carbon.
- The nitrogen enrichment experiment showed relatively large responses in belowground dynamics, but a small effect on overall carbon storage and respiration.

Main conclusion

MIMICS+, with a framework specifically designed to represent high-latitudes, was presented to be a useful contribution to the existing family of microbially explicit models. The analysis indicated that the direct plant-derived fraction of SOM is an important parameter to reproduce observed C:N ratios at the sites. MIMICS+ can be used to further investigate microbe-microbe relationships and, when coupled to a vegetation model, also plant-microbe interactions.

Author contribution

I was responsible for the MIMICS+ model development with help from co-authors and other colleagues. I wrote the MIMICS+ model code and ran the CLM simulations used in the study. I performed the analyses and interpreted the results in collaboration with the co-authors. I also wrote the original paper draft and finalized the manuscript with contributions from the co-authors.

4.2 Paper II: Implications of climate and litter quality for simulations of litterbag decomposition at high latitudes

Objectives

In this paper we investigated three research questions formulated as hypotheses related to microbial decomposition:

- Is the model able to distinguish observed effects of climate and litter quality on mass loss from litterbags? (Hypothesis 1: The model adequately captures observed patterns in mass loss in terms of climate and litter quality.)

- Does MIMICS+ reproduce observed dominating controls on decomposition on short timescales, where litter quality is expected to dominate, and longer timescales, where climate is expected to dominate? (Hypothesis 2: MIMICS+ includes processes thought to be governing on short (12 months) and longer (6 years) timescales, and should capture the evolution of dominating controls on decomposition.)

- Will using improved input data for microclimate improve mass loss predictions with MIMICS+ compared to using default CLM-produced microclimate? (Hypothesis 3: An improved microclimate from observations or site-specific land model configurations improves model predictions of litterbag mass loss.)

Summary

Litterbag decomposition studies are often used to inform or validate decomposition models. The spatial and temporal scales of these experiments do not match the spatial and temporal scales of the models they are used in, and we therefore wanted to investigate consequences using MIMICS+. This was done by replicating litterbag experiments performed in Canada (CIDET; Trofymow and CIDET Working Group, 1998) and Southern Norway (VCG; Vandvik et al., 2022). Figure A1 in paper II shows a map of the sites. The CIDET experiments investigate decomposition of a range of different plant litter types at sites spread across Canada on a relatively long temporal scale (for this paper we used data from three and six years after litterbag burial). The VCG experiment was a one-year study where native litter was buried at sites in Southern Norway with differences in mean annual temperature and precipitation. By testing hypotheses 1 and 2 above we explored if the model could reproduce observed controls on litterbag mass loss. For the VCG sites, CLM simulations with a different configuration, as well as site-specific surface data and measurements of soil microclimate were available. This data provided an opportunity to explore how differently derived input data affected model results (hypothesis 3).

Main findings

- MIMICS+ reproduced mass loss within the observed variation for 12 of the 18 observational points, and broadly captured mass loss ranking among litter types at the CIDET sites.
- Considering the influence of litter quality on mass loss: The metabolic fraction of the litter (i.e. how recalcitrant it is) had a larger and more immediate effect on modeled mass loss than the C:N ratio. Comparison with the observational data indicates that the calculation of the metabolic fraction used in the model might put too much emphasis on the nitrogen content compared to the lignin content of the litter.
- The model performs better on longer timescales ($>$ 1 year) where climatic controls are assumed to dominate mass loss rates, and showed weaker than expected (based on literature) control of litter quality on short time scales ($<$ 1 year). This might be related to inadequate representation of leaching from litter in the model.
- The model gave more variable results for the VCG sites than for the CIDET sites. Using measured and site-specific model-derived microclimatic input data did not improve modeled predictions of mass loss at the VCG sites. Challenges related to local features at the sites and the effect of snow on soil temperature and moisture conditions are believed to contribute to the discrepancy.

Main conclusion

Broad-scale controls of mass loss were captured for the simulations of the CIDET sites, in line with hypothesis 1. Hypothesis 2 was partly proven, as the climatic control on mass loss was identified on a longer time scale, but the control of litter quality on short time scales was smaller than expected. Using observed or site-specific input data did not improve model predictions compared to the default CLM microclimate, and hypothesis 3 was thus not proven but opened for investigations into possible causes. More information about the microbial community, like biomass amount and stoichiometry would provide insights into whether the modeled microbial community is actually representative of the real decomposers. A measure of how much of the mass loss can be attributed to leaching can help interpreting the observations. As frozen soil conditions had a large impact on modeled mass loss, the representation of snow in LSMs will impact the decomposition process belowground.

Author contribution

I designed the study, performed the MIMICS+ simulations and ran all CLM simulations except the "SP" data which was ran by Hui Tang. I wrote the manuscript with contributions from the co-authors.

4.3 Paper III: Ectomycorrhizal turnover times affect soil dynamics in boreal ecosystems; A model study

Objectives

The objective of the study was to test model sensitivity to EcM turnover time and necromass composition, and examine the effects on the rest of the soil system, specifically microbial interactions and carbon storage.

Summary

The results from paper I showed that saprotrophic fungi were the largest contributor to the modeled microbial biomass. Observational studies from Swedish forests suggest that the amount of EcM could be comparable to, or even higher than saprotrophic fungi in these systems. The amount of EcM biomass is partly determined by the turnover time (the lifetime of living biomass in the EcM pool), which is a poorly constrained parameter in the model. We defined a set of plausible turnover times based on a combination of estimates from field data and CLM simulations. These turned out to be longer than the values often used in mechanistic models, giving higher values of EcM biomass. The calculated turnover rates were used to run a series of simulations with MIMICS+ at the same Norwegian podzolic sites as in paper I (Strand et al., 2016), to investigate the consequences of the increased EcM biomass for the rest of the soil dynamics. As recent observational evidence has shown that the chemical recalcitrance of EcM necromass can affect soil carbon sequestration more than previously thought, we also examined the consequences of adding EcM necromass to protected or unprotected SOM pools.

Main findings

- The ratio between EcM and saprotrophic fungi was more in line with observations in the simulations with longer turnover times. However, the total soil carbon decreased, moving model estimates further away from the observed values of total soil carbon at the Norwegian sites.

- We found a linear relationship between modeled living EcM biomass and turnover time, where a one-year increase in turnover time led to a 27 gC/m2 (mean) increase in EcM biomass.

- Higher EcM biomass resulted in more competitive interactions with the saprotrophic pools, by removing more nitrogen from the soil system through the EcM-to-plant pathway. This led to reduced saprotrophic CUE, causing more respiration and significantly lower total soil carbon.

- Adding mycorrhizal necromass to the SOM pool available for saprotrophic decomposition (SOMa) decreased the carbon content in the SOMa pool, as well as the total carbon storage. The relatively low C:N ratio of the mycorrhizal necromass led to a priming effect, where the saporotrophs could build more biomass due to higher CUE, thereby decomposing more substrate.
- Adding mycorrhizal necromass to protected pools increased the carbon content in these pools, leading to a small increase in total carbon storage.

Main conclusion

The lower total soil carbon due to increased fungal competition contrasts the Gadgil-effect theory, which assumes increased soil carbon when there is competition between saprotrophic fungi and EcM, due to decreased saprotrophic decomposition rates. The decrease in total soil carbon brings modeled values away from the mean of the observations from Strand et al. (2016). When EcM necromass was made easily available to the saprotrophic decomposers, total soil carbon also decreased, but now due to increased decomposition rates. This led to our suggestion that the model underestimation of total soil carbon at the sites is partly caused by a too rapid cycling of recalcitrant mycorrhizal biomass and/or a too effective release of labile carbon during the mining process.

Author contribution

I designed the study, performed the analysis and wrote the manuscript with contributions from the co-authors.

Chapter 5

Discussion, outlook and concluding remarks

The main objective of this work was to establish a microbially explicit soil biogeochemistry model which is capable of representing processes relevant to boreal ecosystems but still is simple and general enough to be used in an ESM. The resulting model is MIMICS+, which adds mycorrhizal pools, a nitrogen cycle, and vertical layers to the MIMICS-Wieder framework. Through the model development process and application of the model, the work presented in this thesis has contributed to a deeper understanding about the role of microbial activity for soil carbon dynamics and how microbes potentially can influence carbon-climate feedbacks. The work has also highlighted several challenges related to representing real-world, complex soil dynamics in a modeling framework.

5.1 Discussion

5.1.1 MIMICS+ as a biogeochemistry model

Objective: Establish a microbially explicit soil biogeochemical model, which is capable of representing processes relevant to boreal ecosystems but also simple and general enough to be incorporated into an ESM.

The comparisons between MIMICS+, CLM, and observations in paper I showed that MIMICS+ performs better than, or on par with a traditional soil decomposition model at the Norwegian forested sites. The percentage of carbon in microbes compared to total soil carbon estimated by the model is comparable to literature values (1–3 %), and the experiments in paper II showed that the model captures broad scale controls and rates of litter mass loss during decomposition at high latitudes. Together, these results show that MIMICS+ is a microbially explicit soil model that can be trusted to produce reasonable results also when it is coupled to a larger model.

However, the model does not capture all the small-scale features and variations that comes with the highly heterogeneous nature of real soils. This is evident from the poor one-to-one match of total soil carbon between the modeled and

observed soil profiles in paper I (Fig. 2d–f), and the variable results of the litterbag decomposition experiments for the VCG sites in paper II (Fig. 4). The one-to-one match for the CLM results in paper I was as poor, or worse than the MIMICS+ results, illustrating that this is an issue that also affects the LSMs (Blyth et al., 2021). When developing process models that are intended to represent larger areas, they cannot be expected to capture sub-grid variations that inevitably affect real-world soils. Yet, applying some kind of parameter optimization, like the Monte Carlo method used by Pierson et al. (2022) would likely improve the correlation between MIMICS+ and the soil profiles in paper I. However, such methods can be demanding in terms of time and computational cost and the optimized parameters will be fitted to a certain set of observations. If MIMICS+ is used offline to model a smaller region/specific site, optimizing the parameters using high resolution data from the location can be beneficial. As the main intention for MIMICS+ is to be coupled to CLM, it will be useful to include the MIMICS+ parameters in future parameter sensitivity simulations and Perturbed Parameter Ensembles (PPE) with CLM (Dagon et al., 2020). With these analyses it is possible to quantify parameter uncertainties and how much it contributes to overall uncertainty in LSM projections.

We wanted a model that represents processes that are particularly important at high latitudes. Based on what is known about these systems, we chose to include mycorrhizal pools and a representation of the nitrogen cycle. Although the model is tested against observations from high-latitude systems and provided reasonable results, testing it against observations from other ecosystems with different nutrient conditions and mycorrhizal patterns would improve confidence that the model is general enough to be used in global LSM simulations. Given the close relationship between mycorrhizal fungi and their host plants, it is also essential to test MIMICS+ in a system that is coupled to vegetation.

Going from a simple process representation to a more complex representation of the same process inevitably means that more parameters and equations are introduced. Although going from the six soil carbon pools (three SOM pools and three litter pools) in the current CENTURY-based CLM representation, to nine pools in MIMICS+ (four microbial pools, three SOM pools, and two litter pools) is an increase in complexity, the effect on computational time and cost will not be substantial.

Many of the parameterizations and pools in MIMICS+ are inherited from the MIMICS-Wieder setup. Various versions of the MIMICS model have been developed and applied by other research groups, providing a basis of literature exploring different aspects of the core modeling framework (e.g. alternative nitrogen cycle; Kyker-Snowman et al., 2020, vertical resolution; Wang et al., 2021, parameter optimization; Pierson et al., 2022, model testbed; Wieder et al., 2017). This facilitates model development, as future work can build on insights from previous work, like our choice of increasing the direct plant-derived fraction based on Kyker-Snowman et al. (2022) (Section 3.1.2). However, a pitfall of a rapid expansion in the use of a model is to carry on using initial parameterizations out of convenience (or lack of better options) without careful consideration of the consequences. As an example, we chose to represent the microbial decomposition

using reverse MMK kinetics based on previous MIMICS work (Wieder et al., 2017), and a numerical argument of model stability (Wang et al., 2016). This choice implicates an assumption of plenty available substrate, making the amount of microbial biomass the rate limiting factor (Chandel et al., 2023). Forward MMK assumes the opposite. In the real-world both cases can occur, and it might have been a better choice to use the Equilibrium Chemistry Approximation (ECA) proposed by Tang and Riley (2013), which can account for limitations in both directions. Despite limited evidence that favors forward MMK over reverse or ECA, Chandel et al. (2023) found that 31 out of the 71 microbial models they examined used the forward MMK formulation. Only 14 and 7 models used reverse MMK or ECA, respectively. To broaden the range of soil model formulations in ESMs, the community should make sure all three formulations are represented in the next CMIP model generation.

5.1.2 Microbe-microbe interactions and nutrient competition

Objective: Gain a better understanding of how the availability of nutrients (nitrogen) affects microbial activity and microbe-microbe interactions in nutrient poor environments (Objective 1a).

The amount of nitrogen added in the enrichment experiment in paper I corresponds to the amount that is typically added to Scandinavian forests for fertilization purposes (Högberg et al., 2017). The largest response was seen for saprotrophic bacteria which was expected, since they are modeled to have the strictest stoichiometric constraint, and therefore would benefit the most from more available nitrogen (Fig. 7 in paper I). The response also reflects the general trend of saprotrophic bacteria being more opportunistic in nature than saprotrophic fungi (Chapin et al., 2011). The model results also indicated a negative relationship between inorganic nitrogen and fungal:bacterial ratio, suggesting that we can get a shift towards microbial communities with a higher fraction of bacteria with elevated nitrogen deposition.

Although the microbial pools showed large responses to the nitrogen enrichment, the response in total soil carbon was modest. If MIMICS+ was coupled to a vegetation model, the nitrogen enrichment experiment would increase plant productivity. Findings from the decomposition of different litter types in paper II indicate that the chemical recalcitrance of the litter input is an important control on decomposition rates. How much, and in which direction the microbial pools would respond in a coupled model setup would therefore partly depend on the quality of the litter from the increased productivity.

Another mechanism that is not captured in the offline nitrogen enrichment experiment are shifts in plant allocation to nutrient acquisition through mycorrhiza. Observational evidence suggest that plants allocate less carbon to mycorrhiza when the amount of more readily available nitrogen increases (Högberg et al., 2010). A decrease in EcM due to a decrease in carbon allocation would lead to more saprotrophic biomass according to the findings from paper III.

Paper III illustrates how mycorrhizal presence has the potential to both increase

and decrease saprotrophic biomass, thereby affecting soil carbon storage and exchange through heterotrophic respiration. In the simulations where mycorrhizal biomass was high (due to longer turnover time) more nitrogen was lost from the soils through the mycorrhizal pathway, putting a stronger nitrogen limitation on the saprotrophic decomposers and reducing their efficiency to utilize the available carbon (lower CUE). In the simulations where the mycorrhizal necromass (with a relatively low C:N ratio) was put directly into the SOM pool that is available for saprotrophic decomposition, the higher quality of the substrate led to more efficient saprotrophs and more saprotrophic biomass (higher CUE).

Interestingly, the total soil carbon decreased both in the case of lower and higher saprotrophic biomass. In the first case because the saprotrophs respired a larger fraction of the decomposed substrate. In the latter case because the increase in saprotophic biomass led to higher decomposition rates (Eq. 3.1 in Section 3.1.1), and although the respired fraction was smaller, the total amount of respired carbon was still high because of the larger absolute amount of decomposed carbon. The balance between the absolute amount of decomposed carbon and the fraction which enters the atmosphere as respired CO_2 is important to understand in order to quantify the magnitude and direction of soil responses to anthropogenic changes in climate, nutrient availability and CO_2 concentration.

5.1.3 Controls on decomposition and soil carbon storage

Objectives: Gain a better understanding of how temperature and moisture affect soil carbon storage and decomposition (Objective 1b). Gain a better understanding of how the quality (chemical composition) of plant litter can impact microbial decomposition (Objective 1c).

Climatic controls

Paper I showed that the total soil carbon content was higher for the warmer half of the sites than for the cooler half, for both models and the observations, while paper II showed that litter mass loss was faster at warmer sites than at colder sites (CIDET sites, Fig. 2 in paper II). This apparent contradiction can in part be explained by how substrates are protected from microbial decomposition by physicochemical or chemical mechanisms (see Section 2.1.2). For the sites studied in paper I, there is a positive correlation between mean annual temperature and litter production. As 50 % of the incoming litter to MIMICS+ omits the microbial pathway and is transferred directly to the protected pools (Section 3.1.2), more carbon ends up in the relatively stable protected pools at warmer sites. In contrast to the analysis in paper I, the decomposition experiments in paper II only look at the mass loss from the litter pools, isolating the effect of temperature on decomposition, which showed the expected increase in decomposition rates with temperature.

Within MIMICS+, the direct plant-derived fraction of litter input to SOM, and how fast substrate is moved from the protected pools (SOMp and SOMc) to the pool available for decomposition (SOMa) will largely determine if higher

temperatures will lead to more or less carbon storage. The size of the direct plant-derived SOM fraction is debated (Sokol et al., 2019; Angst et al., 2021; Whalen et al., 2022), and the equations determining the rates at which SOM substrate is made available for microbial decomposition are uncertain (Pierson et al., 2022; Wieder et al., 2015). To gain a better understanding of these mechanisms, observational studies that can inform these rates will be valuable. For example, the turnover of mineral associated organic matter (MAOM, analogous to SOMp) can be measured using radiocarbon measurements, as suggested by Pierson et al. (2022).

The model results and observations from Strand et al. (2016) indicate that the higher plant production and long-term storage of carbon in protected SOM pools more than offsets the effect of increased decomposition rates at warmer sites. If we make the assumption that this pattern also is representative for anthropogenic warming, this indicates that the carbon-climate feedback is negative for these terrestrial systems. However, this is a speculation based on the limited evidence presented in this thesis. A proper quantification of the direction and magnitude of the feedback requires scenario simulations performed within NorESM. Then, the results should be critically evaluated against other models in a CMIP. For global applications of such a study, it is important to separate contributions from different biomes, as increased carbon uptake in one biome can compensate for decreased uptake in another (Shi et al., 2024).

High-latitude soils regularly experience freezing conditions, which impose a strong limitation on microbial decomposition. The simulations for the VCG sites in paper II clearly demonstrated the challenges of representing freezing limitations. In the model, freezing is a special case of moisture limitation, where the soil is perceived as dry by the microbes. For the 50 sites from Strand et al. (2016), MIMICS+ and CLM projected higher soil carbon content for the soils experiencing lower mean annual precipitation, while the observations showed the opposite. This again demonstrates the challenges of modeling moisture effects on decomposition rates. The interactions between soil temperature and moisture further complicate the matter. The complexity of soil moisture effect on microbial processes is reflected in the wide range of functions that is used to represent moisture limitations in various microbial models (Chandel et al., 2023; Sierra et al., 2015).

Litter quality control

Within MIMICS+, the recalcitrance of incoming litter (i.e. the partitioning of litter between the metabolic and the structural pool) has an immediate effect on decomposition rates, while the C:N ratio of incoming litter can gradually affect the amount and composition of microbial biomass by adjusting the CUE. When fresh litter is added to soil, a significant fraction of the most labile carbon is assumed to quickly leach away (especially in wet conditions). This partly explains why observational studies of litter decomposition often report that litter quality is the dominating control on mass loss initially, while climatic factors become more important over time (Trofymow et al., 2002). A lesson learned during the work with paper II was that both the model setup and the observational setup would

have benefited from quantifying the amount of carbon lost during initial leaching of labile compounds.

5.1.4 How forcing affect model results

Objective: Gain a better understanding of how microclimatic forcing can impact model results (Objective 2).

Model results are not only determined by model structure and parameter choices, but also by input data. For the litterbag experiments at the VCG sites (paper II) we therefore experimented with different sources for representing the microclimate; soil moisture and temperature. In addition, we modified surface parameters like slope and organic content in the CLM simulations that produced the input fluxes of carbon and nitrogen. Contrary to our expectations, using soil temperature and moisture observed on site did not improve the model results. Sub-grid local features like slopes, the presence of boulders, and stony, shallow soils make the observations of soil temperature and moisture vulnerable to uncertainties. This shows that we also need to consider how representative the input data is when interpreting the model results. The sub-grid heterogeneity is an obvious reason why models struggle to represent local effects on soil processes. Efforts to improve sub-grid representation through tiling and more refined vegetation models in LSMs (Fisher and Koven, 2020; Blyth et al., 2021) will hopefully improve the representation of modeled surface conditions, which holds important controls of modeled bigeochemical cycles in the soil.

The effect of coarse resolution forcing is also evident on a larger scale, illustrated by the climate categorization in paper I. When dividing the sites into two categories based on either mean annual temperature or moisture, some sites ended up in different categories when we divided based on model forcing than when we divided based on observations from meteorological stations. In offline CLM simulations, the modeled soil temperature and moisture are driven by coarse resolution atmospheric forcing data. When using non-linear representations of soil decomposition as in the MIMICS+ model, such inaccuracies in model forcing could potentially lead to fundamentally different responses to climatic changes, which is important to be aware of when interpreting the model results.

5.1.5 Bridging the gap

Objective: Contribute to bridging the gap between model requirements and measurements by identifying key parameters and processes. (Objective 3).

An essential step towards incorporating new processes into ESMs is to investigate the processes using a simpler modeling framework, like MIMICS+. Besides informing modelers about process behavior and uncertainties, this step also provides valuable insights into the theories that made the process relevant for model incorporation in the first place (Kyker-Snowman et al., 2022). By formalizing ecological processes into a mathematical framework, we enable the

detection of interactions, knowledge gaps, and new hypotheses about process functioning. The development and applications of MIMICS+ presented in this work have contributed to several insights in that regard. Some examples are given here.

First, the fraction of litter that was transferred directly to SOM was shown to be an important control on the SOM C:N ratio (paper I). The C:N ratio is a quantity that is easily accessible, both as model output and through chemical analysis of soil samples. Model sensitivity experiments where the direct plant-derived fraction is varied, combined with observed C:N ratios could benefit the ongoing work of quantifying the plant-derived versus microbially-derived fractions of SOM (Whalen et al., 2022).

Second, a valuable insight from paper II was that we can extract more information from litterbag experiments by including an estimate of how much of the mass loss is due to microbial decomposition, and how much is explained by other processes, such as leaching.

Third, paper III presents the somewhat unconventional idea that total soil carbon storage decreases with increased microbial nutrient competition, due to inefficient saprotrophs. There is little empirical evidence for such behavior, however, evidence for increased carbon storage is also inconsistent (Fernandez and Kennedy, 2016). Thus, empirical data that can increase our understanding of how microbial competition affects CUE will be valuable, from both a modeling and an ecological perspective.

Lastly, MIMICS+ (and other microbially explicit models) would greatly benefit from more quantitative data about microbial biomass amounts, composition, and stoichiometry. Ongoing work in the research project FUNDER[1] aims to provide such information for the Vestland Climate Grid presented in paper II. These data can shine new light on the results presented in the paper, which can enhance our understanding of the ecological processes, and inform future model development.

5.2 Outlook and future research

The obvious next step to continue the work from this thesis, is to couple MIMICS+ to CLM. This will provide a direct coupling between the soil pools and the vegetation above, enabling further investigations into microbe-plant interactions. The long-term plans for the CLM version that is used in NorESM is to use the Functionally Assembled Terrestrial Ecosystem Simulator (FATES) as the default vegetation model. FATES is a more refined vegetation model than what is currently used in CLM, that can track disturbance history and successional stage of cohorts of PFTs (Koven et al., 2020). Coupled to MIMICS+, this approach can give valuable new insights, especially into the role of mycorrhizal associations during treeline migration.

Combining complex process models is not an easy task. Since MIMICS+ has been developed as a stand-alone module, the parameter values have not been tested in a coupled system which might introduce instabilities if the parameters are used

[1] https://betweenthefjords.w.uib.no/funder/

"as-is". Especially parameters related to the mycorrhizal associations and direct nitrogen uptake by plants will need careful consideration and testing in a coupled system before realistic results can be achieved. Although this is cumbersome work, the process might expose connections between above- and below-ground processes in the model that may or may not be representative of the real world. Interdisciplinary collaboration between ecologists and modelers will therefore be valuable throughout the coupling process.

After MIMICS+ has been coupled and tested within the CLM framework, the CLM configuration can be used in fully coupled NorESM runs and participate in future model intercomparisons. If the participating ESMs include a more diverse representation of soil sub-models, the confidence in carbon feedback projections can be increased, although it is likely that the spread among modeled projections will increase due to larger structural differences (Bradford et al., 2016).

5.3 Concluding remarks

A better understanding of how below-ground processes influence carbon-climate feedbacks is necessary for projections of the future climate. The development and application of soil biogeochemistry models that explicitly represent microbial activity is an essential step toward this goal. This thesis has presented MIMICS+ as a valuable tool, both as a future soil sub-model for NorESM, and as a stand-alone model that provides insight into the interplay between microbes and their environment. The thesis further highlights the importance of knowledge exchange between modeling communities and empiricists. As process models always will be a simplified representation of reality, understanding the consequences of these simplifications is necessary for interpreting the model results.

Bibliography

Aas, E. R., H. A. de Wit, and T. K. Berntsen (2024). "Modeling boreal forest soil dynamics with the microbially explicit soil model MIMICS+ (v1.0)." In: *Geoscientific Model Development* 17.7, pp. 2929–2959. DOI: 10.5194/gmd-17-2929-2024.

Angst, G., K. E. Mueller, K. G. Nierop, and M. J. Simpson (May 2021). "Plant- or microbial-derived? A review on the molecular composition of stabilized soil organic matter." In: *Soil Biology and Biochemistry* 156. DOI: 10.1016/J.SOILBIO.2021.108189.

Arora, V. K., G. J. Boer, P. Friedlingstein, M. Eby, C. D. Jones, J. R. Christian, G. Bonan, L. Bopp, V. Brovkin, P. Cadule, T. Hajima, T. Ilyina, K. Lindsay, J. F. Tjiputra, and T. Wu (2013). "Carbon–Concentration and Carbon–Climate Feedbacks in CMIP5 Earth System Models." In: *Journal of Climate* 26.15, pp. 5289–5314. DOI: 10.1175/JCLI-D-12-00494.1.

Arora, V. K. et al. (2020). "Carbon-concentration and carbon-climate feedbacks in CMIP6 models and their comparison to CMIP5 models." In: *Biogeosciences* 17.16, pp. 4173–4222. DOI: 10.5194/BG-17-4173-2020.

Bar-On, Y. M., R. Phillips, and R. Milo (2018). "The biomass distribution on Earth." In: *Proceedings of the National Academy of Sciences* 115.25, pp. 6506–6511. DOI: 10.1073/pnas.1711842115.

Bardgett, R. (2005). *The biology of soil: a community and ecosystem approach*. Oxford university press. ISBN: 0198525036.

Baskaran, P., R. Hyvönen, S. L. Berglund, K. E. Clemmensen, G. I. Ågren, B. D. Lindahl, and S. Manzoni (Feb. 2017). "Modelling the influence of ectomycorrhizal decomposition on plant nutrition and soil carbon sequestration in boreal forest ecosystems." In: *New Phytologist* 213, pp. 1452–1465. DOI: 10.1111/nph.14213.

Blyth, E. M., V. K. Arora, D. B. Clark, S. J. Dadson, M. G. D. Kauwe, D. M. Lawrence, J. R. Melton, J. Pongratz, R. H. Turton, K. Yoshimura, and H. Yuan (2021). "Advances in Land Surface Modelling." In: *Current Climate Change Reports* 7, pp. 45–71. DOI: 10.1007/s40641-021-00171-5.

Bollmeyer, C., J. D. Keller, C. Ohlwein, S. Wahl, S. Crewell, P. Friederichs, A. Hense, J. Keune, S. Kneifel, I. Pscheidt, S. Redl, and S. Steinke (2015). "Towards a high-resolution regional reanalysis for the European CORDEX domain." In: *Quarterly Journal of the Royal Meteorological Society* 141.686, pp. 1–15. DOI: https://doi.org/10.1002/qj.2486.

Bonan, G. B. and S. C. Doney (2018). "Climate, ecosystems, and planetary futures: The challenge to predict life in Earth system models." In: *Science* 359.6375, eaam8328. DOI: 10.1126/science.aam8328.

Bradford, M. A., W. R. Wieder, G. B. Bonan, N. Fierer, P. A. Raymond, and T. W. Crowther (Aug. 2016). "Managing uncertainty in soil carbon feedbacks to climate change." In: *Nature Climate Change* 6 (8), pp. 751–758. DOI: 10.1038/nclimate3071. URL: http://www.nature.com/articles/nclimate3071.

Brzostek, E. R., J. B. Fisher, and R. P. Phillips (Aug. 2014). "Modeling the carbon cost of plant nitrogen acquisition: Mycorrhizal trade-offs and multipath resistance uptake improve predictions of retranslocation." In: *Journal of Geophysical Research: Biogeosciences* 119.8, pp. 1684–1697. DOI: 10.1002/2014JG002660.

Chandel, A. K., L. Jiang, and Y. Luo (2023). "Microbial Models for Simulating Soil Carbon Dynamics: A Review." In: *Journal of Geophysical Research: Biogeosciences* 128.8, pp. 1–27. DOI: 10.1029/2023JG007436.

Chapin, F. S., P. A. Matson, and P. M. Vitousek (2011). *Principles of Terrestrial Ecosystem Ecology*. eng. 2nd ed. 2011. New York, NY: Springer New York : Imprint: Springer. ISBN: 978-1-4419-9504-9.

Crowther, T. W., J. van den Hoogen, J. Wan, M. A. Mayes, A. D. Keiser, L. Mo, C. Averill, and D. S. Maynard (2019). "The global soil community and its influence on biogeochemistry." In: *Science* 365.6455. DOI: 10.1126/science.aav0550.

Dagon, K., B. M. Sanderson, R. A. Fisher, and D. M. Lawrence (2020). "A machine learning approach to emulation and biophysical parameter estimation with the Community Land Model, version 5." In: *Advances in Statistical Climatology, Meteorology and Oceanography* 6.2, pp. 223–244. DOI: 10.5194/ascmo-6-223-2020.

Daly, A. B., A. Jilling, T. M. Bowles, R. W. Buchkowski, S. D. Frey, C. M. Kallenbach, M. Keiluweit, M. Mooshammer, J. P. Schimel, and A. S. Grandy (June 2021). "A holistic framework integrating plant-microbe-mineral regulation of soil bioavailable nitrogen." In: *Biogeochemistry* 154 (2), pp. 211–229. DOI: 10.1007/s10533-021-00793-9.

Danabasoglu, G. et al. (2020). "The Community Earth System Model Version 2 (CESM2)." In: *Journal of Advances in Modeling Earth Systems* 12.2. DOI: https://doi.org/10.1029/2019MS001916.

Del Grosso, S. J., W. J. Parton, A. R. Mosier, D. S. Ojima, A. E. Kulmala, and S. Phongpan (2000). "General model for N2O and N2 gas emissions from soils due to dentrification." In: *Global Biogeochemical Cycles* 14.4, pp. 1045–1060. DOI: https://doi.org/10.1029/1999GB001225.

Du, E., C. Terrer, A. F. Pellegrini, A. Ahlström, C. J. van Lissa, X. Zhao, N. Xia, X. Wu, and R. B. Jackson (2020). "Global patterns of terrestrial nitrogen and phosphorus limitation." In: *Nature Geoscience* 13.3, pp. 221–226. DOI: 10.1038/s41561-019-0530-4. URL: http://dx.doi.org/10.1038/s41561-019-0530-4.

Eyring, V., S. Bony, G. A. Meehl, C. A. Senior, B. Stevens, R. J. Stouffer, and K. E. Taylor (May 2016). "Overview of the Coupled Model Intercomparison Project Phase 6 (CMIP6) experimental design and organization." In: *Geoscientific Model Development* 9 (5), pp. 1937–1958. DOI: 10.5194/gmd-9-1937-2016.

Fernandez, C. W. and P. G. Kennedy (2016). "Revisiting the 'Gadgil effect': do interguild fungal interactions control carbon cycling in forest soils?" In: *New Phytologist* 209.4, pp. 1382–1394. DOI: https://doi.org/10.1111/nph.13648.

Fisher, J. B., S. Sitch, Y. Malhi, R. A. Fisher, C. Huntingford, and S.-Y. Tan (Mar. 2010). "Carbon cost of plant nitrogen acquisition: A mechanistic, globally applicable model of plant nitrogen uptake, retranslocation, and fixation." In: *Global Biogeochemical Cycles* 24.1, pp. 1–17. DOI: 10.1029/2009GB003621.

Fisher, R. A. and C. D. Koven (2020). "Perspectives on the Future of Land Surface Models and the Challenges of Representing Complex Terrestrial Systems." In: *Journal of Advances in Modeling Earth Systems* 12.4, pp. 1–24. DOI: https://doi.org/10.1029/2018MS001453.

Frey, S. D. (2019). "Mycorrhizal Fungi as Mediators of Soil Organic Matter Dynamics." In: *Annual Review of Ecology, Evolution, and Systematics* 50.1, pp. 237–259. ISSN: 1543-592X. DOI: 10.1146/annurev-ecolsys-110617-062331.

Friedlingstein, P. et al. (2006). "Climate–Carbon Cycle Feedback Analysis: Results from the C4MIP Model Intercomparison." In: *Journal of Climate* 19.14, pp. 3337–3353. DOI: 10.1175/JCLI3800.1.

Gadgil, P. D. and R. L. Gadgil (1975). "Suppression of litter decomposition by mycorrhizal roots of Pinus radiata." In: 5, pp. 35–41.

Gadgil, R. L. and P. Gadgil (1971). "Mycorrhiza and litter decomposition." In: *Nature* 233.5315, pp. 133–133.

German, D. P., K. R. B. Marcelo, M. M. Stone, and S. D. Allison (Apr. 2012). "The Michaelis-Menten kinetics of soil extracellular enzymes in response to temperature: A cross-latitudinal study." In: *Global Change Biology* 18 (4), pp. 1468–1479. DOI: 10.1111/j.1365-2486.2011.02615.x.

Grandy, A. S., W. R. Wieder, K. Wickings, and E. Kyker-Snowman (Nov. 2016). "Beyond microbes: Are fauna the next frontier in soil biogeochemical models?" In: *Soil Biology and Biochemistry* 102, pp. 40–44. DOI: 10.1016/j.soilbio.2016.08.008.

Guerra, C. A. et al. (2020). "Blind spots in global soil biodiversity and ecosystem function research." In: *Nature Communications* 11.3870, pp. 1–13. DOI: 10.1038/s41467-020-17688-2.

Halbritter, A. H. et al. (2020). "The handbook for standardized field and laboratory measurements in terrestrial climate change experiments and observational studies (ClimEx)." In: *Methods in Ecology and Evolution* 11.1, pp. 22–37. DOI: https://doi.org/10.1111/2041-210X.13331.

Hansson, A., P. Dargusch, and J. Shulmeister (Feb. 2021). "A review of modern treeline migration, the factors controlling it and the implications for carbon storage." In: *Journal of Mountain Science 2021 18:2* 18 (2), pp. 291–306. DOI: 10.1007/S11629-020-6221-1.

Hawkins, H. J., R. I. Cargill, M. E. Van Nuland, S. C. Hagen, K. J. Field, M. Sheldrake, N. A. Soudzilovskaia, and E. T. Kiers (2023). "Mycorrhizal mycelium as a global carbon pool." In: *Current Biology* 33.11, R560–R573. DOI: 10.1016/j.cub.2023.02.027.

Högberg, M. N., M. J. Briones, S. G. Keel, D. B. Metcalfe, C. Campbell, A. J. Midwood, B. Thornton, V. Hurry, S. Linder, T. Näsholm, and P. Högberg (July

2010). "Quantification of effects of season and nitrogen supply on tree below-ground carbon transfer to ectomycorrhizal fungi and other soil organisms in a boreal pine forest." In: *New Phytologist* 187 (2), pp. 485–493. DOI: 10.1111/j.1469-8137.2010.03274.x.

Högberg, P., T. Näsholm, O. Franklin, and M. N. Högberg (2017). "Tamm Review: On the nature of the nitrogen limitation to plant growth in Fennoscandian boreal forests." In: *Forest Ecology and Management* 403, pp. 161–185. DOI: https://doi.org/10.1016/j.foreco.2017.04.045.

Jia, G., E. Shevliakova, P. Artaxo, N. De Noblet-Ducoudré, R. Houghton, J. House, K. Kitajima, C. Lennard, A. Popp, A. Sirin, R. Sukumar, and L. Verchot (2019). "Emissions Trends and Drivers." In: *Land–climate interactions. In: Climate Change and Land: an IPCC special report on climate change, desertification, land degradation, sustainable land management, food security, and greenhouse gas fluxes in terrestrial ecosystem.* Ed. by P. R. Shukla et al. Cambridge, UK and New York, NY, USA: Cambridge University Press. Chap. 2. DOI: https://doi.org/10.1017/9781009157988.004.

Kaiser, C., M. R. Kilburn, P. L. Clode, L. Fuchslueger, M. Koranda, J. B. Cliff, Z. M. Solaiman, and D. V. Murphy (2015). "Exploring the transfer of recent plant photosynthates to soil microbes: mycorrhizal pathway vs direct root exudation." In: *New Phytologist* 205.4, pp. 1537–1551. DOI: https://doi.org/10.1111/nph.13138.

Koven, C. D., W. J. Riley, Z. M. Subin, J. Y. Tang, M. S. Torn, W. D. Collins, G. B. Bonan, D. M. Lawrence, and S. C. Swenson (2013). "The effect of vertically resolved soil biogeochemistry and alternate soil C and N models on C dynamics of CLM4." In: *Biogeosciences* 10.11, pp. 7109–7131. DOI: 10.5194/bg-10-7109-2013.

Koven, C. D. et al. (2020). "Benchmarking and parameter sensitivity of physiological and vegetation dynamics using the Functionally Assembled Terrestrial Ecosystem Simulator (FATES) at Barro Colorado Island, Panama." In: *Biogeosciences* 17.11, pp. 3017–3044. DOI: 10.5194/bg-17-3017-2020.

Kyker-Snowman, E., W. R. Wieder, S. D. Frey, and A. S. Grandy (2020). "Stoichiometrically coupled carbon and nitrogen cycling in the MIcrobial-MIneral Carbon Stabilization model version 1.0 (MIMICS-CN v1.0)." In: *Geoscientific Model Development* 13.9, pp. 4413–4434. DOI: 10.5194/gmd-13-4413-2020.

Kyker-Snowman, E., D. L. Lombardozzi, G. B. Bonan, S. J. Cheng, J. S. Dukes, S. D. Frey, E. M. Jacobs, R. McNellis, J. M. Rady, N. G. Smith, R. Q. Thomas, W. R. Wieder, and A. S. Grandy (Jan. 2022). "Increasing the spatial and temporal impact of ecological research: A roadmap for integrating a novel terrestrial process into an Earth system model." In: *Global Change Biology* 28.2, pp. 665–684. DOI: 10.1111/GCB.15894.

Lambert, M. (2022). "Modelling the critical role of cold acclimation for vegetation survival during extreme winter weather." PhD thesis. University of Oslo.

Lawrence, D. M. et al. (2019). "The Community Land Model Version 5: Description of New Features, Benchmarking, and Impact of Forcing Uncertainty." In:

Journal of Advances in Modeling Earth Systems 11.12, pp. 4245–4287. DOI: 10.1029/2018MS001583.

Lehmann, J. and M. Kleber (2015). "The contentious nature of soil organic matter." In: *Nature* 528.7580, pp. 60–68.

Lindahl, B. D. and A. Tunlid (2015). "Ectomycorrhizal fungi–potential organic matter decomposers, yet not saprotrophs." In: *New Phytologist* 205.4, pp. 1443–1447. DOI: https://doi.org/10.1111/nph.13201.

Miner, K. R., M. R. Turetsky, E. Malina, A. Bartsch, J. Tamminen, A. D. McGuire, A. Fix, C. Sweeney, C. D. Elder, and C. E. Miller (Jan. 2022). "Permafrost carbon emissions in a changing Arctic." In: *Nature Reviews Earth and Environment* 3 (1), pp. 55–67. DOI: 10.1038/s43017-021-00230-3.

Mooshammer, M., W. Wanek, S. Zechmeister-Boltenstern, and A. A. Richter (2014). "Stoichiometric imbalances between terrestrial decomposer communities and their resources: mechanisms and implications of microbial adaptations to their resources." In: *Frontiers in microbiology*, p. 22.

Nieder, R., D. K. Benbi, and H. W. Scherer (2011). "Fixation and defixation of ammonium in soils: A review." In: *Biology and Fertility of Soils* 47 (1), pp. 1–14. DOI: 10.1007/s00374-010-0506-4.

Parton, W. J., E. A. Holland, S. J. Del Grosso, M. D. Hartman, R. E. Martin, A. R. Mosier, D. S. Ojima, and D. S. Schimel (2001). "Generalized model for NO x and N2O emissions from soils." In: *Journal of Geophysical Research: Atmospheres* 106.D15, pp. 17403–17419. DOI: https://doi.org/10.1029/2001JD900101.

Parton, W. J., A. R. Mosier, D. S. Ojima, D. W. Valentine, D. S. Schimel, K. Weier, and A. E. Kulmala (1996). "Generalized model for N2 and N2O production from nitrification and denitrification." In: *Global Biogeochemical Cycles* 10.3, pp. 401–412. DOI: https://doi.org/10.1029/96GB01455.

Parton, W. J., J. W. B. Stewart, and C. V. Cole (1988). "Dynamics of C, N, P and S in grassland soils: a model." In: *Biogeochemistry* 5.1, pp. 109–131. DOI: 10.1007/BF02180320.

Pelletier, J. D., P. D. Broxton, P. Hazenberg, X. Zeng, P. A. Troch, G.-Y. Niu, Z. Williams, M. A. Brunke, and D. Gochis (2016). "A gridded global data set of soil, intact regolith, and sedimentary deposit thicknesses for regional and global land surface modeling." In: *Journal of Advances in Modeling Earth Systems* 8.1, pp. 41–65. DOI: https://doi.org/10.1002/2015MS000526.

Phillips, R. P., I. C. Meier, E. S. Bernhardt, A. S. Grandy, K. Wickings, and A. C. Finzi (2012). "Roots and fungi accelerate carbon and nitrogen cycling in forests exposed to elevated CO2." In: *Ecology Letters* 15.9, pp. 1042–1049. DOI: https://doi.org/10.1111/j.1461-0248.2012.01827.x.

Pierson, D., K. A. Lohse, W. R. Wieder, N. R. Patton, J. Facer, M.-A. de Graaff, K. Georgiou, M. S. Seyfried, G. Flerchinger, and R. Will (Dec. 2022). "Optimizing process-based models to predict current and future soil organic carbon stocks at high-resolution." In: *Scientific Reports* 12 (1), p. 10824. DOI: 10.1038/S41598-022-14224-8.

Rantanen, M., A. Y. Karpechko, A. Lipponen, K. Nordling, O. Hyvärinen, K. Ruosteenoja, T. Vihma, and A. Laaksonen (2022). "The Arctic has warmed

nearly four times faster than the globe since 1979." In: *Commun Earth Environ* 3.168, pp. 1–10. DOI: 10.1038/s43247-022-00498-3.

Sanderson, B. M. et al. (2023). "The need for carbon emissions-driven climate projections in CMIP7." In: *EGUsphere* 2023, pp. 1–51. DOI: 10.5194/egusphere-2023-2127.

Schädel, C., C. D. Koven, D. M. Lawrence, G. Celis, A. J. Garnello, J. Hutchings, M. Mauritz, S. M. Natali, E. Pegoraro, H. Rodenhizer, V. G. Salmon, M. A. Taylor, E. E. Webb, W. R. Wieder, and E. A. Schuur (Oct. 2018). "Divergent patterns of experimental and model-derived permafrost ecosystem carbon dynamics in response to Arctic warming." In: *Environmental Research Letters* 13 (10), p. 105002. DOI: 10.1088/1748-9326/aae0ff.

Schlesinger, W. H. and E. S. Bernhardt (2013). *Biogeochemistry An Analysis of Global Change*. 3rd ed. Elsevier. ISBN: 9780123858740.

Schmidt, M. W., M. S. Torn, S. Abiven, T. Dittmar, G. Guggenberger, I. A. Janssens, M. Kleber, I. Kögel-Knabner, J. Lehmann, D. A. Manning, P. Nannipieri, D. P. Rasse, S. Weiner, and S. E. Trumbore (Oct. 2011). "Persistence of soil organic matter as an ecosystem property." In: *Nature* 478 (7367), pp. 49–56. DOI: 10.1038/nature10386.

Seland, Ø. et al. (2020). "Overview of the Norwegian Earth System Model (NorESM2) and key climate response of CMIP6 DECK, historical, and scenario simulations." In: *Geoscientific Model Development* 13.12, pp. 6165–6200. DOI: 10.5194/gmd-13-6165-2020.

Shi, M., J. B. Fisher, E. R. Brzostek, and R. P. Phillips (2016). "Carbon cost of plant nitrogen acquisition: Global carbon cycle impact from an improved plant nitrogen cycle in the Community Land Model." In: *Global Change Biology* 22.3, pp. 1299–1314. DOI: 10.1111/gcb.13131.

Shi, Z., F. M. Hoffman, M. Xu, U. Mishra, S. D. Allison, J. Zhou, and J. T. Randerson (Apr. 2024). "Global-Scale Convergence Obscures Inconsistencies in Soil Carbon Change Predicted by Earth System Models." In: *AGU Advances* 5 (2). DOI: 10.1029/2023AV001068.

Sieczka, A. and E. Koda (Oct. 2016). "Kinetic and equilibrium studies of sorption of ammonium in the soil-water environment in agricultural areas of central poland." In: *Applied Sciences (Switzerland)* 6.10, p. 269. DOI: 10.3390/APP6100269.

Sierra, C. A., S. E. Trumbore, E. A. Davidson, S. Vicca, and I. Janssens (2015). "Sensitivity of decomposition rates of soil organic matter with respect to simultaneous changes in temperature and moisture." In: *J. of Adv. Model. Earth Syst.* 7, pp. 335–356. DOI: 10.1002/2014MS000358Key.

Smith, S. L., H. B. O'Neill, K. Isaksen, J. Noetzli, and V. E. Romanovsky (Jan. 2022). "The changing thermal state of permafrost." In: *Nature Reviews Earth and Environment* 3 (1), pp. 10–23. DOI: 10.1038/s43017-021-00240-1.

Soetaert, K. and P. M. Herman (2009). *A practical guide to ecological modelling: using R as a simulation platform*. Springer, p. 372. ISBN: 9781402086236. DOI: 10.1007/978-1-4020-8624-3.

Sokol, N. W., J. Sanderman, and M. A. Bradford (2019). "Pathways of mineral-associated soil organic matter formation: Integrating the role of plant carbon

source, chemistry, and point of entry." In: *Global Change Biology* 25.1, pp. 12–24. DOI: https://doi.org/10.1111/gcb.14482.

Strand, L. T., I. Callesen, L. Dalsgaard, and H. A. de Wit (2016). "Carbon and nitrogen stocks in Norwegian forest soils — the importance of soil formation, climate, and vegetation type for organic matter accumulation." In: *Canadian Journal of Forest Research* 46.12, pp. 1459–1473. DOI: 10.1139/cjfr-2015-0467.

Strickland, M. S. and J. Rousk (Oct. 2010). "Considering fungal:bacterial dominance in soils – Methods, controls, and ecosystem implications." In: *Soil Biology and Biochemistry* 42.9, pp. 1385–1395. DOI: 10.1016/J.SOILBIO.2010.05.007.

Sulman, B. N., J. A. M. Moore, R. Abramoff, C. Averill, S. Kivlin, K. Georgiou, B. Sridhar, M. D. Hartman, G. Wang, W. R. Wieder, M. A. Bradford, Y. Luo, M. A. Mayes, E. Morrison, W. J. Riley, A. Salazar, J. P. Schimel, J. Tang, and A. T. Classen (2018). "Multiple models and experiments underscore large uncertainty in soil carbon dynamics." In: *Biogeochemistry* 141.2, pp. 109–123. DOI: 10.1007/s10533-018-0509-z.

Sulman, B. N., R. P. Phillips, A. C. Oishi, E. Shevliakova, and S. W. Pacala (2014). "Microbe-driven turnover offsets mineral-mediated storage of soil carbon under elevated CO 2." In: *Nature Climate Change* 4 (12), pp. 1099–1102. DOI: 10.1038/nclimate2436.

Sulman, B. N., E. Shevliakova, E. R. Brzostek, S. N. Kivlin, S. Malyshev, D. N. Menge, and X. Zhang (Apr. 2019). "Diverse Mycorrhizal Associations Enhance Terrestrial C Storage in a Global Model." In: *Global Biogeochemical Cycles* 33 (4), pp. 501–523. DOI: 10.1029/2018GB005973.

Tang, J. Y. and W. J. Riley (Dec. 2013). "A total quasi-steady-state formulation of substrate uptake kinetics in complex networks and an example application to microbial litter decomposition." In: *Biogeosciences* 10 (12), pp. 8329–8351. DOI: 10.5194/bg-10-8329-2013.

Taylor, K. E., R. J. Stouffer, and G. A. Meehl (2012). "An overview of CMIP5 and the experiment design." In: *Bulletin of the American Meteorological Society* 93 (4), pp. 485–498. DOI: 10.1175/BAMS-D-11-00094.1.

Trofymow, J. A. and the CIDET Working Group (1998). *The Canadian Intersite Decomposition Experiment (CIDET): Project and Site Establishment Report*. Tech. rep. Victoria, B. C.: Can. For. Serv. Pac. For. Cent. Inf. Rep.

Trofymow, J. A., T. R. Moore, B. Titus, C. Prescott, I. Morrison, M. Siltanen, S. Smith, J. Fyles, R. Wein, C. Camiré, L. Duschene, L. Kozak, M. Kranabetter, and S. V. Trofymow (2002). "Rates of litter decomposition over 6 years in Canadian forests : influence of litter quality and climate." In: *Can. J. For. Res* 32, pp. 789–804. DOI: 10.1139/X01-117.

Vandvik, V., I. H. Althuizen, F. Jaroszynska, L. C. Krüger, H. Lee, D. E. Goldberg, K. Klanderud, S. L. Olsen, R. J. Telford, S. A. Östman, S. Busca, I. J. Dahle, D. D. Egelkraut, S. R. Geange, R. Gya, J. S. Lynn, E. Meineri, S. Young, and A. H. Halbritter (2022). "The role of plant functional groups mediating climate impacts on carbon and biodiversity of alpine grasslands." In: *Scientific Data* 9.1, p. 451. DOI: 10.1038/s41597-022-01559-0.

Vowles, T. and R. G. Björk (Mar. 2019). "Implications of evergreen shrub expansion in the Arctic." In: *Journal of Ecology* 107 (2). Ed. by H. C. Prentice, pp. 650–655. DOI: 10.1111/1365-2745.13081.

Wang, Y. P., J. Jiang, B. Chen-Charpentier, F. B. Agusto, A. Hastings, F. Hoffman, M. Rasmussen, M. J. Smith, K. Todd-Brown, Y. P. Wang, X. Xu, and Y. Q. Luo (2016). "Responses of two nonlinear microbial models to warming and increased carbon input." In: *Biogeosciences* 13 (4), pp. 887–902. DOI: 10.5194/bg-13-887-2016.

Wang, Y. P., H. Zhang, P. Ciais, D. Goll, Y. Huang, J. D. Wood, S. V. Ollinger, X. Tang, and A.-K. Prescher (Apr. 2021). "Microbial Activity and Root Carbon Inputs Are More Important than Soil Carbon Diffusion in Simulating Soil Carbon Profiles." In: *Journal of Geophysical Research: Biogeosciences* 126 (4). DOI: 10.1029/2020JG006205.

Whalen, E. D., A. S. Grandy, N. W. Sokol, M. Keiluweit, J. Ernakovich, R. G. Smith, and S. D. Frey (Dec. 2022). "Clarifying the evidence for microbial- and plant-derived soil organic matter, and the path toward a more quantitative understanding." In: *Global Change Biology* 28 (24), pp. 7167–7185. DOI: 10.1111/gcb.16413.

Wieder, W. R., A. S. Grandy, C. M. Kallenbach, P. G. Taylor, and G. B. Bonan (2015). "Representing life in the Earth system with soil microbial functional traits in the MIMICS model." In: *Geosci. Model Dev* 8, pp. 1789–1808. DOI: 10.5194/gmd-8-1789-2015.

Wieder, W. R., A. S. Grandy, C. M. Kallenbach, and G. B. Bonan (2014). "Integrating microbial physiology and physio-chemical principles in soils with the MIcrobial-MIneral Carbon Stabilization (MIMICS) model." In: *Biogeosciences* 11.14, pp. 3899–3917. DOI: 10.5194/bg-11-3899-2014.

Wieder, W. R., M. D. Hartman, B. N. Sulman, Y.-P. Wang, C. D. Koven, and G. B. Bonan (Apr. 2017). "Carbon cycle confidence and uncertainty: Exploring variation among soil biogeochemical models." In: *Global Change Biology* 24.4, pp. 1563–1579. DOI: 10.1111/gcb.13979.

Part II

Part 2: Papers

Paper I

Modeling boreal forest soil dynamics with the microbially explicit soil model MIMICS+ (v1.0)

***Geoscientific Model Development*, 2024**

Geosci. Model Dev., 17, 2929–2959, 2024
https://doi.org/10.5194/gmd-17-2929-2024

Geoscientific Model Development
Open Access
EGU

Modeling boreal forest soil dynamics with the microbially explicit soil model MIMICS+ (v1.0)

Elin Ristorp Aas[1,3], **Heleen A. de Wit**[2,3], **and Terje K. Berntsen**[1,3]

[1]Department of Geosciences, University of Oslo, Oslo, Norway
[2]Norwegian Institute for Water Research, Økernveien 94, 0579 Oslo, Norway
[3]Centre for Biogeochemistry in the Anthropocene, Department of Geosciences, University of Oslo, Oslo, Norway

Correspondence: Elin Ristorp Aas (ecaas@uio.no) and Terje K. Berntsen (t.k.berntsen@geo.uio.no)

Received: 8 September 2023 – Discussion started: 5 October 2023
Revised: 27 February 2024 – Accepted: 28 February 2024 – Published: 16 April 2024

Abstract. Understanding carbon exchange processes between land reservoirs and the atmosphere is essential for predicting carbon–climate feedbacks. Still, considerable uncertainty remains in the representation of the terrestrial carbon cycle in Earth system models. An emerging strategy to constrain these uncertainties is to include the role of different microbial groups explicitly. Following this approach, we extend the framework of the MIcrobial-MIneral Carbon Stabilization (MIMICS) model with additional mycorrhizal groups and a nitrogen cycle that includes a novel representation of inorganic nitrogen sorption to particles via a Langmuir isotherm. MIMICS+ v1.0 is designed to capture and quantify relationships between soil microorganisms and their environment, with a particular emphasis on boreal ecosystems. We evaluated MIMICS+ against podzolic soil profiles in Norwegian forests as well as the conventional Community Land Model (CLM). MIMICS+ matched observed carbon stocks better than CLM and gave a broader range of C : N ratios, more in line with observations. This is mainly explained by a higher directly plant-derived fraction into the soil organic matter (SOM) pools. The model produces microbial biomass estimates in line with numbers reported in the literature. MIMICS+ also showed better representation of climate gradients than CLM, especially in terms of temperature. To investigate responses to changes in nutrient availability, we performed an N enrichment experiment and found that nitrogen sorbed to particles through the sorption algorithm served as a long-term storage of nutrients for the microbes. Furthermore, although the microbial groups responded considerably to the nitrogen enrichment, we only saw minor responses for carbon storage and respiration. Together, our results present MIMICS+ as an attractive tool for further investigations of interactions between microbial functioning and their (changing) environment.

1 Introduction

Among the carbon (C) stores in the terrestrial biosphere, soils are the largest, containing ca. 1700 Gt C, while vegetation accounts for ca. 450 Gt C globally (Friedlingstein et al., 2022). The active exchange of C between terrestrial pools and the atmosphere is affected by elevated CO_2 concentrations and changes in N deposition, but quantifying the responses has proven to be a central challenge in climate science. Arora et al. (2020) highlight the uncertainty in terrestrial carbon–concentration and carbon–climate feedbacks from the last model intercomparison project, CMIP6. The uncertainty in carbon–cycle feedbacks is up to 1 order of magnitude larger for land than for ocean, illustrating the need to improve model representation of terrestrial processes. To do this, we need to represent complex C and nutrient cycle processes in a modeling framework, a task that requires careful consideration of how to translate real-world processes into an appropriate model form. Fisher and Koven (2020) suggest an approach based on modular complexity. Dividing a full-complexity land model into smaller modules allows for investigation of alternatives for structure and parameter choices, which helps in making good modeling choices and thereby constrain sources of uncertainty.

Large variations in responses between different biomes introduce an extra challenge to C cycle modeling. The impact

of environmental changes on boreal systems is of particular interest for several reasons. For example, studies show that the kinetics of soil microbes accustomed to cooler climates are more temperature sensitive than microbes in warmer climates (German et al., 2012). Koven et al. (2017) also showed that soil carbon turnover times in cold areas are more sensitive to climatological temperature than in warm areas. Many boreal areas also experience treeline migration caused by an expansion of the temperature-limited area where tree species can grow (Hansson et al., 2021). Often this leads to a shift in mycorrhizal associations, for example from arbuscular mycorrhiza (AM) to ectomycorrhiza (EcM), which again can lead to changes in soil carbon dynamics and belowground carbon storage (Taylor et al., 2016; Tonjer et al., 2021). EcM has been found to alter decomposition, either negatively through increased nutrient competition with saprotrophs (Gadgil and Gadgil, 1971, 1975) or positively through priming effects (Brzostek et al., 2015; Phillips et al., 2012) based on environmental context (Fernandez and Kennedy, 2016). Recent findings also suggest that differences in decomposability of necromass from different mycorrhizal groups can impact soil C storage more than previously thought (Huang et al., 2022a, b). In Norwegian forests, vegetation is typically dominated by evergreen, coniferous trees, mainly associated with EcM. The dominating soil type in these forests is podzol (Strand et al., 2016). Podzols are typically nutrient poor, and competition for nutrients is expected to be important for the carbon dynamics in these systems. Despite the importance of boreal systems, many soil model structure and parameter choices are based on temperate or tropical observations. This bias may skew model results and make the modeled responses to climate change in boreal environments more uncertain.

Nitrogen (N) is one of the most important nutrients in an ecosystem, and the cycling of nitrogen between aboveground and belowground reservoirs can greatly affect carbon dynamics. In addition to regulating forest productivity, N availability regulates microbial carbon use efficiency (CUE), as microbes respire excess C to meet their stoichiometrical demand (Mooshammer et al., 2014b). This direct relationship between soil N and the C exchange between the atmosphere and soils emphasizes the importance of including microbial C–N relationships in C cycle models. One factor determining nitrogen availability in an ecosystem is inorganic N deposition from the atmosphere and agricultural fertilization. This inorganic N is subject to physical and chemical processes that affect how readily available the N is to microbes and plants. One such process is cation exchange, which controls storage and release of ammonium (NH_4^+) from negatively charged clay particles and organic molecules (Bonan, 2015) and therefore impacts inorganic N availability for microbes and plants. This is a process that might be extra important in nutrient-poor boreal forest systems. There are studies that have examined this effect in agricultural soils (Sieczka and Koda, 2016), but few have looked at natural soils.

Traditionally, decomposition processes in models have been represented by first-order kinetics for litter, as well as active, slow, and passive pools of soil organic matter (SOM) (Parton et al., 1988). This approach limits the ability to examine the mechanisms and possible responses of the soil system during climate change (Todd-Brown et al., 2012). Newer work has introduced models that in different ways represent microbial activity explicitly (e.g., Wieder et al., 2015; Sulman et al., 2019; Fatichi et al., 2019; Yu et al., 2020; Huang et al., 2018; Wang et al., 2013). These models increase the possibility to capture carbon climate feedbacks of the future (Tang and Riley, 2014; Hararuk et al., 2015). Wieder et al. (2015) illustrated that by representing the functional traits of microbes in the MIMICS model, one can raise important hypotheses about how microbes can determine responses to, for example, N enrichment. Kyker-Snowman et al. (2020) further showed that adding an N cycle to the MIMICS model (MIMICS-CN) produced results in line with measurements from North American sites and comparable models. Wang et al. (2021) presented a vertically resolved C-only version of MIMICS and showed that microbial activity and root carbon inputs were more important than the soil carbon diffusion when simulating soil carbon concentration profiles.

Baskaran et al. (2017) introduced a model that emphasized the influence of EcM on decomposition, however without the ability to capture nutrient competition with saprotrophic microbes. We included EcM with parameterizations from Baskaran et al. (2017) in a modeling framework based on the MIMICS model (Wieder et al., 2015) that also includes explicit saprotrophic pools. To capture possible shifts in mycorrhizal associations, we also included an arbuscular mycorrhizal (AM) pool using methods presented by Sulman et al. (2019). In contrast to the always-available inorganic N pools in Sulman et al. (2019), we introduced an algorithm for representing sorption of ammonium to soil particles based on the Langmuir isotherm (Sieczka and Koda, 2016), which may be an important but underrepresented process determining the availability of inorganic N to soil microbes in boreal forests. We assume that by including processes and parameters thought to be particularly relevant for climate responses in colder areas, we can obtain a better understanding of the C dynamics and thereby reduce uncertainty connected to soil processes. A future goal is to couple the soil model to a land model with interactive vegetation, and although our present emphasis is on boreal systems, the incorporated processes are general and representative on a larger scale.

We introduce a vertically resolved, microbially explicit soil decomposition model, MIMICS+, which represents C and N flows between litter, microbial, and SOM pools. In this study the model is offline and forced with data produced by the Community Land Model v5.1 (CLM; Lawrence et al., 2019). C and N stock estimates from the CLM simulations represent a microbially implicit approach based on the traditional CENTURY model (Parton et al., 1988). Therefore, we compare the CLM and MIMICS+ results to investigate

the implications of including the processes and mechanisms mentioned above. To evaluate the model, we use a collection of soil profile data from forested, podzolic sites in Norway, covering a range of conditions representative of boreal systems (Strand et al., 2016). Our experimental setup is as follows: for a selection of 50 sites in Norway, we ran simulations with the CLM model to produce (a) input data needed to run MIMICS+ and (b) estimates of C and N stocks. We then ran MIMICS+ with the produced forcing data. The aims of the study are (1) to formulate a standalone, microbially explicit model capable of representing soil processes in boreal systems; (2) to evaluate model performance and model structure by comparing simulated vertical soil C content along a climatic gradient with observations and simulated soil carbon from the microbially implicit model CLM; and (3) to apply the model to perform an N enrichment experiment to investigate belowground responses to nutrient changes.

2 Model and methods

2.1 Model description

MIMICS+ is based on the MIMICS framework where microbial groups, litter, and soil organic matter are represented as separate pools (Wieder et al., 2015). In its current state, MIMICS+ is not coupled to a comprehensive land model and therefore needs prescribed C and N input and soil temperature and moisture, which it is set up to read from CLM history files. Mass balance equations, $\mathrm{d}P/\mathrm{d}t = \text{sources} - \text{sinks}$, determine the change at each time step for each pool, P. The model structure with pools and fluxes is illustrated in Fig. 1, and a detailed overview of mass balance and rate equations are provided in the Appendix; Tables A1 and A2 contain mass balance equations for C and N pools, respectively, while Tables A3 and A4 list C and N rate equations. Throughout the model description, fluxes referred to as CX or NX, where X is a number, can be found in the abovementioned tables and are illustrated as arrows in Figs. 1 and A1. A list of parameters is given in Table A5. By representing the same hydrologically and biogeochemically active layers as in CLM, MIMICS+ can represent the depth discretization of temperature- and moisture-dependent processes. For each layer the fluxes between the pools within the layer are calculated first, before the vertical transport is calculated. Unless otherwise stated, the equations below describe transport within one layer. The vertical transport is described in Sect. 2.1.4.

2.1.1 Litter and SOM pools

Organic C and N enter the litter and SOM pools as dead plant material. As in MIMICS (Wieder et al., 2015) and ORCHIDEE-SOM (Camino-Serrano et al., 2018), we separate between metabolic (labile) litter mainly originating from leaves and fine roots and structural litter, in which we also include coarse woody debris (CWD). For SOM we again follow the MIMICS approach with two protected SOM pools and one pool that is available for saprotrophic decomposition. Depolymerization and desorption move organic matter from chemically and physically protected pools, respectively, to the available pool (C11, C12, N11, N12). The depolymerization process represents the enzymatic breakdown of recalcitrant SOM and is thus modeled with an rMMK mechanism, while the desorption is a function of clay content, as this rate represents the physical desorption from mineral surfaces (Wieder et al., 2015). A total of 50 % of the incoming metabolic and structural litter go to physically and chemically protected SOM, respectively, as directly plant-derived SOM (C3, C4, N3, N4). The direct litter fluxes, together with microbial necromass (C13–C24, N13–N24) and a flux representing EcM enzyme production (C27), are the sources of input to the SOM pools. The microbial pools determine the rates of decomposition and thereby the transfer rates between the main storage pools – SOM and litter.

2.1.2 Microbial processes

MIMICS+ represents two different types of microbes: saprotrophs and mycorrhizal fungi. Within these two main groups we separate between two functional traits, giving four different microbial pools in total. We divide between saprotrophic fungi (SAPf; analogous to MIMICS k strategists) and bacteria (SAPb; analogous to MIMICS r strategists). Temperature-sensitive reverse Michaelis–Menten kinetics, together with a moisture modifier (Wieder et al., 2017), determine the rates at which saprotrophs decompose substrate from the two litter pools and the available SOM (C5–C10, N5–N10). The N fluxes are determined by the stoichiometry of the substrate pools. During decomposition, a fraction of the incoming C is lost from the soil as heterotrophic respiration (HR), while the rest contributes to saprotrophic biomass. The respired fraction is determined by the carbon use efficiencies $\mathrm{CUE_b}$ and $\mathrm{CUE_f}$, which have maximum values of 0.4 and 0.7 for bacteria and fungi, respectively, but is reduced under low-nutrient conditions. This is based on the theory that microbes adjust their efficiencies to maintain a relatively constant, low C : N ratio despite the higher C : N ratio of substrates (Mooshammer et al., 2014b). The C : N ratio of the model saprotrophs is assumed to be constant ($\mathrm{CN_b} = 5$ and $\mathrm{CN_f} = 8$, Table A5). To ensure that this ratio is fulfilled in each layer and time step (in addition to potentially reducing CUE), N is exchanged between the saprotrophs and the inorganic pools (N36 and N37). The exchange rates can be positive or negative, leading to either immobilization or mineralization of inorganic N. We first calculate the uptake and demand of N to determine if there is enough to meet the requirement for optimal

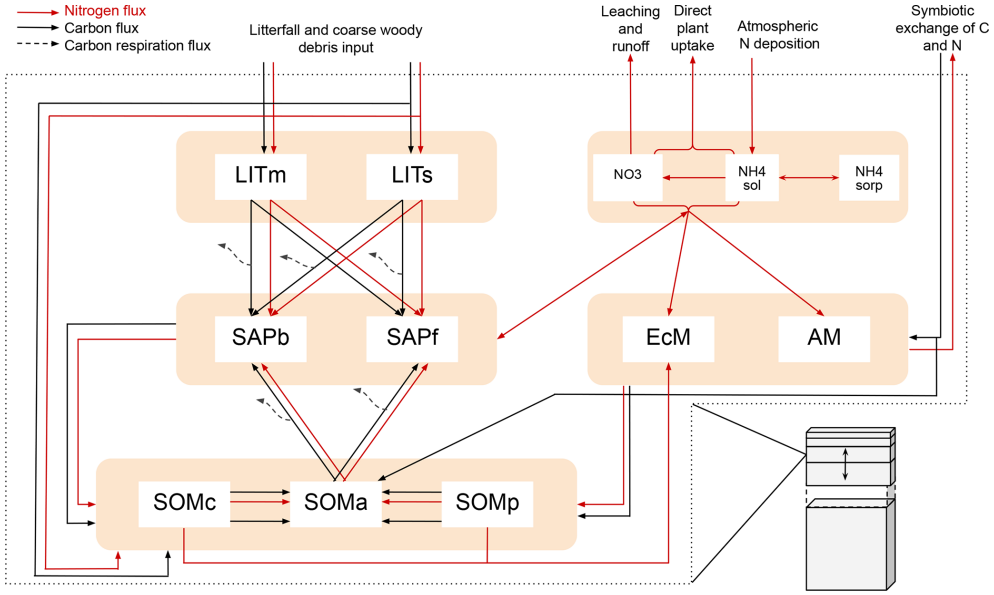

Figure 1. Schematic showing C and N flows within each layer of the model. The black arrows indicate carbon fluxes ($\mathrm{g\,C\,m^{-3}\,h^{-1}}$), while the red arrows indicate nitrogen fluxes ($\mathrm{g\,N\,m^{-3}\,h^{-1}}$). The dashed black arrows symbolize C leaving the system as heterotrophic respiration. Metabolic and structural litter: LITm, LITs. Saprotrophic bacteria and fungi: SAPb, SAPf. Ecto- and arbuscular mycorrhizal fungi: EcM, AM. Chemically protected, available, and physically protected soil organic matter: SOMc, SOMa, SOMp. Inorganic N in the form of NO_3, NH_4 in solution, and NH_4 sorbed to particles: NO_3, $NH4_{sol}$, and $NH4_{sorb}$, respectively.

saprotrophic functioning.

$$N_{\mathrm{demand},x} = \frac{\mathrm{CUE}_x \cdot (\mathrm{FC}_{\mathrm{LITm,SAPx}} + \mathrm{FC}_{\mathrm{LITs,SAPx}} + \mathrm{FC}_{\mathrm{SOMa,SAPx}})}{\mathrm{CN}_x}, \quad (1)$$

$$N_{\mathrm{uptake},x} = \mathrm{NUE} \cdot (\mathrm{FN}_{\mathrm{LITm,SAPx}} + \mathrm{FN}_{\mathrm{LITs,SAPx}} + \mathrm{FN}_{\mathrm{SOMa,SAPx}}) \quad (2)$$

Here, x represents either b (bacteria) or f (fungi), and NUE is nitrogen use efficiency, further described below. This results in one of four possibilities:

1. The N demand is greater than the uptake for both bacteria and fungi, meaning both groups will immobilize inorganic N. In this case we check if there is enough available inorganic N to fulfill the demand from both groups. If not, CUE is reduced (according to Eqs. 3 and 4) so that the saprotrophs utilize all N that is available to them, before the demand is recalculated. Here, $N_{\mathrm{for\_sap}}$ refers to the sum of the available N pools, $N_{\mathrm{NH_4,sol}}$ and $N_{\mathrm{NO_3}}$:

$$\mathrm{CUE_b} = \frac{(f_\mathrm{b} \cdot N_{\mathrm{for\_sap}} + N_{\mathrm{uptake,b}} \cdot \mathrm{d}t) \cdot \mathrm{CN_b}}{(\mathrm{FC}_{\mathrm{LITm,SAPb}} + \mathrm{FC}_{\mathrm{LITs,SAPb}} + \mathrm{FC}_{\mathrm{SOMa,SAPb}}) \cdot \Delta t}, \quad (3)$$

$$\mathrm{CUE_f} = \frac{((1 - f_\mathrm{b}) \cdot N_{\mathrm{for\_sap}} + N_{\mathrm{uptake,f}} \cdot \mathrm{d}t) \cdot \mathrm{CN_f}}{(\mathrm{FC}_{\mathrm{LITm,SAPf}} + \mathrm{FC}_{\mathrm{LITs,SAPf}} + \mathrm{FC}_{\mathrm{SOMa,SAPf}}) \cdot \Delta t}, \quad (4)$$

where f_b determines the division of the available inorganic N between bacteria and fungi and is calculated as

$$f_\mathrm{b} = \frac{(N_{\mathrm{demand,b}} - N_{\mathrm{uptake,b}})}{((N_{\mathrm{demand,b}} - N_{\mathrm{uptake,b}}) + (N_{\mathrm{demand,f}} - N_{\mathrm{uptake,f}}))}. \quad (5)$$

Equations (3) and (4) reduce CUE (and increase the respired fraction) enough to maintain the C : N ratios under the prevailing conditions, and the resulting exchange rates are

$$\mathrm{FN}_{\mathrm{IN,SAPb}} = f_\mathrm{b} \cdot N_{\mathrm{for\_sap}}, \quad (6)$$

$$\mathrm{FN}_{\mathrm{IN,SAPf}} = (1 - f_\mathrm{b}) \cdot N_{\mathrm{for\_sap}}. \quad (7)$$

2. N uptake is larger than demand for both saprotrophic groups, meaning both will mineralize inorganic N. The mineralized N will enter the $N_{\mathrm{NH4_{sol}}}$ pool.

3. Fungi will mineralize N (uptake > demand), while bacteria immobilize N (uptake < demand). In this case bacteria can access the N mineralized by fungi in addition to the inorganic N if needed.

4. Bacteria will mineralize N (uptake > demand), while fungi immobilize N (uptake < demand). In this case fungi can access the N mineralized by bacteria in addition to the inorganic N if needed.

Saprotrophic necromass is transferred to the SOM pools and is partitioned between the three pools based on clay content of the soil and the metabolic fraction of incoming litter (C13–C18 and N13–N18). Only a fraction of the N released during decomposition is directly available to saprotrophs, determined by the NUE (constant NUE = 0.8, Mooshammer et al., 2014a). The remaining fraction is transferred to $N_{NH_4,sol}$.

The model represents two different types of mycorrhizal fungi: EcM and AM. The mycorrhizal pools receive a C supply from plants and in return provides N to its associated plants. How the incoming carbon ($I_{veg,Myc}$, cf. C28 and C29) is partitioned between EcM and AM is determined dynamically through a return on investment (ROI) function based on the method from Sulman et al. (2019). The partition between EcM and AM is determined as a fraction,

$$f_{alloc,i} = \frac{ROI_i}{\Sigma_i ROI_i}, \tag{8}$$

where ROI_i is the nitrogen return of the carbon investment from the mycorrhizal association i (EcM or AM):

$$ROI_i = \frac{N_{acquired,i} \cdot \tau_{myc,som} \cdot CUE_i}{C_i}. \tag{9}$$

EcM acquires N from the protected SOM and inorganic N pools ($N_{acquired,EcM}$ = N25+N26+N27), while AM only acquires inorganic N ($N_{acquired,AM}$ = N28). $\tau_{myc,som}$ is the mycorrhizal turnover time, while CUE_i is the growth efficiency for mycorrhizal association i. N25 and N26 represent ectomycorrhizal mining for N (Lindahl and Tunlid, 2015). By releasing enzymes (C27), EcM accesses N from protected SOM, and at the same time releases C to the available SOM pool (C25 and C26). The enzyme production is modeled as a fraction of the incoming carbon (C28) that is directed into the SOMa pool instead of the EcM pool (C27). The mining algorithm is based on Baskaran et al. (2017), with mycorrhizal "decomposition" modeled as a multiplicative function of mycorrhizal biomass, SOM, and a decay rate (K_{mo}, Table A5). We use this expression together with the C : N ratio of the substrate pool to determine the amount of nitrogen acquired through ectomycorrhizal mining (N25 and N26).

As the mycorrhizal pools are assumed to have constant C : N ratios, a part of the acquired N is used to fulfill the stoichiometric constraint. Any additional acquired N leaves the soil system as N supply to the plant. The prescribed C supply from CLM is zero during the winter months, so to ensure that the mycorrhizal fungi do not provide "free" N to the plant during this time, we introduce the following scaling factor:

$$r_{myc} = \frac{I_{veg,myc}(t)}{\max(I_{veg,myc})}. \tag{10}$$

Here, $I_{veg,myc}(t)$ ($g\,C\,m^{-2}\,h^{-1}$) is the time-varying C supply from vegetation (prescribed from CLM), and $\max(I_{veg,myc})$ is the maximum value of $I_{veg,myc}$ in the current year. This scaling factor means that the mycorrhizal fungi are most effective when they receive the most energy in the form of C. Since $I_{veg,myc}(t)$ is prescribed in the current model version, the input flux will not respond to changes in soil N availability. Constant mortality rates determine the transfer from mycorrhizal fungi to the SOM pools (C19–C24 and N19–N24).

2.1.3 Inorganic N processes

Inorganic N is divided between nitrate and ammonium dissolved in soil water (N_{NO_3} and $N_{NH_4,sol}$) and ammonium sorbed to soil particles ($N_{NH_4,sorb}$). Reactive nitrogen from atmospheric deposition enters $N_{NH_4,sol}$ (N32) where it can undergo nitrification to N_{NO_3} (N34) or become sorbed to particles (N35). N_{NO_3} is exposed to leaching and runoff based on CLM algorithms (N31). Both dissolved pools, $N_{NH_4,sol}$ and N_{NO_3}, can be taken up by mycorrhizal fungi (N27, N28) or directly by plants (N33). Since the model is not coupled to aboveground vegetation, direct plant uptake is a constant loss rate of the available inorganic N (k_{plant}). We assume that processes in boreal forests are relatively slow and that the residence times of the pools are much longer than the 1 h time step. We therefore apply a sequential approach to model the mass balance of the inorganic N pools. Within a time step (1 h) the different processes affecting inorganic N are calculated in a sequence: (1) deposition, leaching, and runoff; (2) nitrification; (3) N from decomposition; (4) direct uptake by vegetation; (5) uptake by mycorrhiza; (6) exchange with saprotrophs; and (7) the Langmuir sorption algorithm. The Langmuir sorption algorithm is based on Sieczka and Koda (2016) and described below. The basis for this process is cation exchange, where positively charged ammonium is adsorbed to negatively charged clay particles. Before step (7) the total concentration of ammonium is

$$N_{NH_4,tot} = N_{NH_4,sorp} + N_{NH_4,sol}. \tag{11}$$

Using Eq. (11) together with the Langmuir isotherm equation, we find the equilibrium partition between $N_{NH_4,sol}$ and $N_{NH_4,sorp}$ given the total concentration $N_{NH_4,tot}$. The Langmuir isotherm equation is given by

$$N_{NH_4,sorp,eq} = \frac{NH4_{sorp,max} \cdot K'_L \cdot N_{NH_4,sol,eq}}{1 + K'_L \cdot N_{NH_4,sol,eq}}, \tag{12}$$

where K'_L is a Langmuir constant related to adsorption energy and a function of soil water content. $NH4_{sorp,max}$ is the maximum adsorption capacity. We assume that the system moves towards the equilibrium value during the time step, via the following mechanism, derived from the pseudo-second-

order kinetic model in Sieczka and Koda (2016):

$$N_{\mathrm{NH_4,sorp}} = \begin{cases} N_{\mathrm{NH_4,sorp,eq}} - \dfrac{1}{\frac{1}{N_{\mathrm{NH_4,sorp,eq}} - \mathrm{NH4_{sorp,prev.}}} + k \cdot \Delta t} & N_{\mathrm{NH_4,sorp,eq}} > N_{\mathrm{NH_4,sorp,prev}}, \\ N_{\mathrm{NH_4,sorp,eq}} + \dfrac{1}{\frac{1}{N_{\mathrm{NH_4,sorp,prev}} - N_{\mathrm{NH_4,sorp,eq}}} + k \cdot \Delta t} & N_{\mathrm{NH_4,sorp,eq}} < N_{\mathrm{NH_4,sorp,prev}}, \\ N_{\mathrm{NH_4,sorp,prev}} & N_{\mathrm{NH_4,sorp,eq}} = N_{\mathrm{NH_4,sorp,prev}}. \end{cases} \quad (13)$$

Here k is a rate constant, and Δt is the time step. The top option corresponds to absorption, the middle option to desorption, and the third option to no N exchange between sorbed $N_{\mathrm{NH_4}}$ and $N_{\mathrm{NH_4}}$ in solution (i.e., equilibrium has already been reached). All parameter values are from Sieczka and Koda (2016), converted to appropriate model units (see Table A5).

2.1.4 Vertical structure

The discrete vertical layers of the model follow the same structure as CLM with increasing layer thickness with depth (Lawrence et al., 2019). This allows incoming litter and N deposition to be distributed following the same vertical profile as in CLM. We use vertically resolved soil temperature and soil moisture from CLM as inputs to MIMICS+. We also use drainage and runoff rates from CLM to determine N leaching. Within each time step the fluxes between the pools are calculated and applied first, then vertical transport is calculated and applied. This transport is calculated as a simple diffusion equation between adjacent layers (Soetaert and Herman, 2009), using a constant diffusion coefficient from Koven et al. (2013). As the vertically resolved soil temperature and soil moisture from CLM are used in MIMICS+, the saprotrophic decomposition rates that are functions of these variables have a depth dependency in the model. The mycorrhizal N uptake is a function of the amount of mycorrhizal biomass and inorganic N (and SOM for EcM) in the soil layer; hence uptake can vary with depth.

2.1.5 Parameter sensitivity analysis

To test the soil C sensitivity to different model parameters, we performed a sensitivity analysis on 16 key parameters. For one parameter at a time, we either increased or decreased the value by 25 % compared to the default, giving a total of 32 experiments which were performed for each of the 50 sites simulated in this study (see Sect. 2.2).

2.2 Soil profile database

For comparison, a forest soil database collected in connection with the International Co-operative Programme on Assessment and Monitoring of Air Pollution Effects on Forests (ICP Forests) monitoring program level 1 sites was used (Lorenz, 1995). These data have been further analyzed by Strand et al. (2016) and provide a unique source of information about boreal soil conditions. A total of 1040 soil profiles were described, sampled, and analyzed between 1988 and 1992 (Esser and Nyborg, 1992). Soil profile descriptions were done according to standardized procedures (Sveistrup, 1984) and classified according to the Canadian System of Soil Classification (CSSC). Relevant information from the database includes C and N stocks, mean annual temperature (MAT), and mean annual precipitation (MAP). Specifically, the database contains C content down to 30, 50, and 100 cm, making it possible to compare vertically modeled C stocks to observations in these depth intervals. The dataset also contains separate measurements of C and N in the organic litter, fermented, and humic (LFH) layer and mineral soil. The organic layer consists of more or less decomposed litter, and although not directly comparable to modeled litter and SOM pools, the C : N ratio in organic vs. mineral soil is still a useful quantity for model evaluation purposes. A more detailed description of the database is given in Strand et al. (2016). Because podzols are the most common soil category in Norwegian forests, we chose to focus on the podzolic sites in the dataset, giving a total of 578 sites. Due to computational resource limitations, we chose a subset of 50 representative sites (out of the 578) for the site simulations with CLM and MIMICS+. The remaining 528 sites were used for further comparison with the modeled carbon stocks. The 50 sites cover an area from 5 to 70° N latitude and from 5 to 29° W longitude. The MAT varies from −1.3 to 7 °C, while MAP ranges from 356 to 2510 mm $\mathrm{yr^{-1}}$.

2.3 Simulation setup

For the subset of 50 sites, we performed single-site simulations using CLM5.1 in biogeochemistry (BGC) mode. Data from these simulations were used both to force MIMICS+ and to compare the C and N stocks as calculated by the standard decomposition model in CLM. The CLM variables that are used to force MIMICS+ are listed in Table A6. For the simulations we assume that all C allocated to active N uptake by plants in CLM is directed to mycorrhiza (in default CLM this C is assumed to directly respire).

The observations were performed during the years 1988–1992, so we ran the models up to and including 1992 and averaged model values over the 5 years. Unless otherwise stated, these averages are what is used for the comparisons. The three datasets each containing data from 50 sites are referred to as observations from the database (OBS), CLM simulations (CLM), and MIMICS+ simulations with CLM forcing (MIMICS+). An overview of the yearly mean input of carbon and nitrogen is shown in Fig. C1.

For the CLM simulations, a single-site configuration with 100 % natural vegetation was used together with atmospheric

forcing from the Global Soil Wetness Project forcing dataset (GSWP3; https://hydro.iis.u-tokyo.ac.jp/GSWP3/, last access: 1 September 2023). This is the default atmospheric forcing for CLM and provides 3 h data with 0.5° resolution. Following CLM spin-up protocol (Lawrence et al., 2019), all sites were spun up for 500 years in "accelerated-decomposition" mode followed by 700 years of "regular spin-up" by recycling atmospheric forcing for 1901–1930. For the 1850–1900 period, the atmospheric forcing cycles the years 1901–1920, then historical forcing was used until the end of the simulation.

As with the CLM simulations, MIMICS+ needs to be spun up to equilibrium before running a historical period. The spin-up was performed from arbitrary initial concentrations by recycling monthly averages of soil temperature and moisture, N deposition, litter, and C input from the CLM history files for the years 1850–1869 (during which atmospheric forcing was used from 1901–1920) for 1000 years.

2.3.1 Comparison of climate gradient profiles

To examine how well the models capture variation with temperature, the three datasets (OBS, MIMICS+, CLM) were sorted by increasing MAT. The first half ($N = 25$) was labeled "cooler", while the second half ($N = 25$) was labeled "warmer". To capture variation in moisture, the sites were sorted by MAP in the same manner, with the first half labeled "drier" and the second half labeled "wetter". Because the MAP and MAT data from the observations and the model forcing differ, some sites ended up in different categories depending on whether they were sorted by the observed or forcing climate data (12 sites for MAT and 8 sites for MAP). We split the dataset in the following way – OBS by observed climate and MIMICS+ and CLM by model forcing climate – because we investigated sensitivities to temperature and precipitation. (Figure S1 in the Supplement shows results of this analysis with all points classified according to their OBS climate.) The MAT and MAP intervals for each category are given in Table 1. For some sites the measured soil depth was shallower than 50 or 100 cm. These sites, where the depth to bedrock was less than 50 or 100 cm, were removed from both the model and the observation datasets before making distribution boxplots for these depth intervals.

2.3.2 N enrichment experiment

To investigate the response modeled by MIMICS+ to N enrichment, we performed an idealized N addition experiment. Starting from spun-up conditions, we ran two parallel simulations for all 50 sites for 30 years: one "control", using N deposition from the CLM runs, and one "treatment", with an extra amount of $15\,\mathrm{g\,N\,m^{-2}\,yr^{-1}}$ deposited. This is a common amount used in forest fertilization (Högberg et al., 2017). The additional nitrogen was added equally in each time step throughout the second simulation year to give a total of $15\,\mathrm{g\,N\,m^{-2}}$. We used these simulations to investigate the temporal response ratios (RRs: treatment : control) for different C and N pools, as well as for HR.

3 Results

3.1 Comparison of modeled and empirical C and N stocks

Observed and modeled soil carbon stocks are shown in Fig. 2. Both models capture the general trend of decreasing C concentration with increasing depth. The modeled mean C stocks of MIMICS+ across the 50 sites are closer to observations in the 0–30 cm depth interval, while the CLM simulations clearly underestimate C stocks (both models are significantly different from the subset of observations, $p < 0.05$). The models both underestimate carbon at the 30–50 cm interval, while there is no significant difference between the modeled and observed C content in the deepest layer. Due to the heterogeneous nature of real soils and the impact of differences in litter production between the sites, a larger variability in the observations compared to the simulations is not unexpected. However, site-to-site comparisons with observations are poor for both models but marginally better for MIMICS+ (Fig. 2d–f). This is likely explained by subgrid variability in the observations that are not captured by the models and their forcing. As the model is intended to work on larger spatial scales within an ESM model, a good one-to-one match with specific sites is of less importance than being able to capture larger patterns in temperature and moisture. By looking at the collection of sites together, we remove some of the uncertainty related to the variability between the sites and focus on larger patterns in our analyses. There is no significant difference between the two observational subsets, meaning that the 50 sites chosen for the direct model comparison are representative of the broader region.

Looking at C : N ratios, the overall picture with a higher ratio in the forest floor (observations) and litter pools (models) than in the total soil is captured by both models, with MIMICS+ again being closer to the observed values (Fig. 3a and b). Both models have significantly lower C : N ratios in the total as well as in the mineral soil, but MIMICS+ has significantly higher values than CLM ($p < 0.05$). For the litter pools, the pattern is the opposite, and the models have significantly higher C : N litter ratios than those observed in the LFH layer. The modeled litter pools are not directly comparable to the LFH layer, but we get an indication of how the modeled C : N ratio compares to the partly decomposed matter. Both models have higher mean values and greater variability than the observations (Fig. 3c). This is expected as the observed LFH layer is partly decomposed and would therefore have lost some C compared to the simulated litter pools which have not yet been affected by the decomposition processes. In addition, the modeled litter pools contain some

Table 1. MAT and MAP intervals for dividing the sites into climate categories.

Data source	Cooler [°C]	Warmer [°C]	Drier [mm yr^{-1}]	Wetter [mm yr^{-1}]
Observed	(−1.3)–2.5	2.6–7.1	355–975	1009–2510
Model forcing	(−1.8)–3.8	3.9–8.1	494–1243	1244–3606

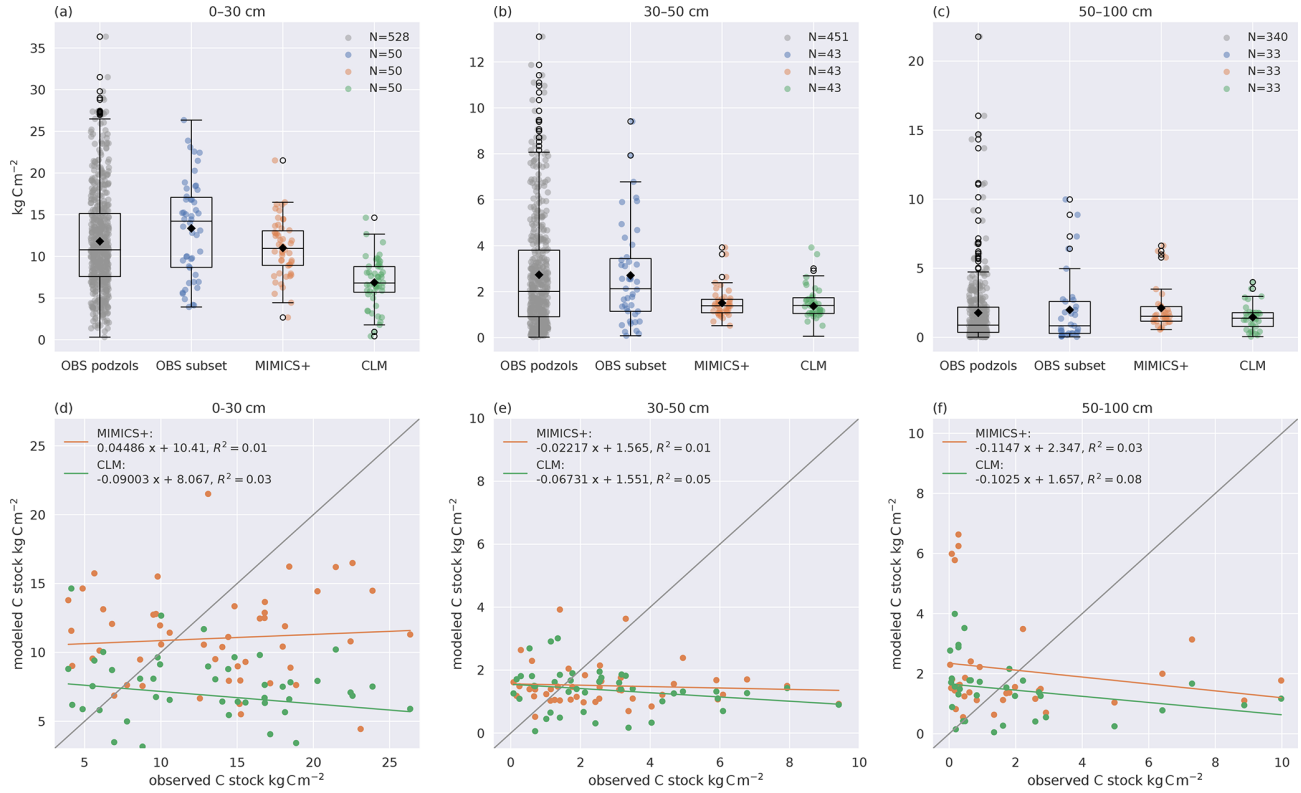

Figure 2. Modeled and observed C stocks. **(a–c)** Boxplots of C stocks in **(a)** 0–30, **(b)** 30–50, and **(c)** 50–100 cm soil depths for all observed podzols except the 50 modeled ones (left) and the 50 modeled sites (center left) from Strand et al. (2016), simulated with MIMICS+ (center right) and with CLM (right). The line in each box is the median, while the diamonds mark the mean values. The box's upper and lower edges are the 75th and 25th percentiles, respectively. The whiskers extend from the box by 1.5 times the interquartile range. Note the different scales on the y axes. As not all observed soil profiles reach a depth of 30–50 or 50–100 cm, these sites are omitted in all boxplots for these depths; hence $N = 43$ for **(b)** and $N = 33$ for **(c)**. **(d–f)** Scatterplots of observed (x axis) and modeled (y axis) C stocks in **(d)** 0–30, **(e)** 30–50, and **(f)** 50–100 cm soil depths. The legend shows the slope, intercept, and R^2 for the linear regression line fitted to the scatter points. The 1 : 1 line is added in grey for reference.

low-quality (high C : N ratio) CWD, which is not included in the LFH samples.

The observed total C : N ratio ranges from 12–45 with a mean value of 28, while MIMICS+ and CLM have mean values of 23 and 11, respectively. The range of C : N values from the models is narrower than that of the observations, with MIMICS+ values ranging from 12–38 and CLM only between 11–12. The large variability among the observations indicates the influence of local conditions on a subgrid scale. The fact that MIMICS+ has a larger variability than CLM indicates that differences in soil quality are captured better with the improved modeling framework. Microbial competition for N and a higher fraction of directly plant-derived SOM are factors contributing to this difference between the modeled C : N ratios. Figure 3d shows the C : N ratios simulated with MIMICS+ at three different depth layers. As expected, the top layer with more litter has the highest ratio, while in the middle and lowest layers the ratios are significantly lower. For the CLM simulations the C : N ratio is constant around 11 for all three depth intervals. Since we do not have access to observed vertical N stocks, it was not possible to produce this plot for the observed sites.

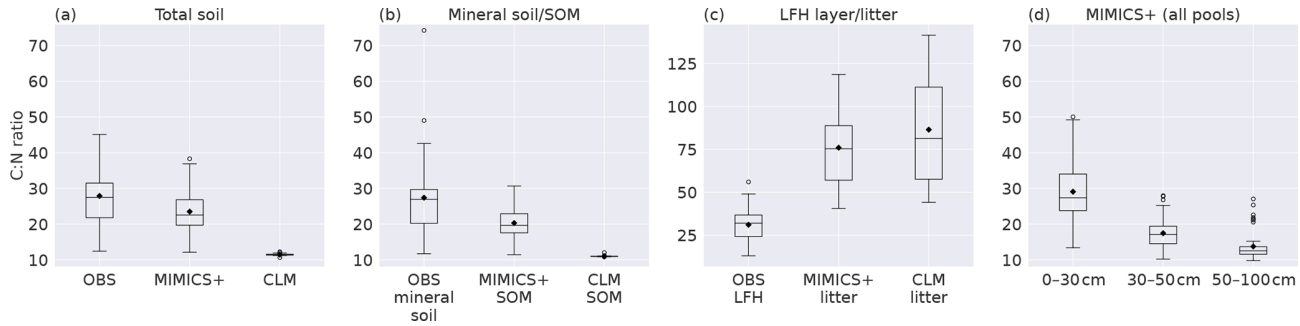

Figure 3. Boxplots of C : N ratios for observed values from Strand et al. (2016), MIMICS+, and CLM simulations of **(a)** the total soil, **(b)** mineral soil (observations) sum of SOM pools (models), **(c)** observed forest floor compared to the C : N ratio of simulated litter pools, and **(d)** total soil at different depths as simulated by MIMICS+. Inorganic N is not considered in any of the plots. The line in each box is the median, while the diamonds mark the mean values. The box's upper and lower edges are the 75th and 25th percentiles, respectively. The whiskers extend from the box by 1.5 times the interquartile range. $N = 50$ sites.

3.2 Modeled C pools in MIMICS+

In this section we look more in detail into model properties of MIMICS+. The sensitivity analysis showed that total soil C change using perturbed parameters was mostly within $\pm 10\,\%$ of the default values (Fig. B1). Modeled soil C was the most sensitive to the fraction of structural litter going directly to protected SOM, as well as mycorrhiza-related parameters (maximum CUE and mining decay rate K_{MO}). The sensitivity of total C to parameter values related to inorganic N was small.

With the current model parameterization, the SOM pools contain about 78 % of the total soil C (all nine pools, ref. Fig. 1), and 62 % of that are in the protected pools (SOMc and SOMp in Fig. 1). The litter pools contain most of the remaining C, while 1.2 % are microbial biomass (Fig. 4). The modeled percentage of microbes ranges from 0.3 %–2 % and is in agreement with the 1 %–3 % microbial biomass C typically reported for soils (Frey, 2019). The microbial respiration (HR) shows a clear seasonal pattern, with a stronger summer peak and winter limitation with MIMICS+ than with CLM (Fig. B4). Figure 4b shows the relative magnitude of each pool within a pool category. Mainly due to the relatively high CWD contribution to the input, the structural pool is the largest litter C pool (18 % of total C, 85 % of total litter C), while metabolic litter consisting of leaf and fine-root litter accounts for ca. 3 % of the total C and 15 % of total litter. The saprotrophic microbial biomass C dominates over the mycorrhizal fungi biomass C, and the saprotrophic fungi dominate over saprotrophic bacteria (mean saprotrophic F : B biomass ratio of 2 and above 1 for all sites). This is largely a consequence of the parameter choices in the model and are further discussed in Sect. 4.

For the focus region of this study (boreal sites in Norway), total C (TOTC) is strongly correlated with both MAT and C input (+0.49 and +0.65, respectively), indicating that higher plant productivity at warmer sites is an important control on total soil C in the MIMICS+ simulations (Fig. 5). The CUE presented in Fig. 5 is calculated as the ratio of the total microbial C uptake in biomass over the total C uptake (including respiration). CUE is positively correlated with available N, pointing to higher microbial efficiencies at sites with higher nutrient content. This is also illustrated by the positive relationship between the percentage of microbial biomass (pct_microbes) and available inorganic N (+0.41 for $N_{\mathrm{NO_3}}$ and +0.62 for $N_{\mathrm{NH_4,sol}}$). The negative correlation between CUE and MAT is likely explained by lower-quality litter input at warmer sites, as there is a positive relationship between the C : N ratio of the litter input and temperature ($+0.46\, p < 0.001$, not shown). The lower litter quality causes reduced CUE and hence a negative relationship between temperature and CUE. The strong correlation between production (C_input) and HR (+0.81) indicates that most sites are close to equilibrium. Lower litter quality at high-production (and high-respiration) sites can explain the negative relationship between CUE and HR. There is a negative correlation (−0.64) between CUE and total C.

The fungal : bacterial saprotrophic biomass ratio (FB ratio) is negatively correlated to available inorganic N (−0.29 for $N_{\mathrm{NO_3}}$ and −0.27 for $N_{\mathrm{NH_4,sol}}$), reflecting the stricter stoichiometrical constrain on bacteria. There is a strong negative correlation between the percentage of microbes and the fungal : bacterial ratio (−0.78), reflecting that sites with more available N are more favorable for microbial growth in both pools but most beneficial for bacteria.

All three inorganic N pools are negatively correlated with MAP (−0.30 for $N_{\mathrm{NO_3}}$, −0.29 for $N_{\mathrm{NH_4,sol}}$, and −0.38 for $N_{\mathrm{NH_4,sorp}}$) and $N_{\mathrm{NH_4,sorp}}$ also with soil water (−0.37). This indicates that the modeled microbes also respond to moisture conditions through the effects of moisture on inorganic N processes (leaching, runoff, and sorption of NH_4), which contribute to making N unavailable, and not only through the modifications of the reverse Michaelis–Menten kinetics.

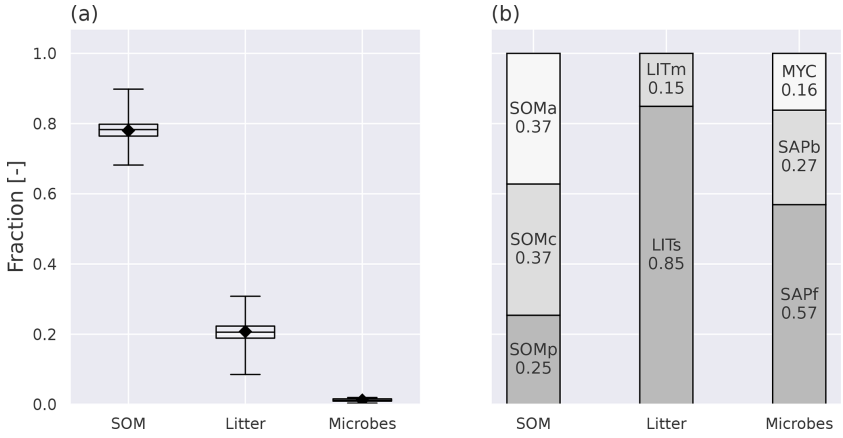

Figure 4. Annual mean pool fractions as simulated by MIMICS+. **(a)** The fractions of total C stored in the main pool categories, soil organic matter (SOM), litter, and microbes. The box's upper and lower edges are the 75th and 25th percentiles, respectively. The whiskers extend from the box by 1.5 times the interquartile range, and $N = 50$ sites. **(b)** The fraction of C in each pool within each main pool category. MYC covers both EcM and AM, as the AM contribution is so small that it would not be visible on its own.

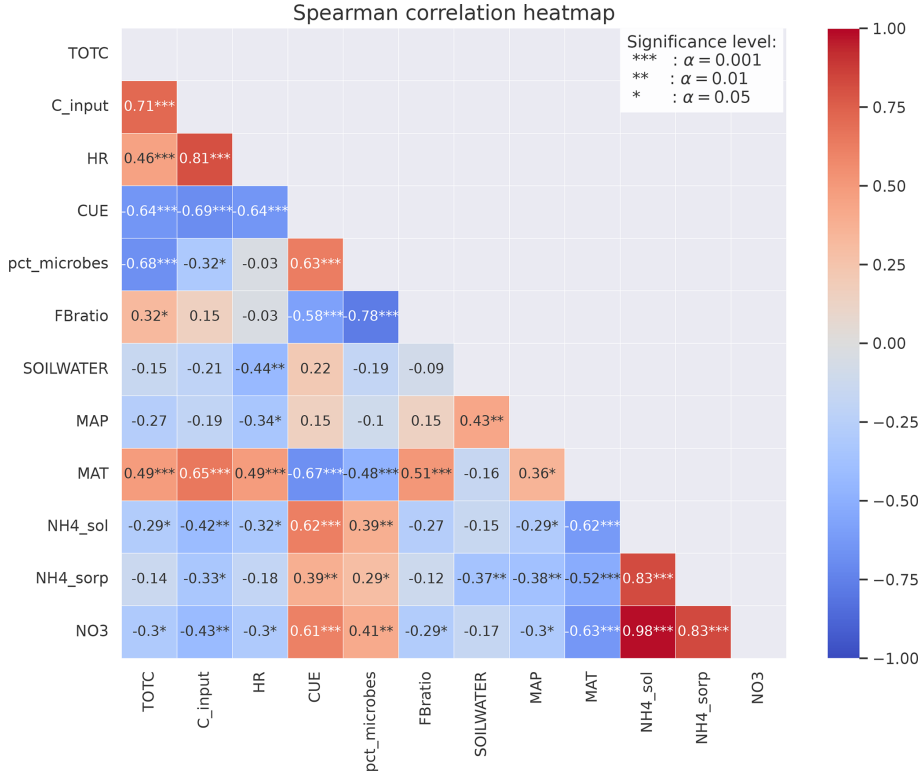

Figure 5. Spearman's correlation coefficients between different variables calculated from MIMICS+ simulations of the 50 sites. The stars represent the significance level of the correlation. Numbers without stars are not significant ($p > 0.05$). The colors indicate whether the correlation is positive (red) or negative (blue), and the shades indicate the strength of the correlation.

3.3 Comparison of climate gradient profiles

In Fig. 6 the 50 sites have been divided into two subsets of 25 sites based on the climate categories described in Sect. 2.3.1. (Figure S1 shows the result of the division of sites based only on the observed climate.) Figure 6a–c show lower carbon stocks for colder sites than for warmer sites for both models and observations for all three depth intervals, indicating that the models are broadly able to capture the temperature-dependent processes that govern the C storage in soils. As shown in Fig. 5, the modeled C input is positively correlated with MAT and total soil C, indicating that the difference is

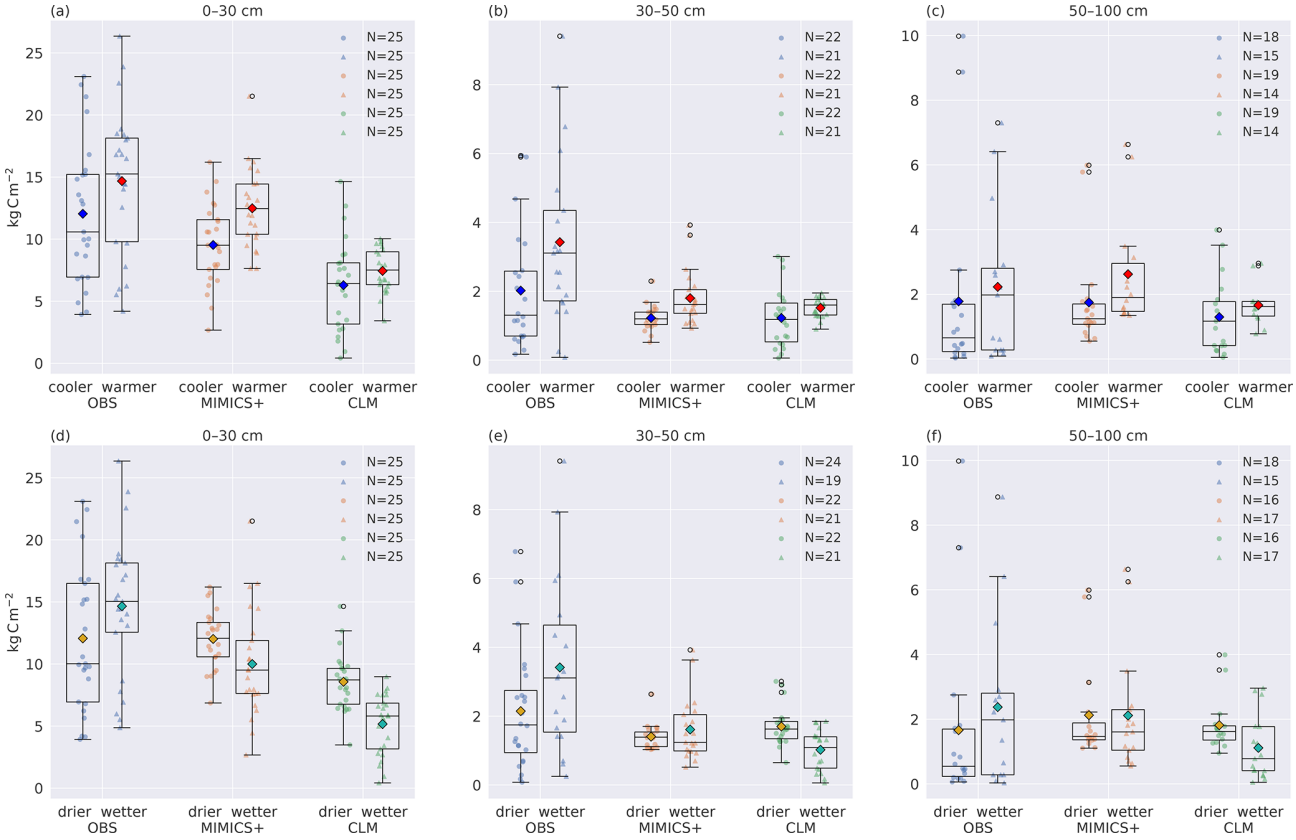

Figure 6. Total carbon stocks for cooler and warmer **(a–c)** and dryer and wetter **(d–f)** parts of the dataset. Boxplots of carbon stocks in the **(a, d)** top 30, **(b, e)** 30–50, and **(c, f)** 50–100 cm soil depths for observed profiles from Strand et al. (2016) (left), simulated with MIMICS+ (center) and with CLM (right). In **(a–c)** the leftmost quartiles represent the coldest 50 % of the dataset, while the rightmost represent the warmest 50 % of the dataset. In **(d–f)** the leftmost boxes represent the drier 50 % of the total subset, while the rightmost represent the wetter 50 %. The line in each box is the median, while the diamonds mark the mean values. The diamond color represents the climate category: yellow – drier, turquoise – wetter, blue – cooler, red – warmer. The box's upper and lower edges are the 75th and 25th percentiles, respectively. The whiskers extend from the box by 1.5 times the interquartile range.

mainly caused by differences in litter input. The MIMICS+ simulations show a significant difference between the cold and warm mean C content ($p < 0.05$) for all depth intervals, while the cold and warm means from the CLM simulations are not significantly different ($0.14 < p < 0.29$). This indicates that MIMICS+ temperature dependencies have a larger impact on soil C sequestration than the standard CLM formulation since the C inputs and soil temperatures are the same for the two models.

Figure 6d–f show that in the observations, the drier sites have a lower mean C stock than the wetter sites (but not significantly). This is the opposite of the modeled results; both models show higher mean C content for the drier sites than for the wetter sites. For MIMICS+ this discrepancy is only evident in the top layer, whereas for the lower layers, there are no significant differences between the drier and wetter sites. For the CLM simulations, the pattern is consistent and significant for all three depth intervals ($p < 0.05$). The influence of moisture on decomposition is represented differently in the two models, which can explain some of the difference between the modeled values. This is further discussed in Sect. 4.3.

3.4 N enrichment experiment

The responses to the N enrichment experiment are a result of how the extra reactive N (15 g N m^{-2} distributed evenly during 1 year) is distributed between the inorganic nitrogen pools after addition (Fig. 7a). All extra N is added to the $N_{NH_4,sol}$ pool, which had the largest response ratio of the three inorganic N pools. Some of this N will gradually move to N_{NO_3} via nitrification or to $N_{NH_4,sorp}$ through sorption. While N is lost from N_{NO_3} relatively fast via plant and microbial uptake and leaching, the extra sorbed N serves as a long-term supply of inorganic N, slowly releasing N back to the dissolved pool. This sustains the higher CUE of the microbes and leads to increased saprotrophic biomass for the duration of the 30-year simulation. Although $N_{NH_4,sol}$ has the

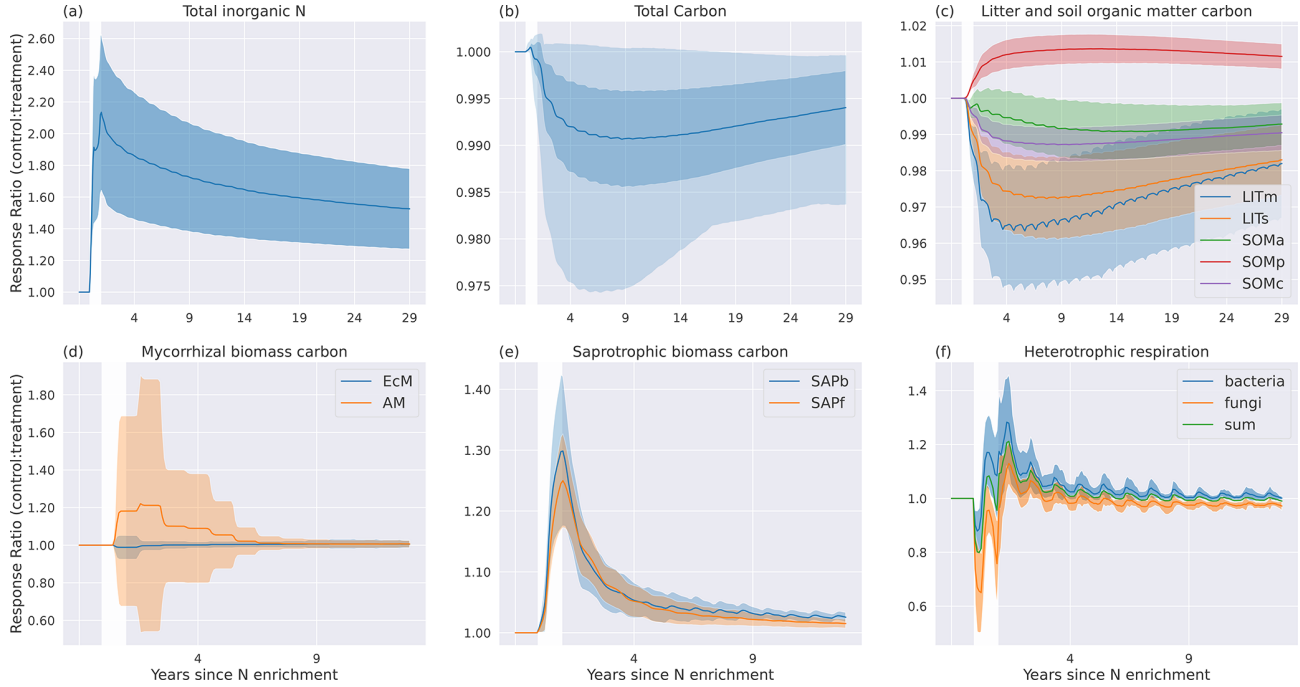

Figure 7. Temporal mean ($N = 50$ sites) response ratios (treatment : control) to experimental N enrichment for **(a)** $N_{NH_4,sol}$, **(b)** $N_{NH_4,sorp}$, **(c)** N_{NO_3}, **(d)** mycorrhizal fungi pools, **(e)** saprotrophic pools, **(f)** heterotrophic respiration, **(g)** total soil C, **(h)** litter pools, and **(i)** soil organic matter pools. The white area marks the year of N enrichment, and the shading indicates the standard deviation. In **(g)** the lighter shading indicates the total spread of the values.

largest relative response to N addition, the change in mass of N is the largest in the $N_{NH_4,sorp}$ pool.

Looking at each C pool response separately, we see the largest responses in the microbial pools (Fig. 7d and e). The extra inorganic N gives a relatively higher return on investment (ROI; Eq. 9) for AM, resulting in more C allocated to AM and less to EcM. The initial large response declines gradually but remains positive throughout the simulation period. Although there is a shift to more AM, the EcM carbon pool is always larger than the AM pool.

Both saprotrophic C pools respond instantly and positively to the N enrichment, with a maximum increase of about 25 % for fungi and 30 % for bacteria at the end of the N addition year. The increase in saprotrophic biomass is a result of higher CUE made possible by more available N. After the N enrichment year, the response gradually decreases until it stabilizes at around 1 % after ca. 5 years. The long-term response is marginally higher for bacteria than for fungi.

The initial response in HR (Fig. 7f) is a result of a lower respired fraction, $(1 - \mathrm{CUE})$, leading to increased saprotrophic biomass and thus gradually increased rates of litter decomposition. After the initial negative response in HR in the N enrichment year, there is a positive response due to the higher decomposition rate. For bacterial HR, the response ratio stabilizes at a low positive value, while for fungi it stabilizes at a slightly negative value. Combined, the response ratio is close to 0 for HR after approximately 4 years.

The positive microbial biomass responses result in initial decreases in the substrate pools, LITm, LITs, and SOMa (Fig. 7c). Most microbial necromass ends up in either the physically protected pool (SOMp) or the available pool (SOMa), leading to a positive response for SOMp, while the increased decomposition of SOMa keeps the response ratio below 1. The chemically protected pool experiences a small negative response because increased microbial biomass increases the rate of the depolymerization process that moves chemically recalcitrant SOM to the available SOM pool (C11). The responses in SOM and litter pools are weak, and following 1 year of N enrichment the mean response of total C is a marginal decrease compared to the control. It is worth noting that some sites experience markedly larger responses in total C than others (shading in Fig. 7b).

The overall response of the model illustrates that shifts in N availability have consequences for microbial C and N dynamics, although not necessarily for the total C storage and respiration. It should be noted that in this experiment we did not increase plant productivity and thus carbon input to the soil, which is expected after N enrichment. This also means that possible changes in plant–microbe competition for N were not captured. The added value of this experiment is that we isolate the in-soil processes and quantify the effects of added nutrients available to microbes and how this affects the soil carbon pools.

4 Discussion

This study aimed to introduce a microbially explicit soil decomposition model, MIMICS+, designed to represent key soil processes that control carbon and nitrogen processing in boreal ecosystems but still be general enough to be used within an ESM. The model was applied to investigate responses to an N enrichment experiment. The results show that the mean C stocks modeled with MIMICS+ match observations reasonably well, and for Norwegian forested podzolic sites the model performs on par with or better than the state-of-the-art land model CLM using a traditional decomposition formulation (Fig. 2a–c). However, both models showed poor one-to-one agreement with the observations (Fig. 2d–f), possibly due to local heterogeneity that is not captured by the models and inaccuracies in the model climate forcings. The C : N ratios from MIMICS+ are closer to observations than CLM, and the predicted fraction of microbial biomass matches well with values reported in the literature (Figs. 3 and 4). Several noteworthy correlations between variables were found from the MIMICS+ simulations (Fig. 5). Both models capture the climatic temperature pattern from the observed soil profiles, although they both struggle to represent the observed pattern in C concentrations emerging from the MAP categories (Fig. 6). The N enrichment experiment demonstrates the implications of adding the Langmuir algorithm for inorganic N, as the sorbed NH_4 works as a long-term supply of N for the microbes. The overall effect of the idealized enrichment experiment on soil C storage and respiration was minor, but it had interesting effects on the relative distribution of the microbial groups and shows the need for further investigation into the role of sorption–desorption processes of inorganic N, especially in N-limited areas like boreal forests (Fig. 7).

4.1 Comparison of modeled and empirical C and N stocks

Looking at the total distribution for the 50 sites, MIMICS+ is closer than CLM to the observations for the top layer (0–30 cm), and models are similar in the middle layer (30–50 cm), while none of the modeled means are significantly different from the observations in the bottom layer (50–100 cm). The site-to-site comparisons with observations were poor for both models, showing that there is a discrepancy between observed and modeled stocks at local scales. This challenge of local factors was illustrated by Pierson et al. (2022), who used the C-only version of MIMICS with optimized parameters based on local observations and showed reduced error in C stocks on smaller scales (catchments $< 50\,km^2$). Such methods would likely also reduce the errors in MIMICS+ at smaller scales. However, it is important to keep in mind that the intention with MIMICS+ is to develop a module that is simple and fast enough to be used in an ESM to simulate the soil carbon dynamics at a grid cell average scale. When forced with grid cell average input, it is not intended to and should not be expected to accurately describe local variation in soil carbon stocks. Upscaling of point observations of soil C stocks to a landscape level in our study area (Norwegian boreal forests) would be useful for comparison of ESM simulations with empirically based estimates of soil C stocks.

With the MIMICS-CN version, Kyker-Snowman et al. (2020) obtained soil C : N ratios that, although within observed ranges, had much lower maximums than the observed ratios. They suggested increasing the fraction of litter going directly to SOM, as forest soils (compared to agricultural and grassland soils) have been shown to contain a high fraction of C in plant residues (Grandy and Robertson, 2007). Our focus area is forested ecosystems, so we increased the fraction of litter going directly to protected SOM without going through microbial decomposition to 50 % for both structural and metabolic litter (these fractions also affect the total C; see Fig. B1). This leads to a longer lifetime of soil C (stored in protected pools) before it becomes available for microbial decomposition and respiration. The higher directly plant-derived fraction in the SOM pools increases the soil C : N ratio, although it is still lower than observed for total and mineral soil (Fig. 3). A recent study by Angst et al. (2021) indicates that the fraction of directly plant-derived SOM may be much higher than previously assumed, especially for forested sites and podzols. The high C : N ratios in our observational dataset point in the same direction, suggesting that the directly plant-derived fraction is an important factor to consider when modeling boreal soils. Our results demonstrate that we get closer to observed C : N ratios with MIMICS+ compared to the CLM formulation, a main reason being the high directly plant-derived fraction. In the CENTURY-based decomposition cascade in CLM, the C : N ratios of the SOM pools are fixed, which gives limited options to account for high C : N ratios and the implications that may have for soil C dynamics.

4.2 Modeled C pools in MIMICS+

The division of C between the different pools in MIMICS+ shows that most soil C is in the SOM pools (78 %), whereof 62 % are protected. This again reflects the relatively high fraction of litter going directly to protected SOM but also the lifetime of C in the protected pools before it is either depolymerized or desorbed into the available SOM pool. Compared to MIMICS-CN we doubled the desorption coefficient (see Table A5), but this is still 1 order of magnitude lower than the value used in the C-only version of MIMICS (Wieder et al., 2015). In the abovementioned studies and the present study, this parameter has been adjusted to match the observed data. In the model formulation, the desorption coefficient is a function of soil clay content, and more observational studies constraining this parameter as a function of clay content or

other observable variables would benefit further model development.

Saprotrophic fungi are the dominant microbial group in our simulations. Fungi are assumed to have a higher maximum CUE than bacteria in the model (0.7 vs. 0.4, respectively) and are more efficient at decomposing structural litter than the bacterial pool (higher V_{max} for decomposition of LITs by SAPf than SAPb). This is based on the assumption that fungal decomposers are more specialized towards recalcitrant substrates, while bacteria thrive on labile, easily accessible metabolic litter (Wardle et al., 2004). The fraction of CWD litter provided by CLM is relatively large at these forested sites, giving more substrate that is preferable for fungi. The Norwegian podzols we are looking at are nutrient poor, and fungal dominance is expected under N-limited conditions (Strickland and Rousk, 2010). Figure 5 indicates a negative relationship between available inorganic N and the F : B ratio, meaning a higher fraction of bacteria in more nutrient-rich conditions, in line with observations. Furthermore, the N enrichment experiment showed that bacteria had a larger positive response to the added N in the long term, which indicates that the model can capture shifts in microbial communities in response to N conditions.

The modeled saprotrophic fungal biomass C dominates over the mycorrhizal fungal biomass C. This is in contrast with an observational study on boreal forests that indicates that EcM can account for as much as 47 %–84 % of fungal biomass (Bååth et al., 2004). Moreover, Clemmensen et al. (2013) challenged the traditional view that C sequestration is mainly driven by the decomposition of aboveground litter by saprotrophs with their study that showed a dominance of root-associated fungi in deeper parts of the LFH in boreal forests. Few studies exist to inform models about fungal dominance in boreal systems, so parameters determining mycorrhizal growth and turnover are poorly constrained and not particularly adjusted for boreal conditions in this model iteration. The sensitivity analysis showed that the EcM mining rate (K_{MO}) and maximum mycorrhizal CUE in particular impact total modeled C (Fig. B1), highlighting the need for informing these parameters with representative observations. The C supply to mycorrhizal pools is prescribed directly from CLM output, and the growth of these pools is therefore governed by this input rate. Coupling MIMICS+ to the aboveground vegetation will allow the plant C supply to react to nutrient conditions in the soil and is a priority in future model development.

Regarding the correlations presented in this study (Fig. 5), one should always keep in mind that correlation does not imply causation, especially in a coupled non-linear system like this model. The analysis should be regarded as a broad investigation into possible relationships within the soil dynamics. Recently, Tao et al. (2023) presented CUE as a strong predictor of SOC globally and argued for a positive correlation between CUE and soil carbon storage (SOC) based on a combination of global-scale datasets, a microbial-process explicit model, data assimilation, deep learning, and meta-analysis. In contrast, our analysis showed a negative correlation between microbial CUE and soil carbon storage, in addition to a strong correlation between total carbon and plant litter input. A relatively large fraction of the litter input in MIMICS+ (50 %) initially omits the microbial pathway (affected by CUE) as directly plant-derived organic matter into protected SOM pools, which weakens the relationship between microbial CUE and TOTC. A high fraction of microbial necromass ends up in SOMa (Eqs. C13–C18 in Table A3 and parameters in Table A5). This leads to a relatively rapid recycling of the C that initially goes through the microbial pathway, which can also contribute to a weaker relationship between CUE and C storage than if larger fractions of the necromass ended up in the protected SOM pools. However, more microbially derived mass in the protected SOM pools will decrease the C : N ratio, taking modeled values further away from the observed C : N ratios in Strand et al. (2016). Tao et al. (2023) used a process-guided deep learning and data-driven modeling (PRODA) approach to optimize parameters in a microbially explicit model (Allison et al., 2010) using observations. Default model parameters prior to optimization gave a negative relationship between CUE and SOC, illustrating how model estimates rely on parameter choices. Using a similar approach to inform MIMICS+ can lead to more robust parameter values in future model iterations.

In MIMICS+ the availability of inorganic N is highly dependent on soil water processes because both N leaching from N_{NO_3} and the Langmuir isotherm algorithm are dependent on soil moisture. This is evident from Fig. 5, where we see a negative correlation between inorganic N pools and moisture-related variables (MAP and SOILWATER). The available inorganic N pools are again positively correlated with the percentage of microbes, giving an indirect dependence of microbes on soil moisture. The total C is negatively correlated with the percentage of microbes and has a high correlation with the incoming C. With higher temperatures, the model gives a higher turnover rate and thereby more release of soil C to the atmosphere. However, increased temperatures also stimulate plant production, especially in boreal and arctic regions, which can exceed or offset the effect of higher decomposition rates (Hobbie et al., 2002). The correlation patterns from our simulation indicate that the effect of temperature on plant production dominates the effect of temperature on decomposition rates in the model. Pierson et al. (2022) found that increased temperature sensitivity of the decomposition kinetics compared to the original MIMICS parameter values reduced error compared to their observational data, indicating that the temperature sensitivity in MIMICS and MIMICS+ may be too weak. However, the agreement between models and observations in Fig. 6a–c indicates that more plant production is the dominating effect of higher temperatures in Norwegian forests.

4.3 Comparison of climate gradient profiles

Although simple, dividing sites into different climatic categories serves as an idealized "space-for-time" investigation of climate change responses. Assuming that the climate in boreal forests in general and Norwegian forests specifically will get warmer and wetter in the future (Hanssen-Bauer et al., 2017), the observations indicate higher soil C content at sites with higher MAP and MAT. The models indicate higher C content for warmer sites but lower C content for the wetter sites, especially in the 0–30 cm layer. There is a positive correlation between MAT and MAP, particularly for the observed climate forcing (Fig. B3). When dividing the observed sites into the climate categories, a large fraction ends up as either cold and dry or warm and wet. We therefore did a simple "temperature-dependence removal" on the total podzol dataset ($N = 578$) by dividing the sites into narrow temperature intervals of 0.5 °C (Fig. S2). This did not reveal a clear pattern between the wetter and drier sites, and it is therefore difficult to disentangle the effects of moisture from the effects of temperature in the observed data. Since the models use soil moisture and not MAP to define parameters, we also analyzed the results using a soil moisture variable from the CLM simulations (SOILWATER_10CM) instead of MAP to discriminate between drier and wetter sites to investigate any effects on the climatic pattern (Fig. S3). This showed the same pattern as in Fig. 6d–f (more C in drier soils for the models and less C in drier soils for observations) for all three distributions, except for the deepest layer, where the trend shifted for the observations, but not significantly. The CLM simulations show a negative correlation between MAP and total C (-0.63, $p < 0.001$, Fig. B2), while this is not evident for MIMICS+, indicating that it is different factors that determine the pattern from the two models. In MIMICS+, the moisture modifier on decomposition works on the fluxes from substrate to the microbial pools. The modeled microbes are the most abundant in the top 0–30 cm, which can explain why we observe a difference between drier and wetter sites only in this layer. In CLM, the moisture modification on decomposition rates works on every step in the decomposition cascade from litter to SOM pools. Since the SOM pools have more C in deeper layers, it can explain why we see the pattern in all three depth intervals for the CLM simulations. The moisture modifier used in MIMICS+ (see r_{moist}, Table A5, and Wieder et al., 2017; Sulman et al., 2014) is a bell-shaped function of soil moisture, limiting decomposition in the case of both very wet and very dry soil conditions. If the optimal soil moisture conditions according to this function do not represent the optimal soil moisture value of the real soils, this could explain why MIMICS+ predicts the opposite pattern between the drier and wetter soils. Moreover, soil moisture can vary with subgrid features like slope and aspect, variations not expected to be captured by CLM. Therefore, discrepancy between actual and modeled soil moisture can also be a contributing factor.

4.4 N enrichment experiment

Meta-analyses of observational N enrichment studies show that microbial biomass tends to decrease after enrichment, while the response in total soil C is relatively modest (Treseder, 2008; Janssens et al., 2010). The small modeled response of total soil C to N enrichment (Fig. 7b) is in line with these observations, but the modeled microbial biomass showed a marginal long-term increase after an initial high response (Fig. 7d and e). Treseder (2008) proposed several mechanisms for N effects on microbial growth (Fig. 1 in Treseder, 2008), some leading to an increase and others leading to a decrease in microbial biomass. The sites studied in our model simulations are mainly N limited (N immobilization via mechanism 1 in Sect. 2.1.2 dominates), and we see an accumulation of microbial biomass as a direct consequence of the increased N availability, which is one of the mechanisms suggested by Treseder (2008) for an increase in microbial biomass. Mechanisms proposed to reduce microbial biomass in response to N enrichment are a decrease in soil pH, a decrease in ligninase activity, an increase in melanoidins, and a decrease in belowground NPP. In this offline iteration of MIMICS+ we are unable to capture potential decreases in belowground NPP allocation. Coupling to a vegetation model will enable this possibility and might affect the modeled response of N enrichment. When dividing results into separate biomes, Treseder's (2008) analyses indicate that for boreal forests the response for bacteria is positive (RR = 1.061), while for fungi it is negative (RR = 0.717) but with a confidence interval covering both positive and negative responses (0.0402–1.434). This points to uncertainties in observations of responses of N enrichment as well. To cover more of the possible mechanisms for microbial biomass decline in the model, one or more of the other mechanisms mentioned above could be included.

The strong N limitation in the model is partly a consequence of using low, constant C : N requirements for the saprotrophic pools ($CN_b = 5$ and $CN_f = 8$, ref. Table A5). A less strict C : N requirement, or a dynamic C : N approach, as presented in the ORCHIMIC model (Huang et al., 2018, 2021), could lead to a weaker modeled N limitation and more microbial N mineralization, which can affect the response to N enrichment. This could also improve the modeled underestimation of the soil C : N ratio, as N in inorganic forms is subject to loss through direct plant uptake and leaching.

In the simulations, the largest loss of soil N is through the ectomycorrhizal pathway (N29). The parameter sensitivity analysis also shows a stronger sensitivity of total C to mycorrhizal parameters than to the plant uptake (Fig. B1). The high microbial immobilization of N, together with the simplified representations of direct plant uptake (constant loss rate of available inorganic N), might cause an overestimation of the loss of organic N through mycorrhiza at the expense of direct plant uptake of inorganic N (N33). To model a more re-

alistic scenario, with increased plant production and changes in plant N acquisition strategies as a response to the extra N, it is therefore necessary to couple MIMICS+ to a vegetation model. In such an experiment, both the increase in litter production and the shifts in plant C allocation will affect the soil dynamics. The enrichment experiment presented in this study showed that the model is able to capture microbial responses, and in a coupled system it can be used to further study plant–microbe competition for nutrients.

4.5 Limitations and future improvements of the MIMICS+ framework

By expanding the MIMICS framework with extra microbial groups and an N cycle, we increase the possibilities to capture microbe–microbe interactions and, after coupling, plant–microbe interactions as well. However, we also introduce additional parameters and a more complex model structure that makes the model more prone to overfitting and equifinality issues. While acknowledging this possible drawback, we believe valuable insights can be gathered through a more detailed process representation, especially as new technologies allow for measurements that are suitable for constraining model parameters. Although the model produces results comparable to the observations from Strand et al. (2016), there are still poorly constrained parameters in the model, especially related to mycorrhizal C and N transfer. Recent insights into the mycorrhizal role in soil C dynamics are valuable contributions to future model development (Huang et al., 2022a, b). A more robust parameter optimization procedure like the PRODA approach (Tao et al., 2023) or a Monte Carlo approach (Pierson et al., 2022) will contribute to constraining model parameters. The model should also be evaluated against observations from other ecosystems, which will increase confidence in the model structure and parameter choices. This offline version of MIMICS+ does not capture plant–microbe interactions and feedbacks, which is essential for capturing terrestrial responses to climate change. Therefore, coupling with a vegetation model is a priority in future model development.

5 Conclusions

The soil model MIMICS+ provides a tool for investigating soil C processes and interactions with the N cycle, particularly relevant for boreal areas. Furthermore, the model framework will serve as a valuable soil module in ESMs as it is general enough to work on larger scales. The model produces soil C and N stocks comparable to observed values in Norwegian forest podzols. The explicit representation of microbial groups enhances performance compared to the traditional CLM and enables detection of soil dynamics not possible with a conventional model. In particular, the novel representation of sorbed inorganic N can be further developed to examine climate responses in N-limited systems like boreal forests but also possible impacts on other ecosystems not limited by N. In this study the MIMICS+ model is decoupled from vegetation, so we cannot directly detect feedbacks between nutrient availability and plant productivity. Coupling MIMICS+ to a dynamical vegetation model like FATES will further enable investigation of the interplay between soil microbes and changing aboveground vegetation.

Appendix A: Model description details

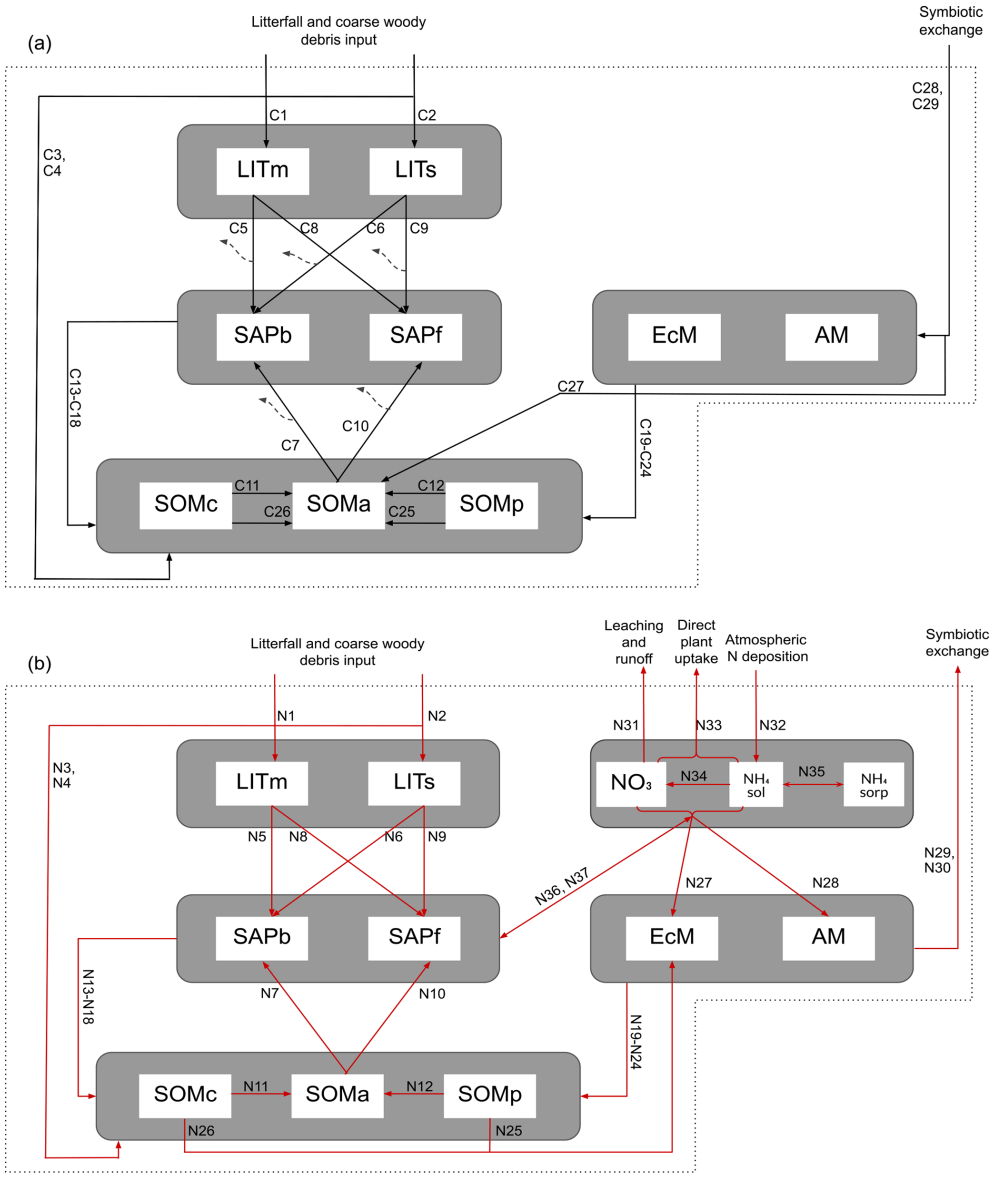

Figure A1. Illustration of all carbon **(a)** and nitrogen **(b)** pools and fluxes in the system. The expressions for each flux can be found with their corresponding numbers in Tables A3 and A4.

Table A1. Mass balance equations for the carbon pools in the model, calculated for each vertical layer (subscript dropped for readability). $FC_{donor,receiver}$: $g\,C\,m^{-3}\,h^{-1}$. Details about the fluxes can be found in Table A3.

Eq.	Stores	Growth rates	Fluxes
(a)	Metabolic litter	$dC_{LITm}/dt =$	$FC_{Veg,LITm} - FC_{LITm,SAPb} - FC_{LITm,SAPf}$
(b)	Structural litter	$dC_{LITs}/dt =$	$FC_{Veg,LITs} - FC_{LITs,SAPb} - FC_{LITs,SAPf}$
(c)	Saprotrophic bacteria	$dC_{SAPb}/dt =$	$CUE_b \cdot FCuptake,SAPb^* - FC_{SAPb,SOMp} - FC_{SAPb,SOMa} - FC_{SAPb,SOMc}$
(d)	Saprotrophic fungi	$dC_{SAPf}/dt =$	$CUE_f \cdot FCuptake,SAPf^* - FC_{SAPf,SOMp} - FC_{SAPf,SOMa} - FC_{SAPf,SOMc}$
(e)	Ectomycorrhiza	$dC_{EcM}/dt =$	$CUE_{EcM} \cdot FC_{Veg,EcM} - FC_{EcM,SOMp} - FC_{EcM,SOMa}$ $- FC_{EcM,SOMc} - FC_{enzEcM,SOMa}$
(f)	Arbuscular mycorrhiza	$dC_{AM}/dt =$	$CUE_{AM} \cdot FC_{Veg,AM} - FC_{AM,SOMp} - FC_{AM,SOMa} - FC_{AM,SOMc}$
(g)	Phys. protected SOM	$dC_{SOMp}/dt =$	$FC_{Veg,SOMp} + FC_{SAPb,SOMp} + FC_{SAPf,SOMp}$ $+ FC_{EcM,SOMp} + FC_{AM,SOMp} - FC_{SOMp,SOMa} - FC_{EcMdecompSOMp}$
(h)	Chem. protected SOM	$dC_{SOMc}/dt =$	$FC_{Veg,SOMc} + FC_{SAPb,SOMc} + FC_{SAPf,SOMc}$ $+ FC_{EcM,SOMc} + FC_{AM,SOMc} - FC_{SOMc,SOMa} - FC_{EcMdecompSOMc}$
(i)	SOM available	$dC_{SOMa}/dt =$	$FC_{SAPb,SOMa} + FC_{SAPf,SOMa} + FC_{EcM,SOMa} + FC_{AM,SOMa}$ $+ FC_{SOMp,SOMa} + FC_{SOMc,SOMa} + FC_{enzEcM,SOMa}$ $+ FC_{EcMdecompSOMc} + FC_{EcMdecompSOMp} - FC_{SOMa,SAPb} - FC_{SOMa,SAPf}$
	Net carbon change	$dC/dt =$	$FC_{Veg,LITm} + FC_{Veg,LITs} + FC_{Veg,SOMp} + FC_{Veg,SOMc}$ $+ CUE_{EcM} \cdot FC_{Veg,EcM} + CUE_{AM} \cdot FC_{Veg,AM} - (1 - CUE_b) \cdot FC_{uptake,SAPb}$ $- (1 - CUE_f) \cdot FCuptake,SAPf^*$

* $FC_{uptake,s} = FC_{LITm,s} + FC_{LITs,s} + FC_{SOMa,s}$.

Table A2. Mass balance equations for the nitrogen pools in the model, calculated for each vertical layer (subscript dropped for readability). $FN_{donor,receiver}$: $g\,N\,m^{-3}\,h^{-1}$. Details about the fluxes can be found in Table A4.

Eq.	Stores	Growth rates	Fluxes
(j)	Metabolic litter	$dN_{LITm}/dt =$	$FN_{Veg,LITm} - FN_{LITm,SAPb} - FN_{LITm,SAPf}$
(k)	Structural litter	$dN_{LITs}/dt =$	$FN_{Veg,LITs} - FN_{LITs,SAPb} - FN_{LITs,SAPf}$
(l)	Saprotrophic bacteria	$dN_{SAPb}/dt =$	$NUE \cdot FN_{uptake,SAPb}{}^{a} - FN_{SAPb,SOMp} - FN_{SAPb,SOMa} - FN_{SAPb,SOMc} + FN_{IN,SAPb}{}^{b,c}$
(m)	Saprotrophic fungi	$dN_{SAPf}/dt =$	$NUE \cdot FN_{uptake,SAPf}{}^{a} - FN_{SAPf,SOMp} - FN_{SAPf,SOMa} - FN_{SAPf,SOMc} + FN_{IN,SAPf}{}^{b,c}$
(n)	Ectomycorrhiza	$dN_{EcM}/dt =$	$FN_{IN,EcM}{}^{b} + FN_{SOMp,EcM} + FN_{SOMc,EcM}$ $- FN_{EcM,SOMp} - FN_{EcM,SOMa} - FN_{EcM,SOMc} - FN_{EcM,Veg}$
(o)	Arbuscular mycorrhiza	$dN_{AM}/dt =$	$FN_{IN,AM}{}^{b} - FN_{AM,SOMp} - FN_{AM,SOMa} - FN_{AM,SOMc} - FN_{AM,Veg}$
(p)	Phys. protected SOM	$dN_{SOMp}/dt =$	$FN_{SAPb,SOMp} + FN_{SAPf,SOMp} + FN_{EcM,SOMp} + FN_{AM,SOMp} + FN_{Veg,SOMp}$ $- FN_{SOMp,SOMa} - FN_{SOMp,EcM}$
(q)	Chem. protected SOM	$dN_{SOMc}/dt =$	$FN_{SAPb,SOMc} + FN_{SAPf,SOMc} + FN_{EcM,SOMc} + FN_{AM,SOMc}$ $+ FN_{Veg,SOMp} - FN_{SOMc,SOMa} - FN_{SOMc,EcM}$
(r)	SOM available	$dN_{SOMa}/dt =$	$FN_{SAPb,SOMa} + FN_{SAPf,SOMa} + FN_{SOMp,SOMa} + FN_{SOMc,SOMa}$ $+ FN_{EcM,SOMa} + FN_{AM,SOMa} - FN_{SOMa,SAPb} - FN_{SOMa,SAPf}$
(s)	Ammonium, solved	$dN_{NH_4,sol}/dt =$	$FN_{DEP} + (1 - NUE)(FN_{uptake,SAPb} + FNuptake,SAPf^{a}) -$ $f_{NH_4}(FN_{IN,EcM} + FN_{IN,AM} + FN_{IN,Veg}) - f_{NH_4}(FN_{IN,SAPb} + FN_{IN,SAPf})$ $- FN_{NH_4,NO_3} + FN_{sol,sorp}$
(t)	Ammonium, sorbed	$dN_{NH_4,sorp}/dt =$	$- FN_{sol,sorp}$
(u)	Nitrate	$dN_{NO_3}/dt =$	$FN_{NH_4,NO_3} - FN_{run+leach} -$ $(1 - f_{NH_4})(FN_{IN,EcM} + FN_{IN,AM} + FN_{IN,Veg}) - (1 - f_{NH_4})(FN_{IN,SAPb} + FN_{IN,SAPf})$
	Net nitrogen change	$dN/dt =$	$FN_{DEP} + FN_{Veg,LITm} + FN_{Veg,LITs} + FN_{Veg,SOMc} + FN_{Veg,SOMp} - FN_{run+leach}$ $- FN_{IN,Veg} - FN_{EcM,Veg} - FN_{AM,Veg}$

[a] $FN_{uptake,s} = FN_{LITm,s} + FN_{LITs,s} + FN_{SOMa,s}$. [b] $FN_{IN,receiver} = FN_{NO3+NH4sol,receiver}$. [c] Can be either positive or negative.

Table A3. Details about C fluxes in the model. The equation numbers correspond to the arrows in Fig. A1a. The letters in the fifth column match those given in Table A1. All $FC_{donor,receiver}$ values are in $g\,C\,m^{-3}\,h^{-1}$. Parameters are described in Table A5.

Eq	Flux name	Rate functions	Used in equations	Notes
C1	$FC_{Veg,LITm} =$	$f_{met} \cdot I_C \cdot (1 - f_{met,SOM})$	(a)	I_C includes litterfall and mortality rates
C2	$FC_{Veg,LITs} =$	$((1 - f_{met}) \cdot I_C + CWD_C) \cdot (1 - f_{struct,SOM})$	(b)	
C3	$FC_{Veg,SOMp} =$	$f_{met} \cdot I_C \cdot f_{met,SOM}$	(g)	
C4	$FC_{Veg,SOMc} =$	$((1 - f_{met}) \cdot I_C + CWD_C) \cdot f_{struct,SOM}$	(h)	
C5	$FC_{LITm,SAPb} =$	$C_{SAPb} \cdot V_{max1} \frac{C_{LITm}}{K_{m1}+C_{SAPb}}$	(a)(c)	Reverse MMK
C6	$FC_{LITs,SAPb} =$	$C_{SAPb} \cdot V_{max2} \frac{C_{LITs}}{K_{m2}+C_{SAPb}}$	(b)(c)	Reverse MMK
C7	$FC_{SOMa,SAPb} =$	$C_{SAPb} \cdot V_{max3} \frac{C_{SOMa}}{K_{m3}+C_{SAPb}}$	(i)(c)	Reverse MMK
C8	$FC_{LITm,SAPf} =$	$C_{SAPf} \cdot V_{max4} \frac{C_{LITm}}{K_{m4}+C_{SAPf}}$	(a)(d)	Reverse MMK
C9	$FC_{LITs,SAPf} =$	$C_{SAPf} \cdot V_{max5} \frac{C_{LITs}}{K_{m5}+C_{SAPf}}$	(b)(d)	Reverse MMK
C10	$FC_{SOMa,SAPf} =$	$C_{SAPf} \cdot V_{max6} \frac{C_{SOMa}}{K_{m6}+C_{SAPf}}$	(i)(d)	Reverse MMK
C11	$FC_{SOMc,SOMa} =$	$\frac{C_{SAPf} \cdot V_{max2} \cdot C_{SOMc}}{KO \cdot K_{m2}+C_{SAPb}} + \frac{C_{SAPb} \cdot V_{max5} \cdot C_{SOMc}}{KO \cdot K_{m5}+C_{SAPf}}$	(h)(i)	As in MIMICS
C12	$FC_{SOMp,SOMa} =$	$C_{SOMp} \cdot k_{desorp}$	(g)(i)	As in MIMICS
C13	$FC_{SAPb,SOMp} =$	$C_{SAPb} \cdot k_{SAPb,som} \cdot f_{SAPb,SOMp}$	(c)(g)	
C14	$FC_{SAPb,SOMc} =$	$C_{SAPb} \cdot k_{SAPb,som} \cdot f_{SAPb,SOMc}$	(c)(h)	
C15	$FC_{SAPb,SOMa} =$	$C_{SAPb} \cdot k_{SAPb,som} \cdot f_{SAPb,SOMa}$	(c)(i)	
C16	$FC_{SAPf,SOMp} =$	$C_{SAPf} \cdot k_{SAPf,som} \cdot f_{SAPf,SOMp}$	(d)(g)	
C17	$FC_{SAPf,SOMc} =$	$C_{SAPf} \cdot k_{SAPf,som} \cdot f_{SAPf,SOMc}$	(d)(h)	
C18	$FC_{SAPf,SOMa} =$	$C_{SAPf} \cdot k_{SAPf,som} \cdot f_{SAPf,SOMa}$	(d)(i)	
C19	$FC_{EcM,SOMp} =$	$C_{EcM} \cdot k_{myc,som} \cdot f_{EcM,SOMp}$	(e)(g)	
C20	$FC_{EcM,SOMc} =$	$C_{EcM} \cdot k_{myc,som} \cdot f_{EcM,SOMc}$	(e)(h)	
C21	$FC_{EcM,SOMa} =$	$C_{EcM} \cdot k_{myc,som} \cdot f_{EcM,SOMa}$	(e)(i)	
C22	$FC_{AM,SOMp} =$	$C_{AM} \cdot k_{myc,som} \cdot f_{AM,SOMp}$	(f)(g)	
C23	$FC_{AM,SOMc} =$	$C_{AM} \cdot k_{myc,som} \cdot f_{AM,SOMc}$	(f)(h)	
C24	$FC_{AM,SOMa} =$	$C_{AM} \cdot k_{myc,som} \cdot f_{AM,SOMa}$	(f)(i)	
C25	$FC_{EcMdecSOMp} =$	$K_{MO} \cdot dz \cdot C_{EcM} \cdot C_{SOMp} \cdot r_{myc}$	(g)(i)	(Baskaran et al., 2017) and mod. term
C26	$FC_{EcMdecSOMc} =$	$K_{MO} \cdot dz \cdot C_{EcM} \cdot C_{SOMc} \cdot r_{myc}$	(h)(i)	(Baskaran et al., 2017) and mod. term
C27	$FC_{enzEcM,SOMa} =$	$f_{enz} \cdot CUE_{EcM} \cdot FC_{Veg,EcM}$	(e)(i)	
C28	$FC_{Veg,EcM} =$	$f_{alloc,EcM} \cdot I_{veg,Myc}$	(e)	
C29	$FC_{Veg,AM} =$	$f_{alloc,AM} \cdot I_{veg,Myc}$	(f)	

Table A4. Details about N fluxes in the model. The equation numbers correspond to the arrows in Fig. A1b. The letters in the fifth column match those given in Table A2. Parameters are described in Table A5.

Eq.	Flux name	Rate functions	Used in equations	Notes
N1	$FN_{Veg,LITm} =$	$f_{met} \cdot I_N \cdot (1 - f_{met,SOM})$	(j)	I_N includes litterfall and mortality rates
N2	$FN_{Veg,LITs} =$	$((1 - f_{met}) \cdot I_N + CWD_N) \cdot (1 - f_{struct,SOM})$	(k)	
N3	$FN_{Veg,SOMp} =$	$f_{met} \cdot I_C \cdot f_{met,SOM}$	(p)	
N4	$FN_{Veg,SOMc} =$	$((1 - f_{met}) \cdot I_N + CWD_N) \cdot f_{struct,SOM}$	(q)	
N5	$FN_{LITm,SAPb} =$	$FC_{LITm,SAPb} \cdot \left(\frac{N_{LITm}}{C_{LITm}}\right)$	(j)(l)	as in MIMICS
N6	$FN_{LITs,SAPb} =$	$FC_{LITs,SAPb} \cdot \left(\frac{N_{LITs}}{C_{LITs}}\right)$	(k)(l)	as in MIMICS
N7	$FN_{SOMa,SAPb} =$	$FC_{SOMa,SAPb} \cdot \left(\frac{N_{SOMa}}{C_{SOMa}}\right)$	(r)(l)	as in MIMICS
N8	$FN_{LITm,SAPf} =$	$FC_{LITm,SAPf} \cdot \left(\frac{N_{LITm}}{C_{LITm}}\right)$	(j)(m)	as in MIMICS
N9	$FN_{LITs,SAPf} =$	$FC_{LITs,SAPf} \cdot \left(\frac{N_{LITs}}{C_{LITs}}\right)$	(k)(m)	as in MIMICS
N10	$FN_{SOMa,SAPf} =$	$FC_{SOMa,SAPf} \cdot \left(\frac{N_{SOMa}}{C_{SOMa}}\right)$	(r)(m)	as in MIMICS
N11	$FN_{SOMc,SOMa} =$	$FC_{SOMc,SOMa} \cdot \left(\frac{N_{SOMc}}{C_{SOMc}}\right)$	(q)(r)	
N12	$FN_{SOMp,SOMa} =$	$FC_{SOMp,SOMa} \cdot \left(\frac{N_{SOMp}}{C_{SOMp}}\right)$	(p)(r)	
N13	$FN_{SAPb,SOMp} =$	$FC_{SAPb,SOMp} \cdot \left(\frac{N_{SAPb}}{C_{SAPb}}\right)$	(l)(p)	
N14	$FN_{SAPb,SOMc} =$	$FC_{SAPb,SOMc} \cdot \left(\frac{N_{SAPb}}{C_{SAPb}}\right)$	(l)(q)	
N15	$FN_{SAPb,SOMa} =$	$FC_{SAPb,SOMa} \cdot \left(\frac{N_{SAPb}}{C_{SAPb}}\right)$	(l)(r)	
N16	$FN_{SAPf,SOMp} =$	$FC_{SAPf,SOMp} \cdot \left(\frac{N_{SAPf}}{C_{SAPf}}\right)$	(m)(p)	
N17	$FN_{SAPf,SOMc} =$	$FC_{SAPf,SOMc} \cdot \left(\frac{N_{SAPf}}{C_{SAPf}}\right)$	(m)(q)	
N18	$FN_{SAPf,SOMa} =$	$FC_{SAPf,SOMa} \cdot \left(\frac{N_{SAPf}}{C_{SAPf}}\right)$	(m)(r)	
N19	$FN_{EcM,SOMp} =$	$FC_{EcM,SOMp} \cdot \left(\frac{N_{EcM}}{C_{EcM}}\right)$	(n)(p)	
N20	$FN_{EcM,SOMc} =$	$FC_{EcM,SOMc} \cdot \left(\frac{N_{EcM}}{C_{EcM}}\right)$	(n)(q)	
N21	$FN_{EcM,SOMa} =$	$FC_{EcM,SOMa} \cdot \left(\frac{N_{EcM}}{C_{EcM}}\right)$	(n)(r)	
N22	$FN_{AM,SOMp} =$	$FC_{AM,SOMp} \cdot \left(\frac{N_{AM}}{C_{AM}}\right)$	(o)(p)	
N23	$FN_{AM,SOMc} =$	$FC_{AM,SOMc} \cdot \left(\frac{N_{AM}}{C_{AM}}\right)$	(o)(q)	
N24	$FN_{AM,SOMa} =$	$FC_{AM,SOMa} \cdot \left(\frac{N_{AM}}{C_{AM}}\right)$	(o)(r)	
N25	$FN_{SOMp,EcM} =$	$FC_{EcMdecompSOMp} \cdot \left(\frac{N_{SOMp}}{C_{SOMp}}\right)$	(g)(e)	
N26	$FN_{SOMc,EcM} =$	$FC_{EcMdecompSOMc} \cdot \left(\frac{N_{SOMc}}{C_{SOMc}}\right)$	(h)(e)	
N27	$FN_{IN,EcM} =$	$V_{max,myc} \cdot N_{IN} \cdot \left(\frac{C_{EcM}}{(C_{EcM} + K_{m,myc}/dz)}\right) \cdot r_{myc}$	(s)(u)(n)	Baskaran et al. (2017) and mod. term, $IN = N_{NO_3} + N_{NH_4,sol}$
N28	$FN_{IN,AM} =$	$V_{max,myc} \cdot N_{IN} \cdot \left(\frac{C_{AM}}{(C_{AM} + K_{m,myc}/dz)}\right) \cdot r_{myc}$	(s)(u)(o)	Baskaran et al. (2017) and mod. term,
N29	$FN_{EcM,Veg} =$	$(FN_{IN,EcM} + FN_{SOMc,EcM} + FN_{SOMp,EcM}) - CUE_{EcM} \cdot FC_{Veg,EcM} \cdot (1 - f_{enz})/CN_{EcM}$ or lower, if N limited (reduced CUE)	(n)	$IN = N_{NO_3} + N_{NH_4,sol}$
N30	$FN_{AM,Veg} =$	$FN_{IN,AM} - CUE_{AM} \cdot FC_{Veg,AM}/CN_{AM}$ or lower, if N limited (reduced CUE)	(o)	$IN = N_{NO_3} + N_{NH_4,sol}$
N31	$FN_{run+leach} =$	$N_{NO_3} \cdot \left(\frac{QDRAI}{H_2O_{tot}} + \frac{QRUNOFF}{H_2O_{top5cm}}\right)$	(u)	see CTSM doc. 2.22.6
N32	$FN_{DEP} =$	NDEP_TO_SMINN · NDEP_PROF	(s)	
N33	$FN_{IN,Veg} =$	$N_{IN} \cdot k_{uptake}$	(s)(u)	$IN = N_{NO_3} + N_{NH_4,sol}$
N34	$FN_{NH_4,NO_3} =$	$NH_4 \cdot k_{nitr}$ or zero if temp. is below freezing	(s)(u)	based on CTSM doc. chapter 2.22.5
N35	$FN_{sol,sorp} =$			
N36	$FN_{IN,SAPb} =$ or =	$(1 - NUE) \cdot U_{Nb} - CUE_b \cdot U_{Cb}/CN_b$ $f_b \cdot N_{for\_sap}$ if N limited	(l)(s)(u)	$IN = N_{NO_3} + N_{NH_4,sol}$
N37	$FN_{IN,SAPf} =$ or =	$(1 - NUE) \cdot U_{Nf} - CUE_f \cdot U_{Cf}/CN_f$ $(1 - f_b) \cdot N_{for\_sap}$ if N limited	(m)(s)(u)	

Table A5. Description of parameters and other relevant sizes used in the model.

Parameter	Description	Expression/value	Units	Notes
f_{met}	Met. fraction of plant litter	$0.75 \cdot (0.85 - 0.013 \cdot \min(40, \text{lignin} : N))$	–	Wieder et al. (2015)
f_{clay}	Clay fraction in soil	0.0–1.0	–	
T	Soil temperature	–	°C	Varies with season and depth
		Michaelis–Menten kinetics parameter for SAP: Wieder et al. (2015), German et al. (2012)		
V_{max}	Max reaction velocity	$\exp(V_{slope} \cdot T + V_{int}) \cdot a_V \cdot V_{mod} \cdot r_{moist}$	$\text{mg}\,(\text{mg})^{-1}\,\text{h}^{-1}$	
K_m	Half-saturation constant	$\exp(K_{slope} \cdot T + K_{int}) \cdot a_K \cdot K_{mod}$	mg C cm^{-3}	
K_{slope}	Regression coefficient	LIT: 0.017, SOMa: 0.027	$\ln(\text{mg C cm}^{-3})\,^{\circ}\text{C}^{-1}$	For all six fluxes
V_{slope}	Regression coefficient	0.063	$\ln(\text{mg}\,(\text{mg})^{-1}\,\text{h}^{-1})\,^{\circ}\text{C}^{-1}$	For all six fluxes
K_{int}	Regression intercept	3.19	$\ln(\text{mg C cm}^{-3})$	Directly from Wieder et al. (2015)
V_{int}	Regression intercept	5.47	$\ln(\text{mg}\,(\text{mg})^{-1}\,\text{h}^{-1})$	Directly from Wieder et al. (2015)
a_V	Tuning coefficient	1.25×10^{-8}	–	
P	Physical protection scalar used in K_{mod}	$1/(2.0 \cdot \exp(-2\sqrt{f_{CLAY}}))$	–	Wieder et al. (2015)
$a_K \cdot K_{mod}$	Tuning coefficients	1.953125, 7.81250, $3.90625 \cdot P$, 7.8125, 3.90625, $2.604167 \cdot P$		As in MIMICS imp. in CLM For LITm, LITs, SOMa
V_{mod}	Modifies V_{max}	10.0, 3.0, 10.0, 3.0, 5.0, 2.0	–	For LITm, LITs, SOMa Entering SAPb, SAPf
KO	Increase km in Eq. (C11)	6	–	Kyker-Snowman et al. (2020)
$k_{myc,som}$	Turnover rate	1.14×10^{-4}	h^{-1}	$1\,\text{yr}^{-1}$ as Sulman et al. (2019) and Baskaran et al. (2017)
$k_{SAPb,som}$	Turnover rate of SAPb	$5.2 \times 10^{-4} \cdot \exp(0.3 \cdot f_{met}) \cdot \max(p_{mod}, m_{mod})$	h^{-1}	Wieder et al. (2015) and mod. term
$k_{SAPf,som}$	Turnover rate of SAPf	$2.4 \times 10^{-4} \cdot \exp(0.1 \cdot f_{met}) \cdot \max(p_{mod}, m_{mod})$	h^{-1}	Wieder et al. (2015) and mod. term
		p_{mod} scales with root profile; $m_{mod} = 0.1$ is the minimum value of the modifier. m_{mod} is used when $T < 0$		
k_{desorp}	Desorption rate	$2 \times 10^{-6} \cdot \exp(-4.5 \cdot f_{clay})$	h^{-1}	Modified from Kyker-Snowman et al. (2020)
K_{MO}	Mycorrhizal decay rate	3.42×10^{-6}	$\text{m}^2\,\text{g C}^{-1}\,\text{h}^{-1}$	Baskaran et al. (2017)
$V_{max,myc}$	Max mycorrhizal uptake of inorganic N	2.05×10^{-4}	$\text{g g}^{-1}\,\text{h}^{-1}$	Baskaran et al. (2017) for EcM; we also use it for AM
$K_{m,myc}$	Half-saturation constant of ectomycorrhizal uptake of inorganic N	0.08	g N m^{-2}	Baskaran et al. (2017) for EcM; we also use it for AM

https://doi.org/10.5194/gmd-17-2929-2024

Table A5. Continued.

Parameter	Description	Expression/value	Units	Notes
CUE_{EcM}	Growth efficiency of mycorrhiza	0–0.5	–	Sulman et al. (2019)
CUE_{AM}	Growth efficiency of mycorrhiza	0–0.5	–	Sulman et al. (2019)
CUE_b	Growth efficiency of sap. bacteria	0–0.4	–	Determined by N availability
CUE_f	Growth efficiency of sap. fungi	0–0.7	–	
NUE	Nitrogen use efficiency of saprotrophs	0.8	–	Mooshammer et al. (2014a)
r_{moist}	Moisture function	$\max\left(0.05, P \cdot \left(\frac{\Theta_{liq}}{\Theta_{sat}}\right)^3 \cdot \left(1 - \frac{\Theta_{liq}}{\Theta_{sat}} - \frac{\Theta_{frozen}}{\Theta_{sat}}\right)^{2.5}\right)$	–	Wieder et al. (2017), Sulman et al. (2014)
r_{myc}	Mycorrhizal modifier	0–1	–	
$f_{SAPb,SOMp}$	Fraction of necromass into SOMp	$0.3 \cdot \exp(1.3 \cdot f_{clay})$	–	
$f_{SAPb,SOMc}$	Fraction of necromass into SOMc	$0.1 \cdot \exp(-3 \cdot f_{met})$	–	
$f_{SAPb,SOMa}$	Fraction of necromass into SOMa	$1 - (f_{SAPb,SOMp} + f_{SAPb,SOMc})$	–	
$f_{SAPf,SOMp}$	Fraction of necromass into SOMp	$0.2 \cdot \exp(0.8 \cdot f_{clay})$	–	
$f_{SAPf,SOMc}$	Fraction of necromass into SOMc	$0.3 \cdot \exp(-3 \cdot f_{met})$	–	
$f_{SAPf,SOMa}$	Fraction of necromass into SOMa:	$1 - (f_{SAPf,SOMp} + f_{SAPf,SOMc})$	–	
$f_{EcM,SOMp}$	Fraction of necromass into SOMp	0.4	–	Assumed
$f_{EcM,SOMc}$	Fraction of necromass into SOMc	0.2	–	Assumed
$f_{EcM,SOMa}$	Fraction of necromass into SOMa	0.4	–	Assumed
$f_{AM,SOMp}$	Fraction of necromass into SOMp	0.3	–	Assumed
$f_{AM,SOMc}$	Fraction of necromass into SOMc	0.4	–	Assumed
$f_{AM,SOMa}$	Fraction of necromass into SOMa	0.3	–	Assumed
f_{enz}	Fraction of EcM C uptake used for enzyme production	0.10	–	Assumed
f_{use}	Fraction of C released by mining taken up by EcM	0.10	–	Assumed
$f_{alloc,i}$	Fraction of C from plant allocation to myc. i	0–1	-	See Sect. 2.1.2
$f_{met,SOM}$	Fraction of met. litter prod. going directly to SOMp	0.5	–	
$f_{struct,SOM}$	Fraction of structural litter production going directly to SOMc	0.5	–	
dz	Soil layer thickness		m	Corresponds to layer thickness in CLM
D	Diffusion coefficient	1.14×10^{-8}	$m^2\,h^{-1}$	Koven et al. (2013): $1\,cm^2\,yr^{-1}$ 1/3 of this value for $N_{NH_4,sorp}$
CN_b	Optimal CN ratio for bacteria	5	–	Mouginot et al. (2014)
CN_f	Optimal CN ratio for sap. fungi	8	–	Mouginot et al. (2014)
CN_m	Optimal CN ratio for myc. fungi	20	–	Baskaran et al. (2017), Wallander et al. (2003)
BD_{soil}	Soil bulk density	1.6×10^6	$g\,m^{-3}$	Sieczka and Koda (2016)
$NH4_{sorp,max}$	Max adsorption capacity	$0.09 \cdot BD_{soil} \cdot 10^{-3} = 144$	$g\,NH_4\,m^{-3}$	Converted from Sieczka and Koda (2016)
K'_L	Modified Langmuir constant	$0.4 \cdot soil\_water\_frac^{-1}$	$m^3\,g\,NH_4{}^{-1}$	Converted from Sieczka and Koda (2016)
k	Rate constant ammonium sorption	$0.0167 \cdot 60 \cdot 10^3 \cdot BD_{soil}^{-1}$	$m^3\,g^{-1}\,h^{-1}$	Converted from Sieczka and Koda (2016)

Table A6. CLM variables used in MIMICS+.

CLM-BGC variable	Units	Long name	Notes
LEAFC_TO_LITTER	$g C m^{-2} s^{-1}$	leaf C litterfall	
FROOTC_TO_LITTER	$g C m^{-2} s^{-1}$	fine-root C litterfall	
CWDC_TO_LITR2C_vr	$g C m^{-3} s^{-1}$	decomposition of coarse woody debris C to litter 2 C	
CWDC_TO_LITR3C_vr	$g C m^{-3} s^{-1}$	decomposition of coarse woody debris C to litter 3 C	
M_LEAFC_TO_LITTER	$g C m^{-2} s^{-1}$	leaf C mortality	
M_FROOTC_TO_LITTER	$g C m^{-2} s^{-1}$	fine-root C mortality	
M_LEAFC_STORAGE_TO_LITTER	$g C m^{-2} s^{-1}$	leaf C storage mortality	input to met. lit. (LITm)
M_LEAFC_XFER_TO_LITTER	$g C m^{-2} s^{-1}$	leaf C transfer mortality	input to met. lit. (LITm)
M_GRESP_STORAGE_TO_LITTER	$g C m^{-2} s^{-1}$	growth respiration storage mortality	input to met. lit. (LITm)
M_GRESP_XFER_TO_LITTER	$g C m^{-2} s^{-1}$	growth respiration transfer mortality	input to met. lit. (LITm)
M_FROOTC_STORAGE_TO_LITTER	$g C m^{-2} s^{-1}$	fine-root C storage mortality	input to met. lit. (LITm)
M_FROOTC_XFER_TO_LITTER	$g C m^{-2} s^{-1}$	fine-root C transfer mortality	input to met. lit. (LITm)
M_LIVECROOTC_XFER_TO_LITTER	$g C m^{-2} s^{-1}$	live coarse-root C transfer mortality	input to met. lit. (LITm)
M_DEADCROOTC_XFER_TO_LITTER	$g C m^{-2} s^{-1}$	dead coarse-root C transfer mortality	input to met. lit. (LITm)
M_LIVECROOTC_STORAGE_TO_LITTER	$g C m^{-2} s^{-1}$	live coarse-root C fire mortality to litter	input to met. lit. (LITm)
M_LIVESTEMC_STORAGE_TO_LITTER	$g C m^{-2} s^{-1}$	live stem C storage mortality	input to met. lit. (LITm)
M_LIVESTEMC_XFER_TO_LITTER	$g C m^{-2} s^{-1}$	live stem C transfer mortality	input to met. lit. (LITm)
M_DEADSTEMC_STORAGE_TO_LITTER	$g C m^{-2} s^{-1}$	dead stem C storage mortality	input to met. lit. (LITm)
M_DEADSTEMC_XFER_TO_LITTER	$g C m^{-2} s^{-1}$	dead stem C transfer mortality	input to met. lit. (LITm)
LEAFN_TO_LITTER	$g N m^{-2} s^{-1}$	leaf N litterfall	partitioned based on f_{MET}
FROOTN_TO_LITTER	$g N m^{-2} s^{-1}$	fine-root N litterfall	partitioned based on f_{MET}
CWDN_TO_LITR2N_vr	$g N m^{-3} s^{-1}$	decomposition of coarse woody debris N to litter 2 C	input to structural litter (LITs)
CWDN_TO_LITR3N_vr	$g N m^{-3} s^{-1}$	decomposition of coarse woody debris C to litter 3 C	input to structural litter (LITs)
M_LEAFN_TO_LITTER	$g N m^{-2} s^{-1}$	leaf N mortality	partitioned based on f_{MET}.
M_FROOTN_TO_LITTER	$g N m^{-2} s^{-1}$	fine-root N mortality	partitioned based on f_{MET}.
M_LEAFN_STORAGE_TO_LITTER	$g N m^{-2} s^{-1}$	leaf C storage mortality	input to met. lit. (LITm)
M_LEAFN_XFER_TO_LITTER	$g N m^{-2} s^{-1}$		input to met. lit. (LITm)
M_FROOTN_STORAGE_TO_LITTER	$g N m^{-2} s^{-1}$		input to met. lit. (LITm)
M_FROOTN_XFER_TO_LITTER	$g N m^{-2} s^{-1}$		input to met. lit. (LITm)
M_LIVECROOTN_XFER_TO_LITTER	$g N m^{-2} s^{-1}$		input to met. lit. (LITm)
M_DEADCROOTN_XFER_TO_LITTER	$g N m^{-2} s^{-1}$		input to met. lit. (LITm)
M_LIVECROOTN_STORAGE_TO_LITTER	$g N m^{-2} s^{-1}$		input to met. lit. (LITm)
M_LIVESTEMN_STORAGE_TO_LITTER	$g N m^{-2} s^{-1}$		input to met. lit. (LITm)
M_LIVESTEMN_XFER_TO_LITTER	$g N m^{-2} s^{-1}$		input to met. lit. (LITm)
M_DEADSTEMN_STORAGE_TO_LITTER	$g N m^{-2} s^{-1}$		input to met. lit. (LITm)
M_DEADSTEMN_XFER_TO_LITTER	$g N m^{-2} s^{-1}$		input to met. lit. (LITm)
M_RETRANSN_TO_LITTER	$g N m^{-2} s^{-1}$		input to met. lit. (LITm)
NPP_NACTIVE	$g C m^{-2} s^{-1}$		partitioned between EcM and AM based on $f_{alloc,i}$
NDEP_TO_SMINN	$g N m^{-2} s^{-1}$	atmospheric N deposition to soil mineral N	N deposition to NH_4 pool
LEAF_PROF	m^{-1}	profile for litter C and N inputs from leaves	Multiplied with LEAF_TO_LITTER to get rates for each layer
FROOT_PROF	m^{-1}	profile for litter C and N inputs from fine roots	Multiplied with FROOT_TO_LITTER to get rates for each layer
CROOT_PROF	m^{-1}	profile for litter C and N inputs from coarse roots	used for input from mortality
STEM_PROF	m^{-1}	profile for litter C and N inputs from stems	used for input from mortality

Table A6. Continued.

CLM-BGC variable	Units	Long name	Notes
NDEP_PROF	m^{-1}	profile for atmospheric N deposition	Multiplied with NDEP_TO_SMINN to get deposition for each layer
		Environmental variables	
TSOI	K	soil temperature	converted to °C
WATSAT	$mm^3\,mm^{-3}$	saturated soil water content (porosity)	used for calculating r_{moist}
SOILLIQ	$kg\,m^{-2}$	soil liquid water	used for calculating r_{moist}
SOILICE	$kg\,m^{-2}$	soil ice water	used for calculating r_{moist}
W_SCALAR	–	moisture (dryness) inhibition of decomposition	used in nitrification algorithm
T_SCALAR	–	temperature inhibition of decomposition	used in nitrification algorithm
QDRAI	$mm\,s^{-1}$	sub-surface drainage	used for calculating leaching
QOVER	$mm\,s^{-1}$	surface runoff	used for calculating runoff
nbedrock	–	index of shallowest bedrock layer	to determine how many layers to use in the simulations
		Read from surface data file	
PCT_CLAY	–	percent CLAY	
PCT_NAT_PFT	–	percent plant functional type on the natural vegetation land unit	

Appendix B: Additional figures

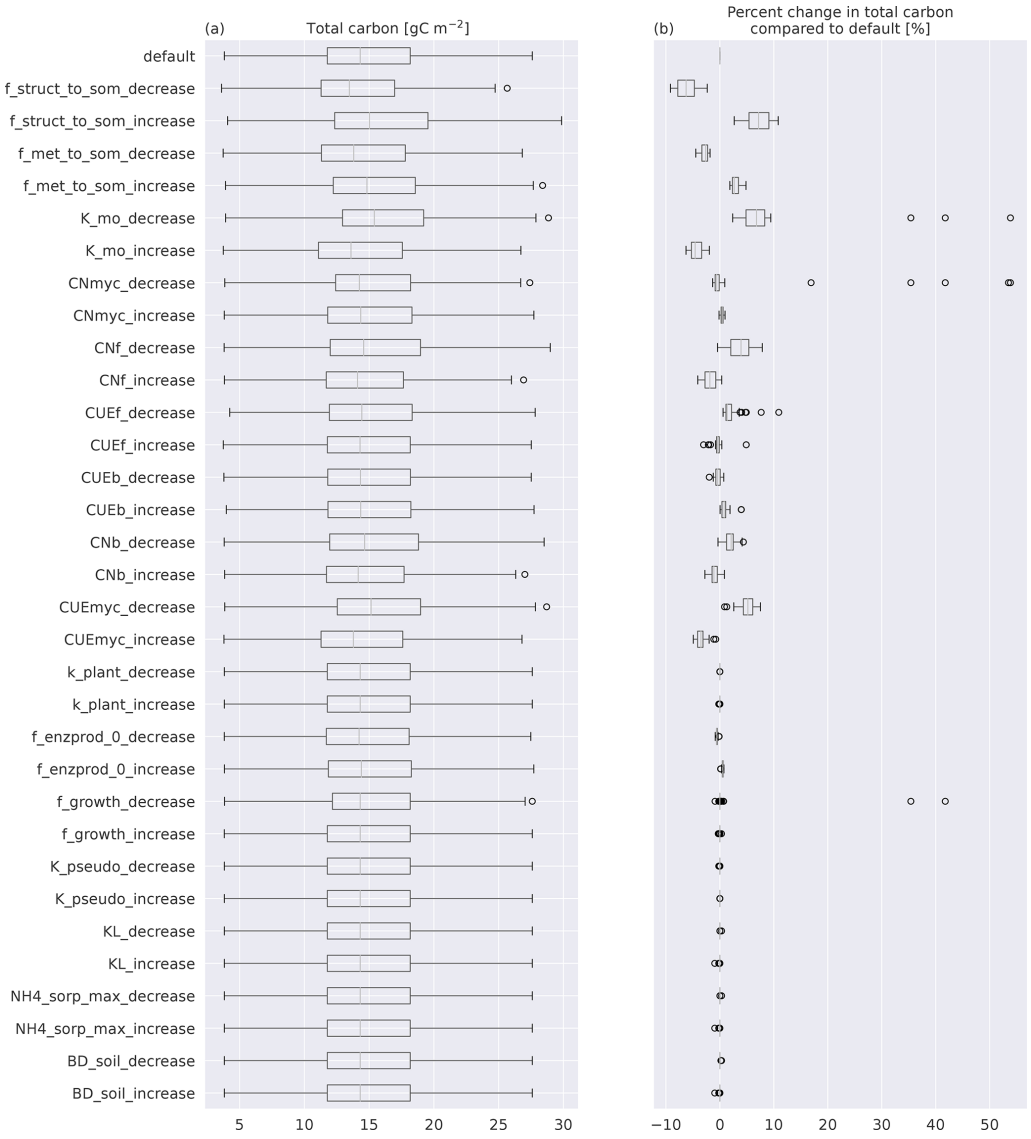

Figure B1. **(a)** Boxplots of total C for the 50 sites modeled with MIMICS+. The top box is the default simulations, while the rest are simulations with one parameter perturbed with either a 25 % increase or a 25 % decrease compared to the default value. **(b)** Boxplots of the percentage change from the default of the same simulations as in **(a)**. The line in each box is the median; the box's upper and lower edges are the 75th and 25th percentiles, respectively. The whiskers extend from the box by 1.5 times the interquartile range.

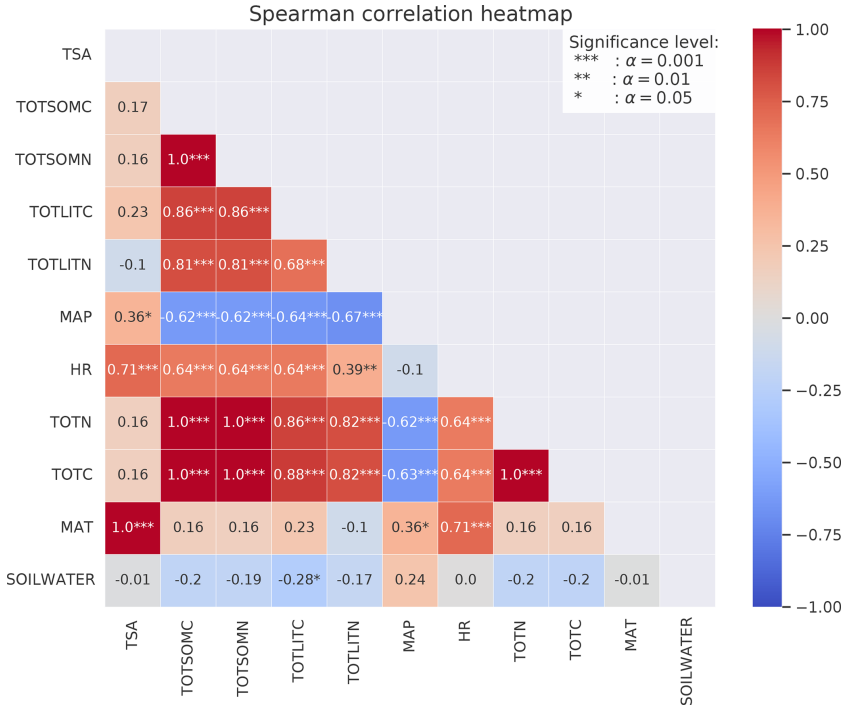

Figure B2. Spearman's correlation coefficients between different variables calculated from the CLM simulations of the 50 sites. The stars represent the significance level of the correlation. Numbers without stars are not significant ($p > 0.05$). The colors indicate whether the correlation is positive (red) or negative (blue), and the shades indicate the strength of the correlation.

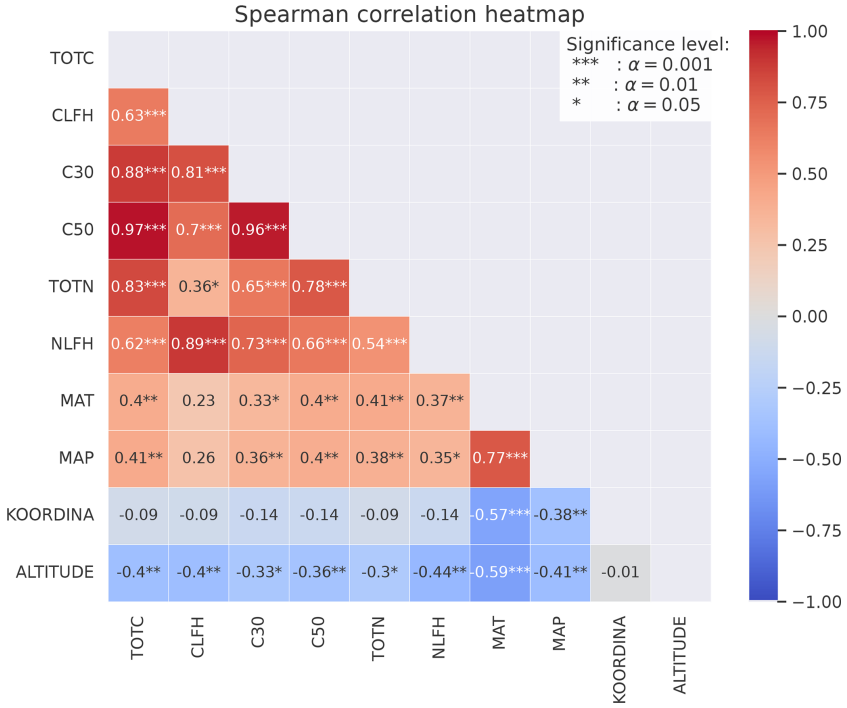

Figure B3. Spearman's correlation coefficients between different observed variables at 50 sites (Strand et al., 2016). The stars represent the significance level of the correlation. Numbers without stars are not significant ($p > 0.05$). The colors indicate whether the correlation is positive (red) or negative (blue), and the shades indicate the strength of the correlation.

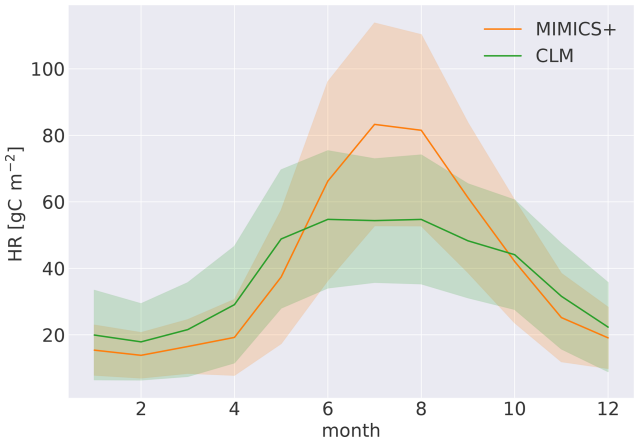

Figure B4. Modeled mean seasonal heterotrophic respiration over the years 1988–1992 and the 50 modeled sites. The shading indicates the standard deviation among the 50 sites.

Appendix C: Input plot

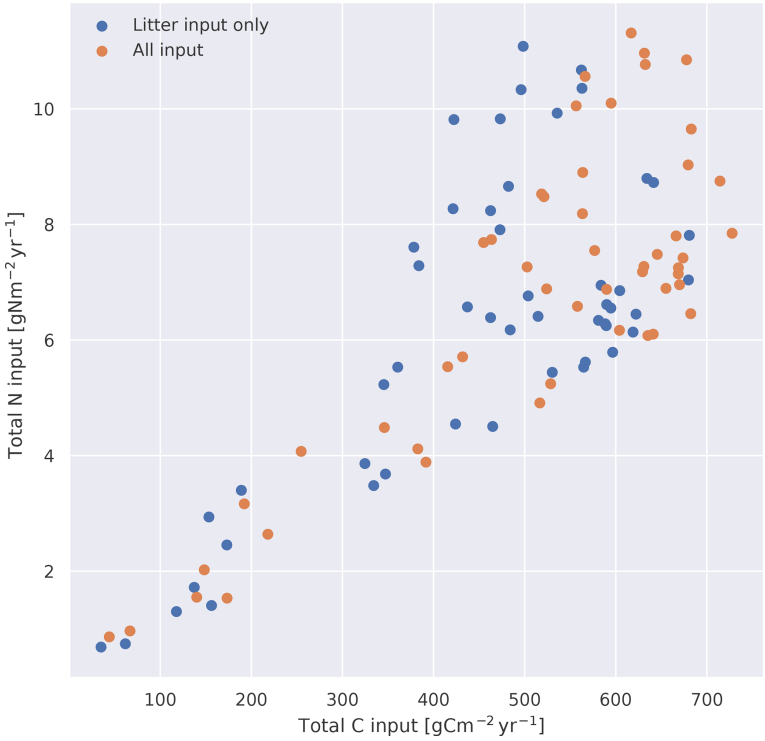

Figure C1. Yearly mean input of carbon and nitrogen to MIMICS+ from CLM for each of the 50 site simulations (averaged over 1988–1992). The blue dots show litter input only, while the orange dots also include the C allocated to mycorrhizal pools and N deposition.

Code and data availability. MIMICS+ (v1.0) is written in Fortran 90. The figures and analyses were produced with Python and Jupyter Notebook. The model code and Jupyter Notebook are available online at https://doi.org/10.5281/zenodo.10610814 (Aas and Woerner, 2024). CLM5.1 is publicly available through the Community Terrestrial System Model (CTSM) GitHub repository (https://github.com/ESCOMP/ctsm, last access: 8 April 2024). The version used for simulations in this paper is archived at https://doi.org/10.5281/zenodo.10946157 (CTSM Development Team, 2024). Input data for CLM and MIMICS+ and output files from MIMICS+ are archived at https://doi.org/10.5281/zenodo.10946217 (Aas, 2024). Access to the soil profile database can be granted upon request to the Norwegian Institute of Bioeconomy Research (NIBIO).

Supplement. The supplement related to this article is available online at: https://doi.org/10.5194/gmd-17-2929-2024-supplement.

Author contributions. ERA and TKB developed the model. ERA ran simulations and wrote the paper. All authors contributed to the analyses and editing of the paper.

Competing interests. The contact author has declared that none of the authors has any competing interests.

Disclaimer. Publisher's note: Copernicus Publications remains neutral with regard to jurisdictional claims made in the text, published maps, institutional affiliations, or any other geographical representation in this paper. While Copernicus Publications makes every effort to include appropriate place names, the final responsibility lies with the authors.

Acknowledgements. We are grateful to Line Tau Strand for providing access to and information about the soil profile database and to Alexander Eiler, Helge Hellevang, Håvard Kauserud, and Rosie Fisher for valuable feedback during the model development process. We are also grateful to Will Wieder and the other scientists at the NCAR lab for their help and discussions regarding MIMICS and CLM.

Financial support. This work has been funded by the University of Oslo and the Research Council of Norway (RCN) through the EMERALD (project no. 294948), FUNDER (project no. 315249), and Green Blue (project no. 287490) research projects. The simulations were performed on resources provided by Sigma2 – the national infrastructure for high-performance computing and data storage in Norway, grant no. NN2806k/NS2806k. Heleen de Wit was supported by the Research Council of Norway (contract no. 160016; Global Change at Northern Latitudes) and the CatchCaN project (the fate and future of carbon in forests), funded by the Technology Agency of the Czech Republic (TACR; project no. TO 01000220).

Review statement. This paper was edited by Sam Rabin and reviewed by two anonymous referees.

References

Aas, E. R.: Model inputs and outputs for "Modeling boreal forest soil dynamics with the microbially explicit soil model MIMICS+ (v1.0)", Zenodo [data set], https://doi.org/10.5281/zenodo.10946217, 2024.

Aas, E. R. and Woerner, E.: ecaas/MIMICSplus: MIMICSplus v1.0.1 with DOI, Zenodo [code], https://doi.org/10.5281/zenodo.10610814, 2024.

Allison, S. D., Wallenstein, M. D., and Bradford, M. A.: Soil-carbon response to warming dependent on microbial physiology, Nat. Geosci., 3, 336–340, https://doi.org/10.1038/ngeo846, 2010.

Angst, G., Mueller, K. E., Nierop, K. G., and Simpson, M. J.: Plant- or microbial-derived? A review on the molecular composition of stabilized soil organic matter, Soil Biol. Biochem., 156, 108189, https://doi.org/10.1016/J.SOILBIO.2021.108189, 2021.

Arora, V. K., Katavouta, A., Williams, R. G., Jones, C. D., Brovkin, V., Friedlingstein, P., Schwinger, J., Bopp, L., Boucher, O., Cadule, P., Chamberlain, M. A., Christian, J. R., Delire, C., Fisher, R. A., Hajima, T., Ilyina, T., Joetzjer, E., Kawamiya, M., Koven, C. D., Krasting, J. P., Law, R. M., Lawrence, D. M., Lenton, A., Lindsay, K., Pongratz, J., Raddatz, T., Séférian, R., Tachiiri, K., Tjiputra, J. F., Wiltshire, A., Wu, T., and Ziehn, T.: Carbon–concentration and carbon–climate feedbacks in CMIP6 models and their comparison to CMIP5 models, Biogeosciences, 17, 4173–4222, https://doi.org/10.5194/bg-17-4173-2020, 2020.

Bååth, E., Nilsson, L. O., Göransson, H., and Wallander, H.: Can the extent of degradation of soil fungal mycelium during soil incubation be used to estimate ectomycorrhizal biomass in soil?, Soil Biol. Biochem., 36, 2105–2109, https://doi.org/10.1016/j.soilbio.2004.06.004, 2004.

Baskaran, P., Hyvönen, R., Berglund, S. L., Clemmensen, K. E., Ågren, G. I., Lindahl, B. D., and Manzoni, S.: Modelling the influence of ectomycorrhizal decomposition on plant nutrition and soil carbon sequestration in boreal forest ecosystems, New Phytol., 213, 1452–1465, https://doi.org/10.1111/nph.14213, 2017.

Bonan, G.: Ecological climatology: concepts and applications, Cambridge University Press, https://doi.org/10.1017/cbo9781107339200.022, 2015.

Brzostek, E. R., Dragoni, D., Brown, Z. A., and Phillips, R. P.: Mycorrhizal type determines the magnitude and direction of root-induced changes in decomposition in a temperate forest, New Phytol., 206, 1274–1282, https://doi.org/10.1111/nph.13303, 2015.

Camino-Serrano, M., Guenet, B., Luyssaert, S., Ciais, P., Bastrikov, V., De Vos, B., Gielen, B., Gleixner, G., Jornet-Puig, A., Kaiser, K., Kothawala, D., Lauerwald, R., Peñuelas, J., Schrumpf, M., Vicca, S., Vuichard, N., Walmsley, D., and Janssens, I. A.: ORCHIDEE-SOM: modeling soil organic carbon (SOC) and dissolved organic carbon (DOC) dynamics along vertical soil profiles in Europe, Geosci. Model Dev., 11, 937–957, https://doi.org/10.5194/gmd-11-937-2018, 2018.

Clemmensen, K. E., Bahr, A., Ovaskainen, O., Dahlberg, A., Ekblad, A., Wallander, H., Stenlid, J., Finlay, R. D., Wardle, D. A., and Lindahl, B. D.: Roots and associated fungi drive long-term

carbon sequestration in boreal forest, Science, 340, 1615–1618, https://doi.org/10.1126/science.1231923, 2013.

CTSM Development Team: ecaas/CTSM_Norway_sites: Version1 (Norway_site_runs), Zenodo [code], https://doi.org/10.5281/zenodo.10946157, 2024.

Esser, J. M. and Nyborg, Å.: Jordsmonn i barskog : en oversikt for Norge, Norwegian Institute of Land Inventory, ISBN 82-7464-034-9, 1992.

Fatichi, S., Manzoni, S., Or, D., and Paschalis, A.: A Mechanistic Model of Microbially Mediated Soil Biogeochemical Processes: A Reality Check, Global Biogeochem. Cy., 33, 620–648, https://doi.org/10.1029/2018GB006077, 2019.

Fernandez, C. W. and Kennedy, P. G.: Revisiting the "Gadgil effect": do interguild fungal interactions control carbon cycling in forest soils?, New Phytol., 209, 1382–1394, https://doi.org/10.1111/nph.13648, 2016.

Fisher, R. A. and Koven, C. D.: Perspectives on the Future of Land Surface Models and the Challenges of Representing Complex Terrestrial Systems, J. Adv. Model. Earth Sy., 12, e2018MS001453, https://doi.org/10.1029/2018MS001453, 2020.

Frey, S. D.: Mycorrhizal Fungi as Mediators of Soil Organic Matter Dynamics, Annu. Rev. Ecol. Evol. S., 50, 237–259, https://doi.org/10.1146/annurev-ecolsys-110617-062331, 2019.

Friedlingstein, P., Jones, M. W., O'Sullivan, M., Andrew, R. M., Bakker, D. C. E., Hauck, J., Le Quéré, C., Peters, G. P., Peters, W., Pongratz, J., Sitch, S., Canadell, J. G., Ciais, P., Jackson, R. B., Alin, S. R., Anthoni, P., Bates, N. R., Becker, M., Bellouin, N., Bopp, L., Chau, T. T. T., Chevallier, F., Chini, L. P., Cronin, M., Currie, K. I., Decharme, B., Djeutchouang, L. M., Dou, X., Evans, W., Feely, R. A., Feng, L., Gasser, T., Gilfillan, D., Gkritzalis, T., Grassi, G., Gregor, L., Gruber, N., Gürses, Ö., Harris, I., Houghton, R. A., Hurtt, G. C., Iida, Y., Ilyina, T., Luijkx, I. T., Jain, A., Jones, S. D., Kato, E., Kennedy, D., Klein Goldewijk, K., Knauer, J., Korsbakken, J. I., Körtzinger, A., Landschützer, P., Lauvset, S. K., Lefèvre, N., Lienert, S., Liu, J., Marland, G., McGuire, P. C., Melton, J. R., Munro, D. R., Nabel, J. E. M. S., Nakaoka, S.-I., Niwa, Y., Ono, T., Pierrot, D., Poulter, B., Rehder, G., Resplandy, L., Robertson, E., Rödenbeck, C., Rosan, T. M., Schwinger, J., Schwingshackl, C., Séférian, R., Sutton, A. J., Sweeney, C., Tanhua, T., Tans, P. P., Tian, H., Tilbrook, B., Tubiello, F., van der Werf, G. R., Vuichard, N., Wada, C., Wanninkhof, R., Watson, A. J., Willis, D., Wiltshire, A. J., Yuan, W., Yue, C., Yue, X., Zaehle, S., and Zeng, J.: Global Carbon Budget 2021, Earth Syst. Sci. Data, 14, 1917–2005, https://doi.org/10.5194/essd-14-1917-2022, 2022.

Gadgil, P. D. and Gadgil, R. L.: Suppression of litter decomposition by mycorrhizal roots of Pinus radiata, J. Genet., 5, 35–41, 1975.

Gadgil, R. L. and Gadgil, P.: Mycorrhiza and litter decomposition, Nature, 233, 133–133, 1971.

German, D. P., Marcelo, K. R. B., Stone, M. M., and Allison, S. D.: The Michaelis-Menten kinetics of soil extracellular enzymes in response to temperature: A cross-latitudinal study, Global Change Biol., 18, 1468–1479, https://doi.org/10.1111/j.1365-2486.2011.02615.x, 2012.

Grandy, A. S. and Robertson, G. P.: Land-use intensity effects on soil organic carbon accumulation rates and mechanisms, Ecosystems, 10, 58–73, https://doi.org/10.1007/s10021-006-9010-y, 2007.

Hanssen-Bauer, I., Førland, E. J., Haddeland, I., Hisdal, H., Mayer, S., Nesje, A., Nilsen, J., Sandven, S., Sandø, A., Sorteberg, A., and Ådlandsvik, B.: Climate in Norway 2100 – a knowledge base for climate adaptation, Tech. Rep. April, The Norwegian Environment Agency, https://www.researchgate.net/profile/Ingjerd-Haddeland/publication/316922280_Climate_in_Norway_2100/links/59194fab4585152e19a24c98/Climate-in-Norway-2100.pdf (last access: 7 April 2024), 2017.

Hansson, A., Dargusch, P., and Shulmeister, J.: A review of modern treeline migration, the factors controlling it and the implications for carbon storage, J. Mt. Sci., 18, 291–306, https://doi.org/10.1007/S11629-020-6221-1, 2021.

Hararuk, O., Smith, M. J., and Luo, Y.: Microbial models with data-driven parameters predict stronger soil carbon responses to climate change, Global Change Biol., 21, 2439–2453, https://doi.org/10.1111/GCB.12827, 2015.

Hobbie, S. E., Nadelhoffer, K. J., and Högberg, P.: A synthesis: The role of nutrients as constraints on carbon balances in boreal and arctic regions, Plant Soil, 242, 163–170, https://doi.org/10.1023/A:1019670731128, 2002.

Högberg, P., Näsholm, T., Franklin, O., and Högberg, M. N.: Tamm Review: On the nature of the nitrogen limitation to plant growth in Fennoscandian boreal forests, Forest Ecol. Manag., 403, 161–185, https://doi.org/10.1016/j.foreco.2017.04.045, 2017.

Huang, W., Van Bodegom, P. M., Declerck, S., Heinonsalo, J., Cosme, M., Viskari, T., Liski, J., and Soudzilovskaia, N. A.: Mycelium chemistry differs markedly between ectomycorrhizal and arbuscular mycorrhizal fungi, Communications Biology, 5, 398, https://doi.org/10.1038/s42003-022-03341-9, 2022a.

Huang, W., van Bodegom, P. M., Viskari, T., Liski, J., and Soudzilovskaia, N. A.: Implementation of mycorrhizal mechanisms into soil carbon model improves the prediction of long-term processes of plant litter decomposition, Biogeosciences, 19, 1469–1490, https://doi.org/10.5194/bg-19-1469-2022, 2022b.

Huang, Y., Guenet, B., Ciais, P., Janssens, I. A., Soong, J. L., Wang, Y., Goll, D., Blagodatskaya, E., and Huang, Y.: ORCHIMIC (v1.0), a microbe-mediated model for soil organic matter decomposition, Geosci. Model Dev., 11, 2111–2138, https://doi.org/10.5194/gmd-11-2111-2018, 2018.

Huang, Y., Guenet, B., Wang, Y. L., and Ciais, P.: Global Simulation and Evaluation of Soil Organic Matter and Microbial Carbon and Nitrogen Stocks Using the Microbial Decomposition Model ORCHIMIC v2.0, Global Biogeochem. Cy., 35, e2020GB006836, https://doi.org/10.1029/2020GB006836, 2021.

Janssens, I. A., Dieleman, W., Luyssaert, S., Subke, J. A., Reichstein, M., Ceulemans, R., Ciais, P., Dolman, A. J., Grace, J., Matteucci, G., Papale, D., Piao, S. L., Schulze, E. D., Tang, J., and Law, B. E.: Reduction of forest soil respiration in response to nitrogen deposition, Nat. Geosci., 3, 315–322, https://doi.org/10.1038/NGEO844, 2010.

Koven, C. D., Riley, W. J., Subin, Z. M., Tang, J. Y., Torn, M. S., Collins, W. D., Bonan, G. B., Lawrence, D. M., and Swenson, S. C.: The effect of vertically resolved soil biogeochemistry and alternate soil C and N models on C dynamics of CLM4, Biogeosciences, 10, 7109–7131, https://doi.org/10.5194/bg-10-7109-2013, 2013.

Koven, C. D., Hugelius, G., Lawrence, D. M., and Wieder, W. R.: Higher climatological temperature sensitivity of soil carbon

in cold than warm climates, Nat. Clim. Change, 7, 817–822, https://doi.org/10.1038/nclimate3421, 2017.

Kyker-Snowman, E., Wieder, W. R., Frey, S. D., and Grandy, A. S.: Stoichiometrically coupled carbon and nitrogen cycling in the MIcrobial-MIneral Carbon Stabilization model version 1.0 (MIMICS-CN v1.0), Geosci. Model Dev., 13, 4413–4434, https://doi.org/10.5194/gmd-13-4413-2020, 2020.

Lawrence, D. M., Fisher, R. A., Koven, C. D., Oleson, K. W., Swenson, S. C., Bonan, G., Collier, N., Ghimire, B., van Kampenhout, L., Kennedy, D., Kluzek, E., Lawrence, P. J., Li, F., Li, H., Lombardozzi, D., Riley, W. J., Sacks, W. J., Shi, M., Vertenstein, M., Wieder, W. R., Xu, C., Ali, A. A., Badger, A. M., Bisht, G., van den Broeke, M., Brunke, M. A., Burns, S. P., Buzan, J., Clark, M., Craig, A., Dahlin, K., Drewniak, B., Fisher, J. B., Flanner, M., Fox, A. M., Gentine, P., Hoffman, F., Keppel-Aleks, G., Knox, R., Kumar, S., Lenaerts, J., Leung, L. R., Lipscomb, W. H., Lu, Y., Pandey, A., Pelletier, J. D., Perket, J., Randerson, J. T., Ricciuto, D. M., Sanderson, B. M., Slater, A., Subin, Z. M., Tang, J., Thomas, R. Q., Martin, M. V., and Zeng, X.: The Community Land Model Version 5: Description of New Features, Benchmarking, and Impact of Forcing Uncertainty, J. Adv. Model. Earth Sy., 11, 4245–4287, https://doi.org/10.1029/2018MS001583, 2019.

Lindahl, B. D. and Tunlid, A.: Ectomycorrhizal fungi – potential organic matter decomposers, yet not saprotrophs, New Phytol., 205, 1443–1447, https://doi.org/10.1111/nph.13201 2015.

Lorenz, M.: International co-operative programme on assessment and monitoring of air pollution effects on forests -ICP forests-, Water Air Soil Poll., 85, 1221–1226, 1995.

Mooshammer, M., Wanek, W., Hämmerle, I., Fuchslueger, L., Hofhansl, F., Knoltsch, A., Schnecker, J., Takriti, M., Watzka, M., Wild, B., Keiblinger, K. M., Zechmeister-Boltenstern, S., and Richter, A.: Adjustment of microbial nitrogen use efficiency to carbon : nitrogen imbalances regulates soil nitrogen cycling, Nat. Commun., 5, 1–7, https://doi.org/10.1038/ncomms4694, 2014a.

Mooshammer, M., Wanek, W., Zechmeister-Boltenstern, S., and Richter, A.: Stoichiometric imbalances between terrestrial decomposer communities and their resources: Mechanisms and implications of microbial adaptations to their resources, Front. Microbiol., 5, 22, https://doi.org/10.3389/fmicb.2014.00022, 2014b.

Mouginot, C., Kawamura, R., Matulich, K. L., Berlemont, R., Allison, S. D., Amend, A. S., and Martiny, A. C.: Elemental stoichiometry of Fungi and Bacteria strains from grassland leaf litter, Soil Biol. Biochem., 76, 278–285, https://doi.org/10.1016/j.soilbio.2014.05.011, 2014.

Parton, W. J., Stewart, J. W. B., and Cole, C. V.: Dynamics of C, N, P and S in grassland soils: a model, Biogeochemistry, 5, 109–131, https://doi.org/10.1007/BF02180320, 1988.

Phillips, R. P., Meier, I. C., Bernhardt, E. S., Grandy, A. S., Wickings, K., and Finzi, A. C.: Roots and fungi accelerate carbon and nitrogen cycling in forests exposed to elevated CO_2, Ecol. Lett., 15, 1042–1049, https://doi.org/10.1111/j.1461-0248.2012.01827.x, 2012.

Pierson, D., Lohse, K. A., Wieder, W. R., Patton, N. R., Facer, J., de Graaff, M.-A., Georgiou, K., Seyfried, M. S., Flerchinger, G., and Will, R.: Optimizing process-based models to predict current and future soil organic carbon stocks at high-resolution, Sci. Rep.-UK, 12, 10824, https://doi.org/10.1038/S41598-022-14224-8, 2022.

Sieczka, A. and Koda, E.: Kinetic and equilibrium studies of sorption of ammonium in the soil-water environment in agricultural areas of central poland, Appl. Sci.-Basel, 6, 269, https://doi.org/10.3390/APP6100269, 2016.

Soetaert, K. and Herman, P. M.: A practical guide to ecological modelling: using R as a simulation platform, Springer, https://doi.org/10.1007/978-1-4020-8624-3, 2009.

Strand, L. T., Callesen, I., Dalsgaard, L., and de Wit, H. A.: Carbon and nitrogen stocks in Norwegian forest soils – the importance of soil formation, climate, and vegetation type for organic matter accumulation, Can. J. Forest Res., 46, 1459–1473, https://doi.org/10.1139/cjfr-2015-0467, 2016.

Strickland, M. S. and Rousk, J.: Considering fungal : bacterial dominance in soils – Methods, controls, and ecosystem implications, Soil Biol. Biochem., 42, 1385–1395, https://doi.org/10.1016/j.soilbio.2010.05.007, 2010.

Sulman, B. N., Phillips, R. P., Oishi, A. C., Shevliakova, E., and Pacala, S. W.: Microbe-driven turnover offsets mineral-mediated storage of soil carbon under elevated CO_2, Nat. Clim. Change, 4, 1099–1102, https://doi.org/10.1038/nclimate2436, 2014.

Sulman, B. N., Shevliakova, E., Brzostek, E. R., Kivlin, S. N., Malyshev, S., Menge, D. N., and Zhang, X.: Diverse Mycorrhizal Associations Enhance Terrestrial C Storage in a Global Model, Global Biogeochem. Cy., 33, 501–523, https://doi.org/10.1029/2018GB005973, 2019.

Sveistrup, T. E.: Retningslinjer for beskrivelse av jordprofil, Jord og Myr, http://hdl.handle.net/11250/2489357 (last access: 5 July 2023), 1984.

Tang, J. and Riley, W. J.: Weaker soil carbon–climate feedbacks resulting from microbial and abiotic interactions, Nat. Clim. Change, 5, 56–60, https://doi.org/10.1038/nclimate2438, 2014.

Tao, F., Huang, Y., Hungate, B. A., Manzoni, S., Frey, S. D., Schmidt, M. W. I., Reichstein, M., Carvalhais, N., Ciais, P., Jiang, L., Lehmann, J., Wang, Y.-P., Houlton, B. Z., Ahrens, B., Viatkin, K., Vargas, R., Yigini, Y., Omuto, C., Malik, A. A., Peralta, G., Cuevas-Corona, R., Di Paolo, L. E., Luotto, I., Liao, C., Liang, Y.-S., Saynes, V. S., Huang, X., and Luo, Y.: Microbial carbon use efficiency promotes global soil carbon storage, Nature, 618, 981–985, https://doi.org/10.1038/s41586-023-06042-3, 2023.

Taylor, M. K., Lankau, R. A., and Wurzburger, N.: Mycorrhizal associations of trees have different indirect effects on organic matter decomposition, J. Ecol., 104, 1576–1584, https://doi.org/10.1111/1365-2745.12629, 2016.

Todd-Brown, K. E. O., Hopkins, F. M., Kivlin, S. N., Talbot, J. M., and Allison, S. D.: A framework for representing microbial decomposition in coupled climate models, Biogeochemistry, 109, 19–33, https://doi.org/10.1007/s10533-011-9635-6, 2012.

Tonjer, L. R., Thoen, E., Morgado, L., Botnen, S., Mundra, S., Nybakken, L., Bryn, A., and Kauserud, H.: Fungal community dynamics across a forest–alpine ecotone, Mol. Ecol., 30, 4926–4938, https://doi.org/10.1111/mec.16095, 2021.

Treseder, K. K.: Nitrogen additions and microbial biomass: a meta-analysis of ecosystem studies, Ecol. Lett., 11, 1111–1120, https://doi.org/10.1111/J.1461-0248.2008.01230.X, 2008.

Wallander, H., Nilsson, L. O., Hagerberg, D., and Rosengren, U.: Direct estimates of C : N ratios of ectomycorrhizal mycelia collected from Norway spruce forest soils, Soil Biol. Biochem.,

35, 997–999, https://doi.org/10.1016/S0038-0717(03)00121-4, 2003.

Wang, G., Post, W. M., and Mayes, M. A.: Development of microbial-enzyme-mediated decomposition model parameters through steady-state and dynamic analyses, Ecol. Appl., 23, 255–272, https://doi.org/10.1890/12-0681.1, 2013.

Wang, Y.-P., Zhang, H., Ciais, P., Goll, D., Huang, Y., Wood, J. D., Ollinger, S. V., Tang, X., and Prescher, A.-K.: Microbial Activity and Root Carbon Inputs Are More Important than Soil Carbon Diffusion in Simulating Soil Carbon Profiles, J. Geophys. Res.-Biogeo., 126, e2020JG006205, https://doi.org/10.1029/2020JG006205, 2021.

Wardle, D. A., Bardgett, R. D., Klironomos, J. N., Setälä, H., Van Der Putten, W. H., and Wall, D. H.: Ecological linkages between aboveground and belowground biota, Science, 304, 1629–1633, https://doi.org/10.1126/science.1094875, 2004.

Wieder, W. R., Grandy, A. S., Kallenbach, C. M., Taylor, P. G., and Bonan, G. B.: Representing life in the Earth system with soil microbial functional traits in the MIMICS model, Geosci. Model Dev., 8, 1789–1808, https://doi.org/10.5194/gmd-8-1789-2015, 2015.

Wieder, W. R., Hartman, M. D., Sulman, B. N., Wang, Y.-P., Koven, C. D., and Bonan, G. B.: Carbon cycle confidence and uncertainty: Exploring variation among soil biogeochemical models, Global Change Biol., 24, 1563–1579, https://doi.org/10.1111/gcb.13979, 2017.

Yu, L., Ahrens, B., Wutzler, T., Schrumpf, M., and Zaehle, S.: Jena Soil Model (JSM v1.0; revision 1934): a microbial soil organic carbon model integrated with nitrogen and phosphorus processes, Geosci. Model Dev., 13, 783–803, https://doi.org/10.5194/gmd-13-783-2020, 2020.

Supplement of Geosci. Model Dev., 17, 2929–2959, 2024
https://doi.org/10.5194/gmd-17-2929-2024-supplement

Geoscientific Model Development
Open Access
EGU

Supplement of

Modeling boreal forest soil dynamics with the microbially explicit soil model MIMICS+ (v1.0)

Elin Ristorp Aas et al.

Correspondence to: Elin Ristorp Aas (ecaas@uio.no) and Terje K. Berntsen (t.k.berntsen@geo.uio.no)

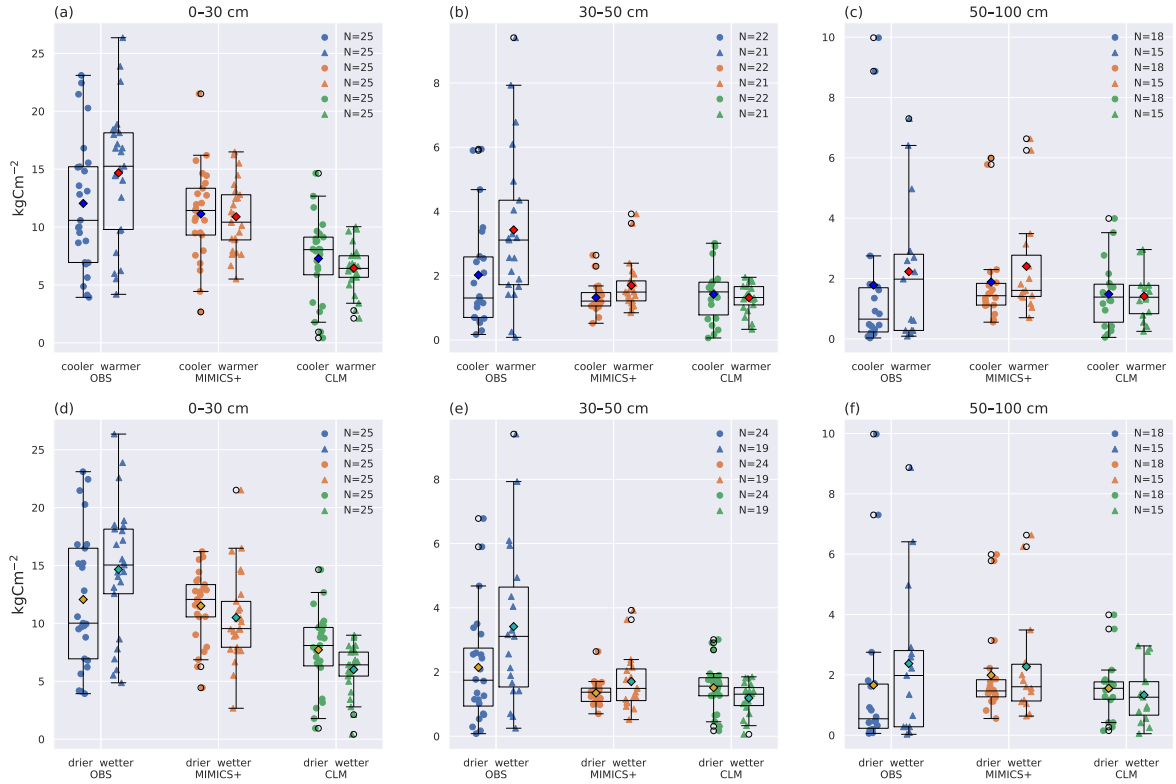

S1: Total carbon stocks for cooler/warmer (a--c) and dryer/wetter (d--f) parts of the dataset. All three datasets (OBS, MIMICS+, CLM) are sorted after the climatic gradient of the observations. Box plots of carbon stocks in the (a), (d) top 30 cm, (b), (e) 30--50 cm, (c), (f) 50--100 cm soil depths for observed profiles from Strand et al. 2016 (left), simulated with MIMICS+ (center) and with CLM (right). In (a--c) the leftmost quartiles represent the coldest 50 % of the dataset, while the rightmost represent the warmest 50 % of the dataset. In (d--f) the leftmost boxes represent the drier 50 % of the total subset, while the rightmost represent the wetter 50 %.

S2: Each panel contains boxplots of carbon stocks in the depth interval indicated in the top right corner, at sites from the total podzol dataset (N=578), that falls into the MAT interval indicated in the top left corner. The sites in each plot is divided into MAP categories described in main text, Table 1. The line in each box is the median, while the diamonds mark the mean values. The box upper and lower edges are the 75th and 25th percentiles, respectively. The whiskers extend from the box by 1.5 times the inter-quartile range.

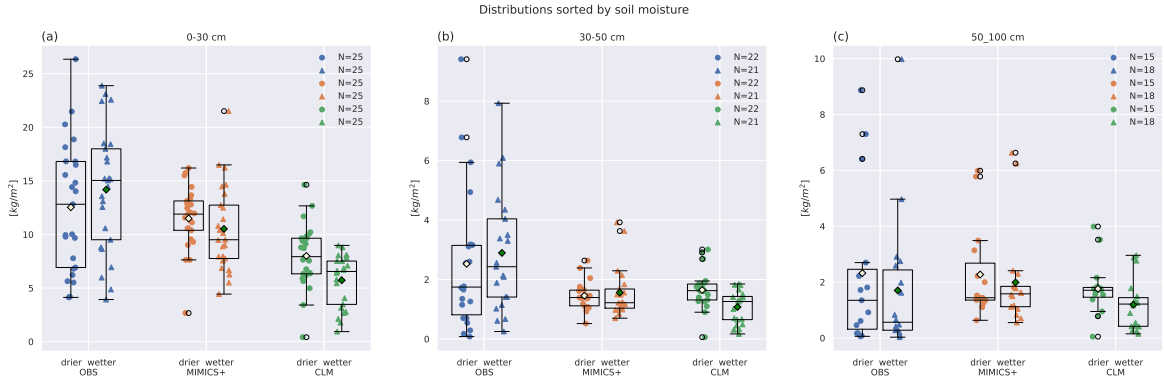

S3: Carbon concentrations for dryer/wetter parts of the datasets divided by the CLM variable SOILWATER_10CM. Box plots of carbon concentrations in the (a) 0--30 cm, (b) 30--50 cm, (c) 50--100 cm soil depths for observed profiles from Strand et al. 2016 (left), simulated with MIMICS+ (center) and with CLM (right). The line in each box is the median, while the diamonds mark the mean values. The diamond color correspond to the climate category; yellow: drier, turquoise: wetter. The box upper and lower edges are the 75th and 25th percentiles, respectively. The whiskers extend from the box by 1.5 times the inter-quartile range.

Paper II

Implications of climate and litter quality for simulations of litterbag decomposition at high latitudes

In review for *Biogeosciences*

Paper III

Ectomycorrhizal turnover times affect soil dynamics in boreal ecosystems; A model study

In prep. for *Soil Biology and Biochemistry*